INDOMETHACIN-AMIDES AS A MOLECULAR PROBE TO INVESTIGATE THE STRUCTURE AND FUNCTION OF CYCLOOXYGENASES, THROMBOXANE SYNTHASE, AND STEROL 14α-DEMETHYLASE FROM *TRYPANOSOMA CRUZI*

By

Mary E. Konkle

Dissertation

Submitted to the Faculty of the Graduate School of Vanderbilt University

In partial fulfillment of the requirements for the degree of

DOCTOR OF PHILOSOPHY

In

Chemistry

December, 2008

Nashville, Tennessee

Approved:

Dr. Lawrence J. Marnett

Dr. Terry P. Lybrand

Dr. Richard N. Armstrong

Dr. Jens Meiler

ACKNOWLEDGEMENTS

All of this work was accomplished with the aid of helpful colleagues, knowledgeable mentors, encouraging friends and family, and the Grace of God.

I would like to thank my advisor Dr. Lawrence Marnett for providing me with the opportunity and means to experience scientific freedom. My PhD Committee, Dr. Terry Lybrand, Dr. Richard Armstrong, Dr. Carmelo Rizzo, and Dr. Jens Meiler for their expertise and interest in this work.

For the work with cyclooxygenases, I am indebted to Dr. Jeffery Pruskiewicz and Dr. Scott Rowlinson for providing purified enzyme. Additionally, the Eicosanoid sub groups; Kebreab Ghebreselasie, Brenda Crews, Dr. Carol Rouzer, Dr. Annie Blobaum and particularly Melissa Turman for the helpful scientific discussions. I have enjoyed my musical collaborator Dr. Chris Moth for his creativity and unique perspective. I had assistance with molecular biology whenever it was needed from Dr. Aaron Jacobs, Dr. James West and Dr. Robyn Jannetta. Phil Kingsley and Dawn Overstreet were selfless with their time and talents for all things Mass Spec. I appreciate all the humor and insightful science provided by Dr. Charles Knutson. For introducing an unexpected project into my graduate studies, I am particularly grateful for Dr. Galena Lepesheva and Dr. Mike Waterman for their willingness to take a chance on an idea. I am also indebted to the openness of Dr. C.S. Raman in sharing the protocol for thromboxane synthase expression.

The support of friends and family during this time is priceless. To all the women of the Belcourt House; Lori, Monica, Jocelyn, Amber, Elizabeth, thanks for your vulnerability and willingness to create a Sanctuary. My heart gives thanks to the First

Pres YAMS, Ben, Hannah, Monica, Les, Jocelyn, and Megan for striving to do it better, everyday. My world would not have color without my Muses, Marianna and Jamie and Piano Man Nate. Music beautifies the simplest deed! I credit Melissa for making the toil of the everyday a little bit brighter.

I want to acknowlege the scores of excellent teachers I have been blessed to encounter during my public education. Dr. Terry Kruger, Dr. Patricia Lang, Mr. Buck McIntyre, Ms. Diane Barton and Mr. Everett Hornbarger warrant particular recognition for making the world my classroon.

I have been fortunate to have a supportive large extended family. In particular, my parents and grandparents, Steve and Hester Konkle and Bill and Mary (A.) Konkle for their support and weekly calls even when the "why" was unclear. I am appreciative of my sister, Carol Konkle Sundheimer that we have each been given the opportunity to find our own calling. My surrogate family, the McLellan clan, has kept me Midwestern grounded and loved through many a trial and gifting me rest whenever required.

Finally, I cannot express the wonder at the path my husband Ryan Mahoney and I have followed. God has truly blessed our trials and been Providence Proven. For all the things he has done to support my calling, my cup overfloweth.

TABLE OF CONTENTS

LIST OF FIGURES

LIST OF TABLES

LIST OF ABBREVIATIONS

2-AG	2-Arachidonoylglycerol
AA	Arachidonic Acid
AEA	Anandamide
ASA	Aspirin
CB	Cannabinoid
COX	Cyclooxygenase
COXIB	COX-2 Selective Inhibitor
CYP51	Sterol 14α–Demethylase
DAH	Diarylheterocycles
GPCR	G-Proteins Coupled Receptor
HHT	12-hydroxyheptadecatrienoic acid
HTS	High Throughput Screen
INDO	Indomethacin
LC	Liquid Chromatography
MBD	Membrane Binding Domain
MD	Molecular Dynamics
MDA	Malondialdehyde
MS	Mass Spectrometry
NSAID	Non-Steroidal Anti-Inflammatory Drug
PG	Prostaglandin

PGG	Prostaglandin Glycerol
POX	Peroxidase
RCS	Rabbit Contractile Substance
RPM	Resident Peritoneal Macrophages
TC	*Trypanosoma cruzi*
TX	Thromboxane
WHO	World Health Organization

CHAPTER I

INTRODUCTION

Function and Biochemistry of Cyclooxygenases

Cyclooxygenases (COX), originally known as prostaglandin endoperoxide H synthases (PGHS), catalyze the *bis*-dioxygenation and subsequent reduction of endogenous fatty acid substrates[1, 2]. The most biologically relevant of these is the twenty-carbon all-*cis* tetraene fatty acid arachidonic acid (AA) which is transformed to the prostanoid precursor prostaglandin H_2 (PGH_2)[2-4]. COX accomplishes this transformation through two separate active sites, the cyclooxygenase site and the peroxidase site[5]. Initial transformation of AA in the cyclooxygenase site is accomplished through exquisite stereospecific-cyclization to form the relatively unstable endoperoxide moiety and peroxy moiety of prostaglandin G_2 (PGG_2)(Figure 1)[6-11]. PGG_2 then diffuses into the peroxidase site, which contains a heme cofactor, and the peroxy moiety is reduced to the alcohol moiety of PGH_2[11-16].

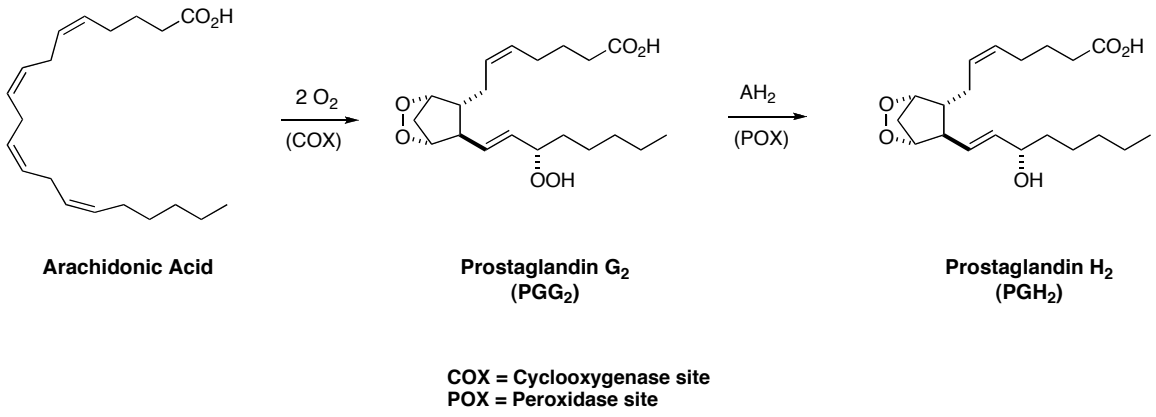

Figure 1. Metabolism of arachidonic acid (AA) to PGH_2 by Cyclooxygenases

The bioactivity of a class of lipids termed prostaglandins were characterized from seminal fluid by the American gynecologist Kurzrok and Lieb in 1930. These compounds caused uterine muscle contractions and were originally thought to originate from the prostate gland. Thus, they were named by Swedish physiologist von Euler even though they actually are formed in the seminal vesicle[17, 18]. Further work in the laboratories of both von Euler and Goldblatt elucidated the varied activities of prostaglandins on several tissue types, but their structures were not elucidated until the 1960's by Bergstrom and colleagues[19]. Considering that the structures of the PGs all had a common 20-carbon skeleton and contained identical patterns of unsaturation, the conclusion that these molecules were downstream of AA metabolism was readily made[1, 2, 19-34]. The regulation of PG production is maintained by the expression of tissue specific synthases for each unique prostaglandin and thromboxane; prostaglandin E_2 (PGE_2), prostaglandin D_2 (PGD_2), prostaglandin $F_{2\alpha}$ ($PGF_{2\alpha}$), prostacylcin or prostaglandin I_2 (PGI_2), and thromboxane A_2 (TXA_2) which are metabolites of PGH_2 (Figure 2.)[35, 36].

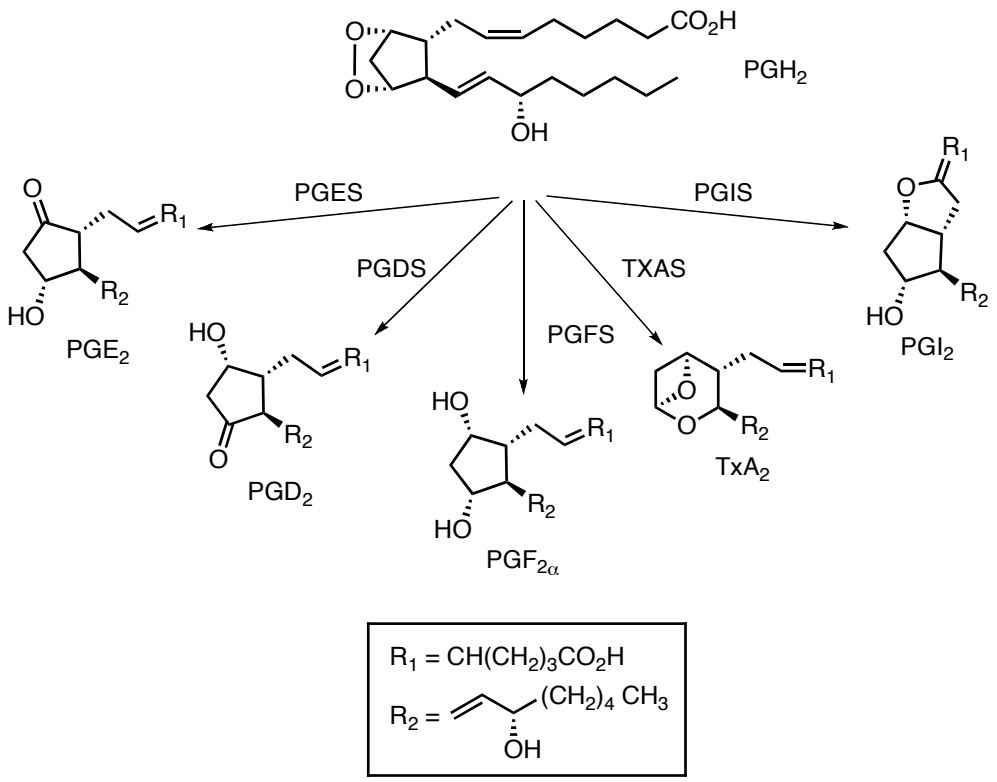

Figure 2. Production of prostaglandins by various synthases from PGH_2

These bioactive lipids signal through g-protein coupled receptors (GPCRs) specific for each PG/TX and are designated $XP_{\#}$ (e.g. EP_3 for the third prostaglandin E_2 receptor). The lack of cross-reactivity by the various PGs at alternative receptors is noteworthy considering their structural similarity. Through signaling at the various receptors, PGs can exert physiological control of processes paramount to both homeostasis and/or an organism's reaction to invasion or injury such as control of vascular tone (PGI_2 and TXA_2), cytoprotection of gastric muscosa (PGE_2), inflammatory responses (PGE_2 and PGD_2), and ocular pressure ($PGF_{2\alpha}$)[24, 26, 28, 31, 33, 34, 37-41]. Since PGH_2

is the common intermediate for all of the downstream PGs, its production by COX represents the committed step in PG synthesis and, as such, a target for therapeutic intervention.

From the early 1970s until the 1990s, it was assumed that all PGs produced came from PGH_2 production by a single isoform of COX. Several groups, through biochemical and pharmacological studies, identified a second COX isoform in the early 1990s[42-47]. This discovery both excited vigorous experimental activity and confounded the framework of bioactive lipid production and signaling. The pharmacological studies, especially, indicated that the regulation of expression of the newly discovered COX isoform, denoted COX-2, was sensitive to both cytokine stimulation and glucocorticoid treatment. This is in stark contrast to COX-1, which appeared to have a basal and relatively constant level of activity in most tissues and whose expression level was impervious to the same stimuli. The two isoforms metabolize AA equally well, which indicated that the reason for two seemingly redundant enzymes could be differential environments for activity[48]. The paradigm that developed, and that has only begun to be seriously challenged in recent years, was that COX-1 activity governed the "housekeeping" (healthful) functions of PG production and COX-2 expression and activity were called upon only in situations of illness or injury (unhealthful)[48]. Recent developments indicate that this view is an oversimplification. What is certain is that COX-1 is constituitively expressed in a large number of tissues whereas COX-2 *in most, but not all, tissues* is expressed minimally prior to oft dramatic induction by growth factors, cytokines, or tumor promoters.

In addition to AA (20:4), COX enzymes can turn over other fatty acid substrates such as dihomolinolenic acid (20:3) and eicosapentaenoic acid (20:5) which go on to produce the 1 (PGX_1) and 3 (PGX_3) series of PGs[49-53]. COXs are not nearly as efficient at turnover of these additional fatty acids as with AA, and as such these other fatty acids can act as competitive physiological inhibitors of PG production. In addition, the endocannabinoids, which are neutral derivatives of AA, 2-arachidonoyl glycerol (2-AG) and arachidonoyl ethanolamide (AEA or anandamide) were initially reported as selective substrates for COX-2 (Figure 3.).

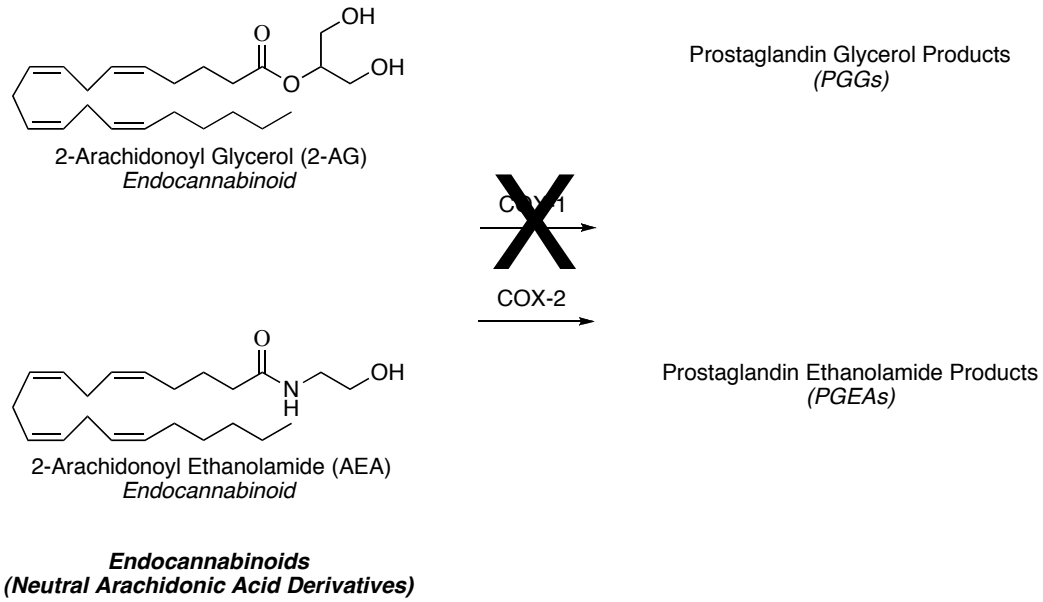

Figure 3. Metabolism of the endocannabinoids by cyclooxygenases to prostaglandin derivatives

The endocannabinoids, so named because they are endogenous ligands for the cannabinoid receptors (CB_1 and CB_2), are bioactive lipids released by various phospholipases from membrane phospholipids. The identification of a receptor prior to the identification of its endogenous ligand is somewhat unique and was motivated in this case by the interest in the pharmacology of its pharmacological ligand, Δ^9–tetrahydrocannabinol, the principle psychotropic component of marijuana[54, 55]. 2-AG was isolated from mammalian tissues and shown to bind to both cannabinoid receptors in 1997[56]. COX-2 can metabolize both 2-AG and AEA, but turnover efficiency of 2-AG is similar to AA, whereas COX-2 oxygenation of AEA is so poor (70% less that that of AA), in fact, that the physiologic relevance of this *in vitro* activity is unclear[57, 58]. The subsequent downstream products of this activity (PG-Gs and PG-EAs respectively) were shown to be produced in *in vitro* experiments by the appropriate PG-synthases (with the exception of thromboxane). Additionally, PGD_2-G was shown to be produced in the RAW264.7 macrophage cellular system by inducing COX-2 expression with lipopolysaccharide and then treating with exogenous 2-AG. As for the relevance of these products in cellular signaling, subsequent work that demonstrated that PGE_2-G could induce calcium mobilization in a dose-dependent fashion in RAW264.7 cells motivates the hypothesis that COX-2 action has some physiological roles not fulfilled by COX-1 expression[59-61].

Structure of Cyclooxygenases

COXs are membrane bound, functional homodimeric (C_2 symmetry), heme-containing enzymes. The molecular weight of the mature protein is 70 kDa per

monomer[62, 63]. Each monomer is anchored into a single leaflet of the membrane by the four amphipathic helices of the membrane binding domain (MBD) which frames an open region called the "lobby"[64]. The first of the catalytic sites, the cyclooxygenase active site, can only be accessed by moving through the lobby. The second of the catalytic site, the peroxidase site, is open to solution and contains the heme cofactor[48]. The two COX isoforms have remarkable fidelity of structure[65](Overlay of COX isoform crystal structures, Figure 4.).

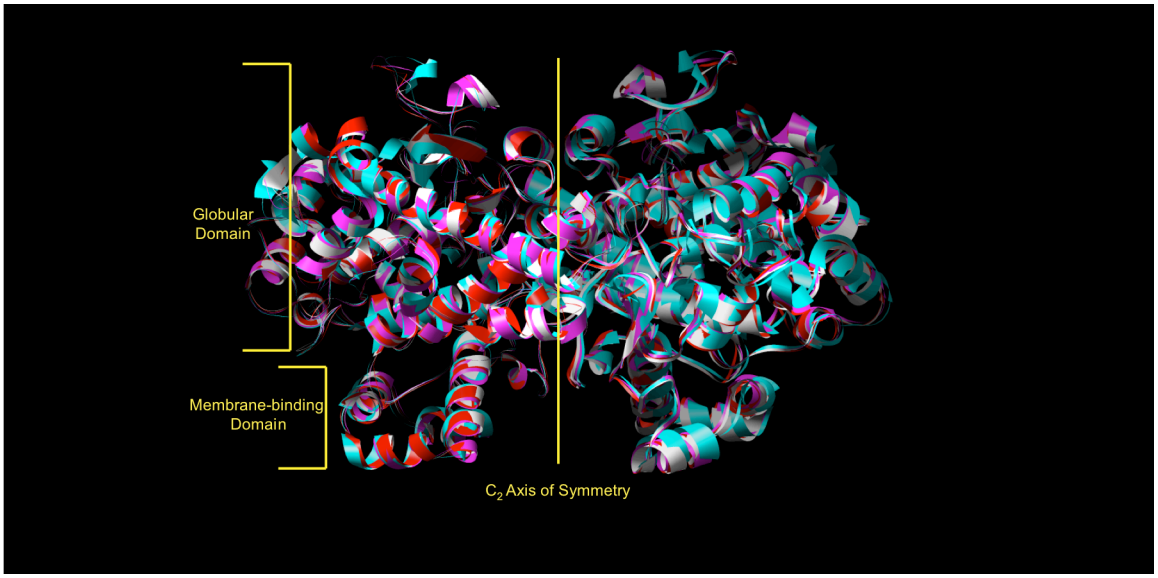

Figure 4. Overlay of backbone trace from COX-2 and COX-1 crystal structures; *6COX* (red), *4COX* (white), *1PTH* (blue), *1EQG* (magenta)

The global sequence identity between the human isoforms is 63.3% and the identity of the residues that make up the 25 A hydrophobic channel of the cyclooxygenase site is >85%. The crystal structures of both isofoms with a variety of

small molecules bound in the cyclooxygenase active site have been determined over the last twenty years and are virtually superimposable with an root mean squared deviation of only 0.9 A despite a variety of ligands and substrate analogues being bound. This minimal variation in structures has been taken to mean that there is no gross conformational change between the bound and unbound states of the enzyme, though admittedly crystallization conditions are far from a a fair *in vivo* simulation[64, 66-74].

For consideration of the work in this dissertation, the focus will be on the structural details of the cyclooxygenase site but not the peroxidase site. Considering substrates, the hydrophobic pocket for AA binding and turnover requires the fatty acid to adopt an upside-down bent L-shaped conformation beginning at Gly–533 which is located near the dimer interface and makes hydrophobic contact with the omega end of AA[64, 75]. The unique conformation of the fatty acid positions the 13 pro-*S* hydrogen at the catalytic tyrosine, Tyr-385, whose transformation to a tyrosyI radical by the priming of the peroxidase site allows the abstraction of the 13 pro-*S* hydrogen as the first step in the highly stereo specific cyclization to PGG_2. It is noteworthy that the substrate conformation and the importance of Tyr-385 was predicted by biochemical and mutagenesis studies prior to solving the crystal structure of the enzyme–substrate complex[9, 10, 66, 74-83].

To enter the cyclooxygenase active site, a small molecule must travel through a constriction site. The hydrogen-bonding network of the constriction site, which consists of the three residues Tyr-355, Glu-524, and Arg-120, is conserved within all isoforms of COX and interacts with the carboxylate of fatty acid substrates[66, 71]. This is the only interaction in the substrate-enzyme complex that is not exclusively of a van Der Waals

character. While conserved across both isoforms, the role of residue-120 is not the same for each COX. Mutagenesis of Arg-120 to the residue Gln, which maintains hydrogen-bonding possibility but not ionic bonding, in COX-1 dramatically raised the K_m of AA (1000-fold) but did not effect the K_m or V_{max} for AA metabolism by the same mutant in COX-2[80-85].

Further consideration was given to the role of constriction site residues in lipid metabolism when studies to describe the structural determinants for endocannabinoid metabolism by COX-2 were undertaken. Although 2-AG and AEA are structurally similar in that both are neutral derivatives of AA, determinants for binding and subsequent turnover are not the same. In this dissertation, the focus will be limited to the study of 2-AG. Mutation of Arg-120 to Gln in mCOX-2 background diminished the oxygenation rate of 2-AG by 9-fold. In stark contrast, the mutation of Tyr-355 to Phe did not affect the rate of endocannabinoid oxygenation. Mutation of Glu-524 to leucine also decreases 2-AG metabolism further indicating the hydrogen-bonding pair of Glu-524/Arg-120 plays a key role in this COX-2 activity[85, 86].

Another area, called the "side-pocket", was investigated to understand the isoform specificity of 2-AG metabolism. The side-pocket is the most divergent region of the cyclooxygenase active sites between COX-1 and COX-2. This side pocket is a hydrophobic region located near the carboxylate binding region which is made accessible in COX-2 but not in COX-1 due to a substitution at residue at 523 from Val (COX-2) to Ile (COX-1). Two other residues in this area are divergent between the two enzymes at position 434 and 513. Position 434, similarly to 523, is Val in COX-2 and Ile in COX-1.

Position 523 is Arg in all COX-2 enzymes but is His in h/oCOX-1 and glutamine in rodent COX-1 enzymes. By making mutations (single, double, and triple) that were COX-2 → COX-1 (human or ovine) in a mCOX-2 background, it was demonstrated that the rank order of impact of the side-pocket residues on 2-AG metabolism is 513 > 424 > 523. It is noteworthy that the 2-AG metabolism capacity measured after completely converting the side-pocket from COX-2 → COX-1 by the construction of a triple mutant was still higher than that achieved by wt oCOX-1.

Inhibition of Cyclooxygenases; Structure and Selectivity

The first description of cyclooxygenase inhibition was made when Sir John Vane demonstrated in 1970 that the blockade of PG production was the mechanism of action of the non-steroidal anti-inflammatory drugs (NSAID) aspirin and indomethacin. Aspirin, or acetyl salicylic acid (ASA), is a derivative of the natural product salicylate. Salicylate is found in high concentrations in willow bark that was first used as a remedy for rheumatic-type pains by the Egyptians around 200 B.C. So the discovery by Smith and Vane et. Al. settled a question that had baffled scientists for nearly 2000 years. Felix Hoffman first made the derivative ASA to make the drug more palatable and subsequently made it commercially available in 1899. Indomethacin (INDO), commercially known as Indocin, was first marketed by Merck 1963. It wasn't until 1971 that the mechanism of action of ASA and INDO was discovered by both Smith and Vane [87-89]. Using radiolabeled ASA and INDO, further studies showed that while ASA covalently modified COX, INDO did not[90]. The mechanism of COX inhibition by ASA was later confirmed by using a brominated derivative of aspirin to form a co-crystal

structure with COX-1 to show the Br-acetyl group covalently bonded to residue Ser-530 (Figure 5.)[69, 91, 92].

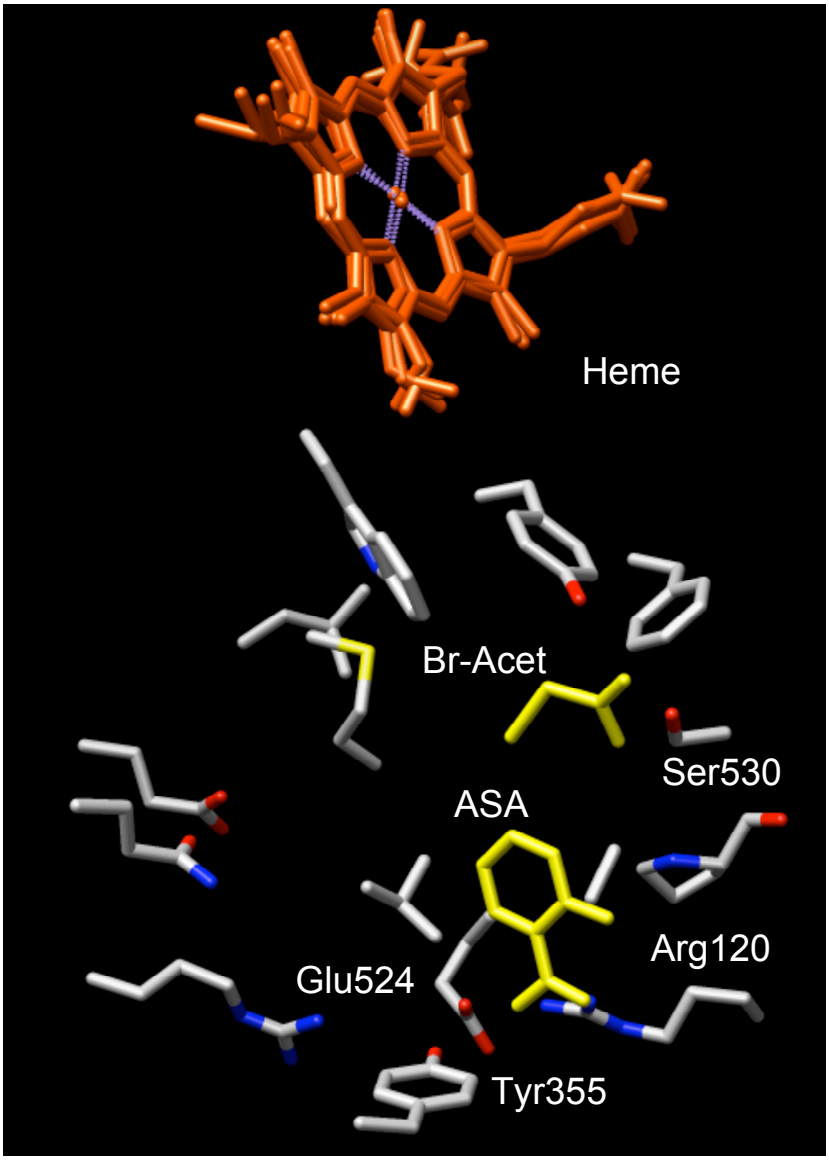

Figure 5. Br-ASA crystal structure with COX (*1PTH*). Key residues including the constriction site Residues Glu524, Tyr355, and Arg120 can be seen coordinated to the carboxylate of ASA (yellow). Ser530 has been acetylated by the Br-Acet group (yellow). The heme groups in the POX site from several overlayed structures (Figure 4) is shown as a reference.

Structural studies coupled with site-directed mutagenesis over the next 40 years revealed many of the structural determinants for ASA and INDO as well as other NSAIDs. It is important to remember that any studies with inhibitors prior to 1990's assumed only one isoform of COX. While the term NSAIDs literally means any compound that attenuates inflammation but is not a steroid, it has colloquially (and in this dissertation) come to mean a non-selective inhibitor of COX activity through competitive binding in the cyclooxygenase site. Nearly all NSAIDs contain a carboxylate group. Not surprisingly, the constriction site mutant R120E as well as crystal structures showed that nearly all of the NSAIDs orient their carboxylate group to form either a salt-bridge with Arg-120 similarly to the binding of the substrate AA to COX-1[85, 93].

One important exception is diclofenac as the R120E mutant did not attenuate its potency nearly as much as the other NSAIDs[85]. Additionally, the mutant S530A greatly diminished the potency of diclofenac but no other NSAID. It was therefore postulated that diclofenac binds in an "inverted" conformation with the carboxylate at the top of the cyclooxygenase channel making the stabilizing hydrogen bonds with Ser-530 and Tyr-385[74]. A crystal structure of diclofenac with COX-2 was subsequently solved and provided further support to this hypothesis (Figure 6.)[94].

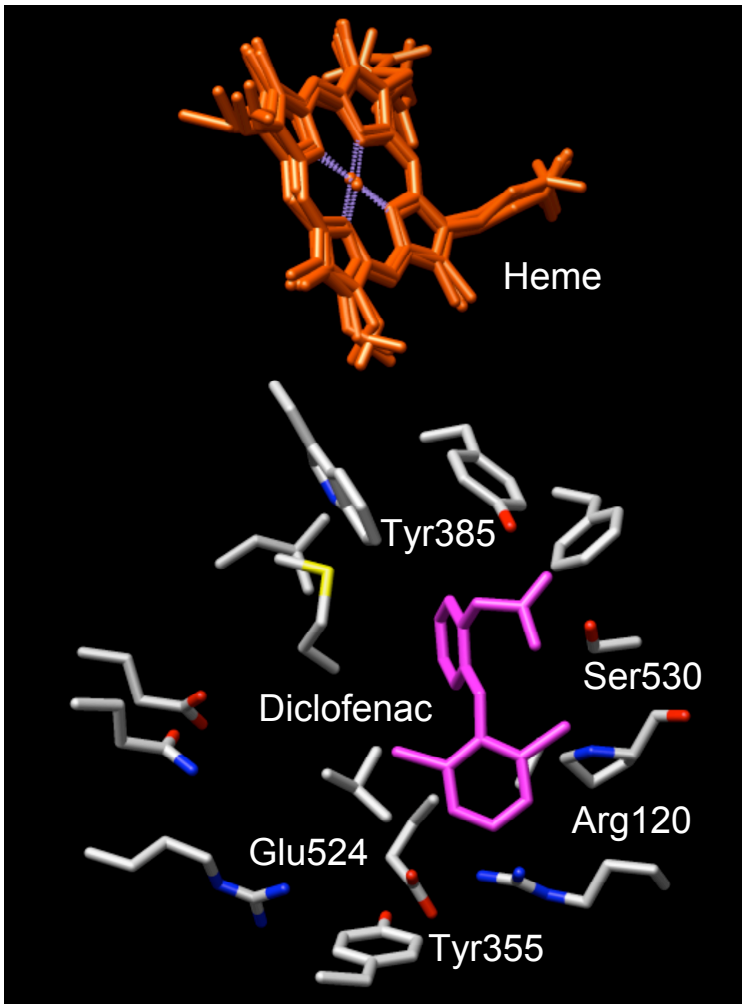

Figure 6. Diclofenac crystal structure with COX-2 (*1PXX*). Key residues including the constriction site residues Glu524, Tyr355, and Arg120 are notated. Ser530 and Tyr385 can be seen coordinated to the carboxylate of diclofenac (pink) in this inverted binding mode. The heme groups in the POX site from several overlayed structures (Figure 4) is shown as a reference.

The discovery of COX-2 as the COX isoform whose expression and activity is responsible for the pathophysiological processes of pyresis, inflammation, and pain catalyzed the urgent efforts of multiple pharmaceutical companies to discover COX-2

selective inhibitors. Despite the extremely high homology between COX isoforms, these efforts were successful with the discovery and development of the diarylheterocycle (DAH) class of inhibitors. DAH have a central heterocyclic ring with two aryl groups connected in a vicinal fashion. One aryl ring is substituted at the *para* position with either a sulfonamide of sulfone moiety. It was determined through mutagenesis studies that the structures of these inhibitors exploit the accessibility of the side-pocket in COX-2, but not in COX-1, to confer selectivity (Figure 7).

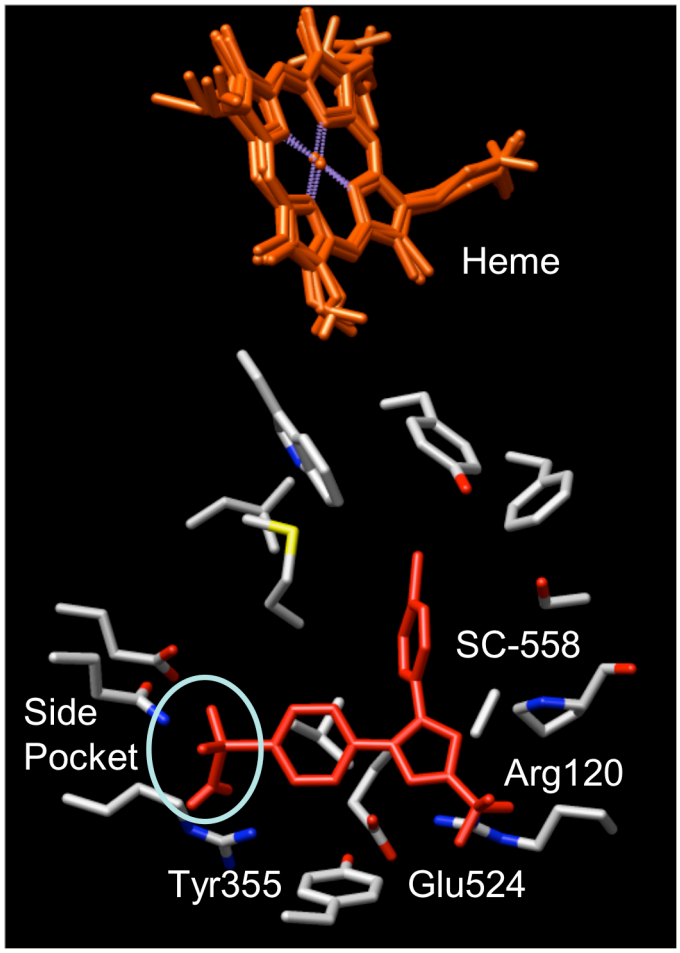

Figure 7. SC-558 (a DAH) crystal structure with COX-2 (*6COX*). Key residues including the constriction site residues Glu524, Tyr355, and Arg120 are notated. The portion of SC-558 that protrudes into the side pocket is noted. The heme groups in the POX site from several overlayed structures (Figure 4) is shown as a reference.

The potency of DAH is greatly diminished by the V523I mutation in mCOX-2 but enhanced by the I523V mutant of COX-1. The medicinal chemistry efforts in this direction were well-rewarded with the commercial launch of rofecoxib (Vioxx) by Merck and celecoxib (Celebrex) by GD Searle in 1999.

In addition to efforts to discover novel scaffolds for COX-2 selective inhibitors, both industrial and academic scientists attempted to confer selectivity through chemical modification of existing NSAID scaffolds. Mutagenesis studies had indicated that Arg-120 played a key role in binding the carboxylate of AA for both isoforms. However, a ionic interaction between Arg-120 and the substrate was required for binding to COX-1 whereas only a hydrogen-bonding interaction was required between this residue and a substrate for COX-1. Logic then follows that neutralization of the carboxylate of NSAIDs to a hydrogen-bonding competent ester or amide would be tolerated for a ligand of COX-2 but not COX-1.

Using INDO as one scaffold, this logic was borne out by finding selectivity could be nearly universally conferred by forming esters and amides of highly varied size and chemical characteristics (Figure 8).

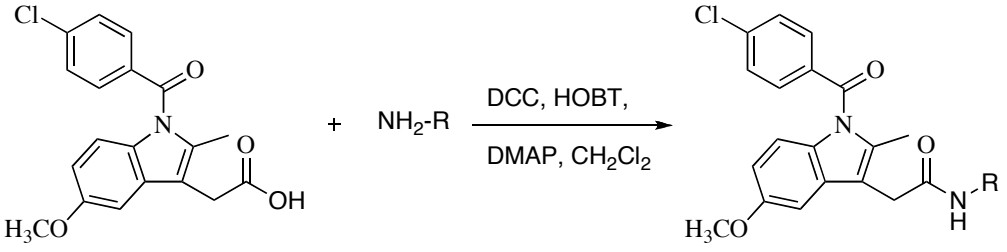

Indomethacin
Non-selective

Indomethacin Amide
Selective for COX-2

Figure 8. Transformation of the non-selective NSAID Indomethacin to a COX-2 selective inhibitor can be accomplished through facile chemistry such as amidation

From mutagenesis experiments it has been concluded that the INDO portion of INDO-esters and amides binds similarly to INDO itself as seen in the *4COX* crystal structure (Figure 9) with the carbonyl group secured by interactions with the constriction site residues. The amide or ester portions of the molecules are assumed to project through the constriction site into the lobby region, but no crystal structures have been solved with these inhibitors and mutagenesis data from the lobby region is minimal[95-98]. Two clear limitations on SAR emerged from these studies. First, hydrogen-bonding capability had to be conserved. As such, tertiary amides were not potent against any COX isoforms. Second, there is definite stereoselectivity bias in the SAR, with *R*-configured amides being COX-2 selective[99]. The molecular basis for this observation has been studied using both computational as well as crystallographic techniques but remains unresolved [100, 101].

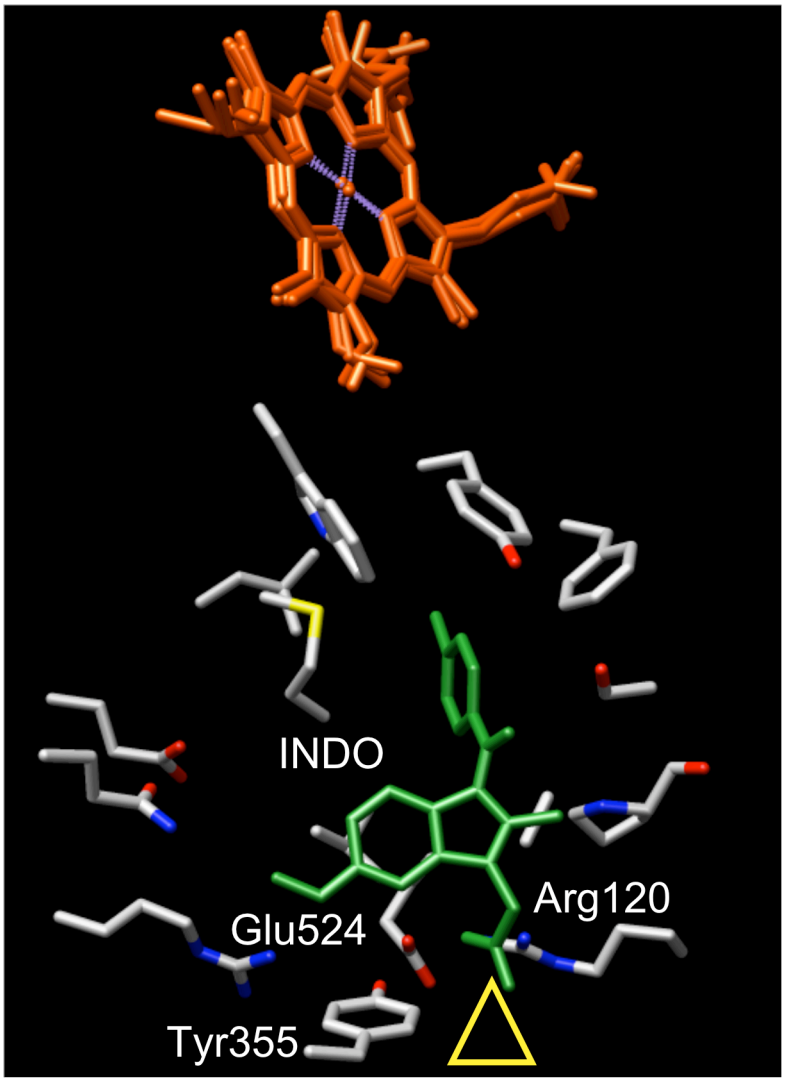

Figure 9. Indomethacin (INDO) crystal structure with COX-2 (*4COX*). Key residues including the constriction site residues Glu524, Tyr355, and Arg120 can be seen coordinating with the carboxylate of INDO (green). The yellow triangle denotes the open lobby region where esters or amides tethered to INDO are expected to project. The heme groups in the POX site from several overlayed structures (Figure 4) are shown as a reference.

Inhibition of Cyclooxygenases; Kinetic Mechanisms

Smith and Lands reported in 1971 that inhibition of COX by some NSAIDs had a time-dependent component[87]. By pre-incubating the enzyme preparation with certain inhibitors prior to the addition of substrates, their potency could be increased. This was the case with INDO and diclofenac, but not for ibuprofen. Interestingly, simple chemical modification, such as the addition of a methyl group, is able to modulate this property[93, 102].

With the discovery of COX-2, understanding the molecular basis of this phenomenon became even more complicated. Compounds considered as a drug candidate by a mechanism of COX inhibition now had to be tested against both isoforms for both time-dependent and time-independent inhibition. These efforts by both academic and industrial labs was greatly aided with the development and dissemination of key techniques in enzymology such as recombinant expression and purification from insect cells as well as mammalian cell transfection of these membrane-bound and glycosylated enzymes[14, 45, 77, 103-105]. Additionally, a wide-array of experimental techniques have been used to evaluate inhibition including the use of oxygen-uptake monitoring, radiolabeled substrate consumption, assessment of intrinsic enzyme fluorescence quenching, LC/MS/MS quantification of whole-cell treatments[21, 27, 30, 106-109]. Taking all this work into consideration, there are three general categories of kinetics of COX inhibition; fast reversible (ibuprofen), slow, tight-binding that are functionally irreversible (INDO and DAH), and covalent modifiers (ASA) (Figure 10.).

Fast reversible inhibitors bind competitively with the substrate AA in the cyclooxygenase site. Ibuprofen, a typical inhibitor of this class, has a relatively small

molecular weight and volume. The main molecular interaction assumed to enable ibuprofen binding is the interaction between the carboxylate of ibuprofen and Arg-120 of the enzyme constriction site. Inhibitors in this class, up to this point, all contain this signature carboxylate, are non-selective, and do not have a time-dependent component to their inhibtion. Additionally, testing ibuprofen (or other molecules like it) for COX inhibition using a high level of substrate would make ibuprofen seem like a poor drug candidate. As such, great care needs to be taken in designing assays for inhibition of COX [110-112].

Slow tight-binding inhibitors can be further divided into inhibitors that bind in two or three steps. Two step binders, such as INDO, characteristically bind in a first fast reversible step (E → EI) followed by a rate-limiting slow second step (EI → EI*) that leads to a functionally irreversible, but non-covalent, complex. Similarly to fast reversible inhibitors, INDO and the like bind competitively with AA in the cyclooxygenase active site. Unlike the previous category, slow tight-binders in two steps can be either selective or selective. INDO and diclofenac are non-selective members of this class. Work by Prusakiewicz et. al. showed through both mutagenesis and inhibitor modification that the second step of INDO binding is related to the insertion of the methyl on the indole ring into a hydrophobic pocket in the cyclooxygenase site[113]. The biophysical action that relates to the rate of the first step has yet to be described for INDO as no mutation has affected those rate constants. INDO-esters and amides are COX-2 selective, but also bind to COX-2 via a kinetic model similar to INDO itself [114].

Inhibitors that are slow, tight-binders in three steps are all COX-2 selective inhibitors that have a time-dependent component to their inhibition. Inhibitors in this

class are often referred to commonly as “COXIBs”, though this term is only loosely defined. DAHs, including rofecoxib and celecoxib, were shown to utilize the side pocket available in the COX-2 active site but not in COX-1 by insertion of the sulfone or sulfonamide by the publication of COX-2 co-crystallized with the DAH SC-558[78, 111, 115-117]. The third step of inhibition of COX-2 was discovered by Lanzo et. al. using fluorescence techniques[118, 119]. Additionally, these studies showed that the DAH do bind to COX-1, but significant reverse rate constants explain the lack of potency against this isoform. Opening access to the side pocket through a Ile523Val mutation in COX-1 confers potency of the DAH [120]. Conversely, closing access to the side pocket through at Val523Ile mutation in COX-2 diminishes DAH potency [120-122].

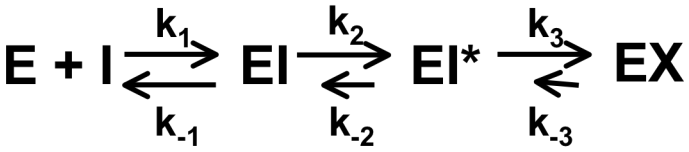

Figure 10. Kinetic equilibria for different classes of COX inhibitors; fast reversible (to EI complex): slow tight binding in two steps (to EI*); and slow tight binding in three steps (to EX)

Biology and Inhibition of Thromoxane A_2

Piper and Vane reported in 1969 the characterization of a novel aortic contractile substance produced by antigen challenged guinea pig lung that had been pre–treated with antigen to cause anaphalaxis[123]. This substance was named rabbit aorta-contracting substance (RCS) for its observed pharmacological effects. RCS was shown to be very unstable ($t_{1/2} < 2$ min) and its production was shown to be blocked by treatment with NSAIDs, such as aspirin and INDO, similarly to other prostaglandins [124-126]. This

observation among other experimental work led to the identification of RCS, later known as thromboxane A_2 (TXA_2), is produced from a precursor, PGH_2, in common with the other prostaglandins. It was subsequently demonstrated that TXA_2 had an even shorter half-life than originally estimated ($t_{1/2}$ = 30 s) and could be produced by coupling platelet preparations with PGH_2 produced by adding arachidonic acid to seminal vesicles[52, 127, 128].

The structure of TXA_2 was definitively elucidated by Samuelsson and colleagues in 1975 by using $^{18}O_2$ to label and methanol, ethanol and sodium azide to trap the unstable compound. These trapping experiments clearly demonstrated that TXA_2 is an endoperoxide derivative of arachidonic acid that contained the characteristically unstable acetal functionality. Additionally, these experiments investigated the mechanism by which thromboxane B_2 (TXB_2) is formed from TXA_2. TXB_2 is the biologically inactive stable non-enzymatic hydrolysis product of TXA_2 that is commonly used as a surrogate marker for TXA_2 quantification (TXAS Scheme)[35].

It was discovered in 1976 by Samuelssson and Vane et. al. that this unstable product was produced from PGH_2 by an enzyme found and later isolated from platelet microsomes named thromboxane synthase (TXAS)[129-131]. TXAS is a member of the cytochrome P450 family as the lone member of family 5A1[132]. TXAS catalyzes the isomerization of PGH_2 to TXA_2 without the need of a reductase. It can, in equimolar amounts, produce the scission products from the substrate PGH_2 to 12-L-hydroxy-5,8,10-heptadecatrienoic acid (HHT) and malondialdehyde (MDA) }(Figure 11.)[20, 133, 134]. Correspondingly, PGH_1 is converted to HHD and MDA with no TXA_1 produced[135]. While HHT has been shown to have neither specific bioactivity nor detriment in the vascular system, MDA can, in fact, be mutagenic. The biological significance of this

TXAS activity remains unclear. TXAS is expressed at highest levels in platelets and at measurable levels in the lung, bone marrow, and umbilical endothelial cells[136]. The lack of ability to monitor ligand binding to TXAS by spectroscopic analysis standard to other P450s (i.e. CO reduction) makes ligand studies difficult[137].

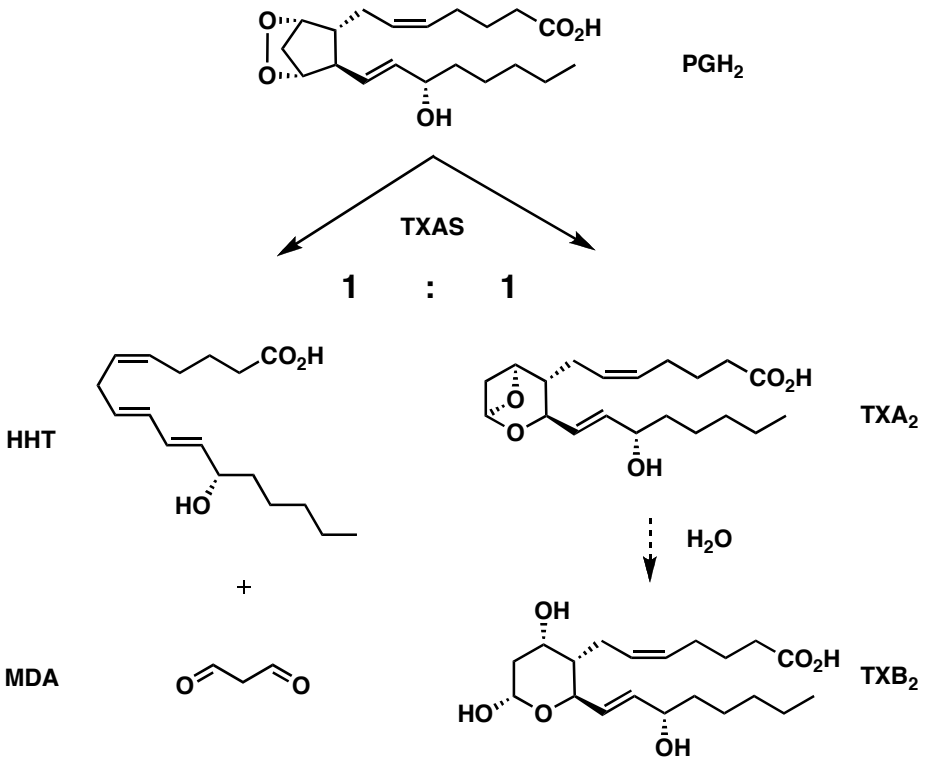

Figure 11. Metabolism of PGH_2 by thromboxane synthase (TXAS). Three products are formed enzymaticallyl HHT, malondialdehyde (MDA) and TXA_2. The dotted arrow denotes non-enzymatic degradation to the biologically inactive TXB_2.

TXA_2 has two receptors that are GPCRs, TPα and TPβ, through which it exerts modulation of vasoconstriction and activation of platelets[138-142]. An opposing system for vascular control exists within the AA cascade. Prostacyclin, or PGI_2, is another unstable prostaglandin that is also produced by a P450 (PGIS, CYP8A family) that is most highly expressed endothelial cells. Regulation of the TXA_2–PGI_2 balance are

found in the interaction of platelets and the vessel wall where TXA_2 released from stimulated platelets causes PGI_2 formation in the endothelium that inhibits platelet activity. In general, TXA_2 represents the activating principle and PGI_2 the corresponding antagonist causing the conversion back to the resting non-activated state[20, 53, 143, 144].

The initial inhibitor for TXAS described was imidazole that although potent for TXAS, was indiscriminate for inhibition of other P450 enzymes[145]. Inhibition of TXAS was the target of the efforts of several academic labs and pharmaceutical companies in the 1970's and 1980's. Assuming inhibition of TXAS activity wouId attenuate vasoconstriction and platelet aggregation, cardiovascular disease was the main target of these efforts. Structure-activity relationships for a TXAS inhibitors emerged from these efforts that were based, in part, by considering the structural requirements for binding substrate and in part from evaluating newly synthesized small molecules. The main SAR garnered from analyzing substrate was the requirement of a free carboxylate. The requirement for a specific nitrogen heterocycle, either a 3-pyridyl or l-imidazolyl, a certain distance from the carboxylate (6.8-8.0 A) was the SAR that has, until recently, been assumed to be required[146]. Programs in medicinal chemistry were very successful at producing extremely potent inhibitors such as ozagrel (IC_{50} = 10 nM) and furegrelate (IC_{50} = 500 nM) (Figure 12.)[147, 148]. Unfortunately, these compounds were not as successful *in vivo* as *in vitro*. The failure of these compounds is assumed to be due to the ability of the TXAS substrate, PGH_2, to activate the thromboxane receptors, albeit at concentrations ten-times higher than TXA_2[149]. As such, blocking the production of TXA_2 while simultaneously increasing the level of another agonist for the same receptor is a biological wash.

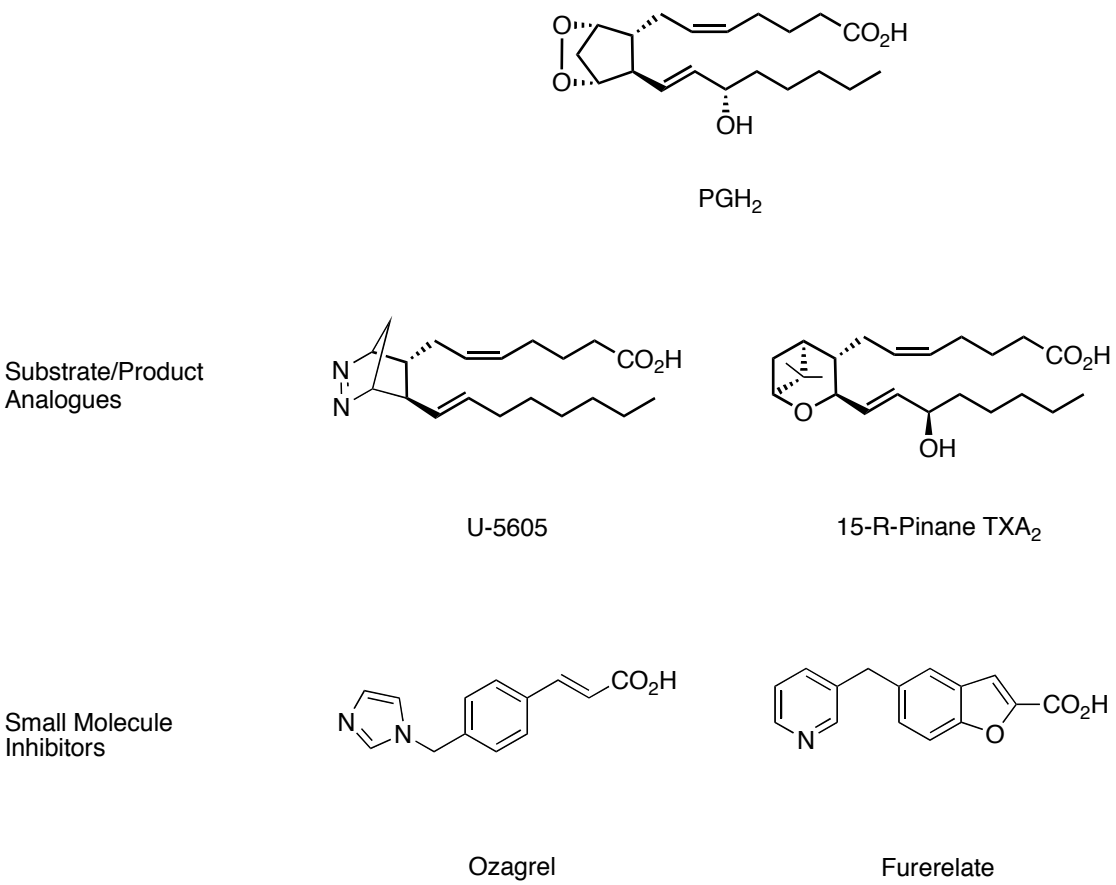

Figure 12. Inhibitors of thromboxane synthase (TXAS) that either directly resemble the substrate or product or small molecule inhibitors with key chemical features maintained.

The interest in TXAS/TP as a therapeutic target reemerged due to developments in the area of COX-2 inhibition. Results published by McAdam et. al. in 1999 showed that administration of the COX-2-selective inhibitor celecoxib diminished the level excreted by patients of 6-keto-$F_{1\alpha}$ and 2,3-dinor-6-keto-$PGF_{1\alpha}$, the stable metabolites used as a surrogate to measure level of *in vivo* prostacyclin. The levels of the

TXA_2 metabolite, TXB_2, were unaffected by celecoxib administration. This is not surprising considering that the vast majority of TXA_2 is produced from platelets which only express COX-1[150, 151]. While an interesting result, it is important to recall that both prostacyclin and thromboxane are released and controlled physiologically in a very immediate way via their short half-lives. A chronic decrease in the anti-thrombotic prostacyclin without a corresponding decrease in the pro-thrombotic TXA_2 could lead to hemostatic dysregulation. Subsequent clinical trials, including the halting of the APC clinical trial that was considering Vioxx as a treatment for familial adematomous polyposis, led to the withdrawal of Vioxx from the market in 2004 due to an increased risk of cardiovascular events. The mechanism by which these compounds cause these side effects remains unclear, but the likelihood that thromboxanes play a role remains a viable possibility.

Discovery of Chagas Disease and Challenges of Therapy Development

Neglected tropical diseases are defined by the World Health Organization (WHO) as largely ancient infectious diseases that thrive in impoverished settings, especially in the heat and humidity of tropical climates. Diseases classified as neglected tropical diseases include malaria, African sleeping sickness, Schistosomiasis, Guinea worm disease, and Chagas disease. Most, though not all, are parasitic and are grouped together not because of similar pathologies, but rather for the shared conditions and populations under which they occur [http://www.who.int/neglected_diseases/en/]. These conditions place additional burdens on the design, distribution, and application of therapeutics. First, the therapeutic agent for a neglected tropical disease needs to be made in minimal

chemical steps from readily available starting materials so that the overall cost can remain low. Second, the agent should be stable under the harsh conditions of long-term sun exposure, high heat, and humidity so that it can be distributed with minimal burden for storage and transport. Lastly, the therapeutic should not have high demands on health care professionals or infrastructure that is often highly lacking in areas where neglected tropical diseases are endemic. The optimal situation would be a theasrapeutic administered orally with minimal frequency and for a limited time[152].

Chagas disease is a neglected tropical disease that infects 16 to 18 million people predominantly within 21 countries in Latin America[153, 154]. Carlos Chagas first described the infection by a novel protozoan, which he named *Trypanosoma cruzi* after his mentor Oswaldo Cruz, in Lassance, Brazil when he was sent to confront a malaria outbreak among railroad workers there in 1909. Chagas went on to correctly describe a new parasitic infectious disease called either Chagas disease or *American Trypanosomiasis*: its pathogen (*Trypanosoma cruzi*), vector (*Triatomine*), hosts (humans and selected animals), clinical manifestations (Chagasic cardiomyopathy), and epidemiology solely and completely and was the only researcher thus far to do so[155-157].

The parasite *Trypanosoma cruzi* is a kinetoplastid that has three forms within its life cycle. The epimastigote is found exclusively in the invertebrate vector, multiplies in the midgut, and is characterized by the emergence of the flagellum from the kinetoplast anterior to the nucleus. The epimastigote differentiates into the metacyclic trypomastigote that is characterized by the flagellum/kinetoplast being located posterior to the nucleus and is the form contained in insect feces that transfers the parasite to the vertebrate host when the insect defecates after a blood meal. After the motile

trypomastigote enters cells in the vertebrate host, it differentiates into the amastigote form of the parasite. Amastigotes are rounded with a very stubby flagellum that is sometimes unobservable and are the dividing form of the parasite. Once the cells fill with amastigotes, the parasite redifferentiates into trypamastigotes through a poorly understood mechanism and the cell bursts to release trypomastigotes into the bloodstream where it can be transmitted again to the vector, completing the life-cycle (Figure 13, http://www.dpd.cdc.gov/dpdx/HTML/TrypanosomiasisAmerican.htm)[158-160].

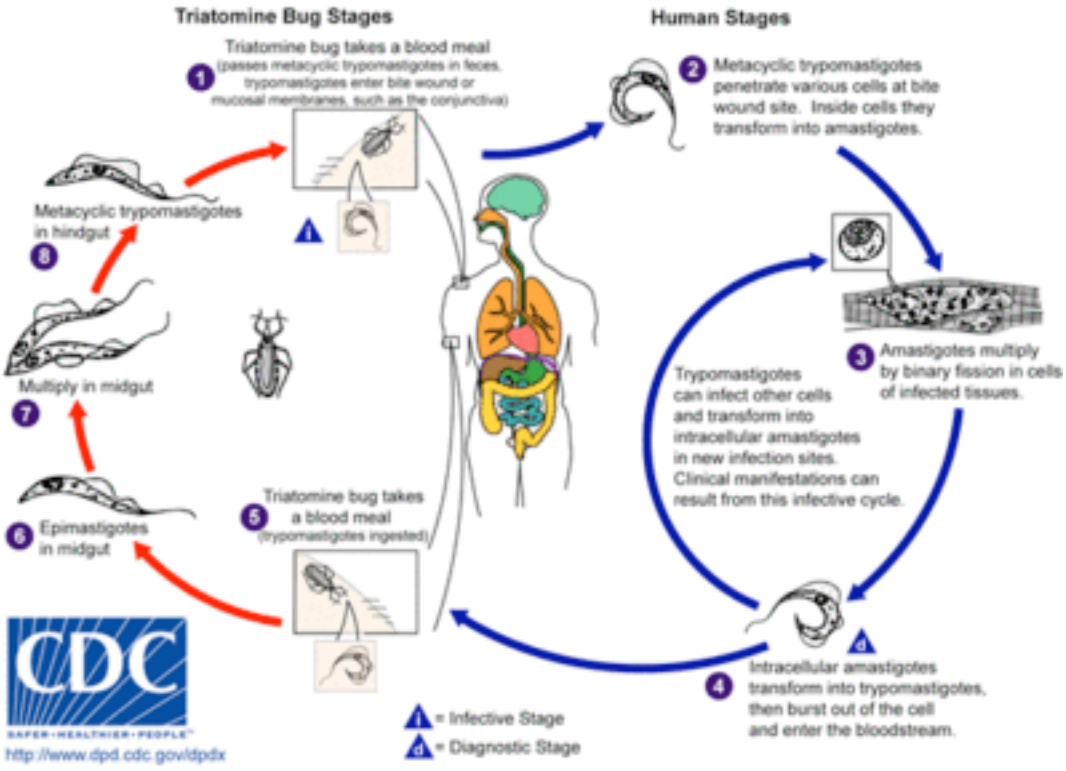

Figure 13. Life cycle of *Trypanosoma cruzi* (figure courtesy of the Center for Disease Control, http://www.dpd.cdc.gov/dpdx/HTML/TrypanosomiasisAmerican.htm)

The vector *Triatominae*, also known colloquially as the "kissing bug" or "assassin bug", is a haematophagous insect that was first described by Charles Darwin in *The*

Voyage of the Beagle after his encounter with the bug in Argentina in 1835. All of the 138 species of triatomines are capable of transmitting Chagas disease, but the subset called "domestic triatomines" (including *Triatoma infestans*, *Rhodnius prolixus*, *Triatoma dimidiata*, *Triatoma brasiliensis*, *Panstrongylus megistus*) are the most epidemiologically relevant when considering human-to-human transmission of Chagas disease. The domestic triatomines reside in mud and thatching building materials commonly used in rural housing in South America. The insects emerge, especially at night, to bite sleeping vertebrates to have a blood meal. The volume of these insects can increase 10-fold from pre-meal to post-meal and their mobility is markedly limited in this voluminous state. Identification of infestation in a home is readily accomplished by visualizing their eggs (white to pale pink in color), their feces (either white or black strikes on walls), or the insect themselves[158, 160-162].

The hosts of *Trypanasoma cruzi* parasites are vertebrates includes humans, dogs, cats, armadillos, opossums, mice, rats, rabbits, hamsters, and guinea pigs. Amphibians and birds are refactory to infection by *T. cruzi* but no experiments have been able to elucidate the mechanism by which the parasites are lysed in the bloodstream of these animals immediately following their injection[158]. After introduction of the parasite into humans, Chagas disease can progress in three stages; acture, indeterminate, and chronic. Initial transmission can be recognized by a skin lesion at the site of infection, particularly around the eye (Romana's sign). This is followed by a flu-like illness and the highest load of observed parasitemia. In up to 10% of cases, almost exclusively in children, the acute stage is fatal by either myocarditis or meningoencephalitis. However, in a recent study 99.3% of the surveyed patients in the chronic stage of the disease did not remember the

original infection. An indeterminate stage, which can last up to a decade, follows and is characterized by lack of symptoms and decreased parasite load but observable IgG antibodies to the parasite[158, 160, 163-165].

Approximately one-third of patients with indeterminate stage will go on to develop chronic Chagas disease that manifests itself in the cardiac system and/or gastrointestinal system. The main life-threatening conditions resulting from Chagasic heart disease are heart failure, arrhythmias, and thromboembolism. Electrocardiogram abnormalities become more frequent after twenty-years from the time of the infection and include ventricular premature contractions, right bundle branch block, and intraventricular conduction disturbance. Eventual cardiomyopathy, occurring in an estimated 57% of chronic patients, is an ominous sign as prognosis for survival after its onset is less than five years. Chagas mega syndromes are inflammatory on smooth muscle fibers of the walls of the hollow viscera in the digestive system. It is found most commonly in the esophagus and the colon. Autoimmunity against both heart and digestive organs has been a suggested mechanism to explain the progression of this disease, but this is still a highly controversial view[154, 158, 164, 166].

The first experimental treatments of Chagas disease with chemotherapy began soon after its discovery in 1909. The earliest, and fully unsuccessful, treatments tried consisted of mostly organometallic agents including the metals arsenic, antimony, and mercury. CL Brener, in 1961, catalogued all chemicals that had been used up to that point to treat Chagas disease and none were without heavy metals. Two drugs that were developed empirically and have been in use for treatment of Chagas disease since the late 1960's are nifurtimox and benznidazole. Despite the rapid discovery of the cause and

pathology of Chagas disease by Carlos Chagas, the development of treatments has been at a near standstill since the early 1970's[167]. While both nifurtimox and benznidazole are effective (up to 80%) in the acute stage of the disease, they are nearly completely ineffective in the chronic stage of the disease [167, 168]. These drugs can have dose-limiting side effects and resistance in certain strains has been documented [169]. Developing strategies to overcome this resistance in nearly impossible considering that not only is the biological method of resistance unknown, but also the mechanism of action for either of these drugs. This is shocking considering they have been used in clinics for nearly 50 years. There has been a recent report that nitroreductase is a possible target for both nifurtimox and benznidazole as both compounds contain nitro groups[170].There have been recent pre-clinical developments that have been encouraging. The most promising target is C14 sterol-α demethylase against which triazole compounds have shown favorable results *in vitro* [171-173]. Additional targets in the pre-clinical stage include the parasite specific cruzipain, N-alkyl-bisphosphonates against farnesyl pyrophosphate synthase, and inhibition of trypanothione synthesis and metabolism [171, 174-177].

Despite the wealth of both structural and functional knowledge from mutagenesis studies, crystallographic studies, and inhibitor development there are many still many questions surrounding COX isoforms. The physiological role of each COX isoform is still not fully understood. A small molecule developed as a drug whose molecular target is COX, INDO, has proved to be a useful molecular scaffold for the development of inhibitors for other enzymes.

References

1. Bergstrom, S.; Samuelsson, B., Isolation of prostaglandin E1 from human seminal plasma. Prostaglandins and related factors. 11. *J Biol Chem* **1962,** 237, 3005-6.
2. Hamberg, M.; Samuelsson, B., Oxygenation of unsaturated fatty acids by the vesicular gland of sheep. *J Biol Chem* **1967,** 242, (22), 5344-54.
3. Hemler, M. E.; Lands, W. E., Evidence for a peroxide-initiated free radical mechanism of prostaglandin biosynthesis. *J Biol Chem* **1980,** 255, (13), 6253-61.
4. Schreiber, J.; Mason, R. P.; Eling, T. E., Carbon-centered free radical intermediates in the hematin- and ram seminal vesicle-catalyzed decomposition of fatty acid hydroperoxides. *Arch Biochem Biophys* **1986,** 251, (1), 17-24.
5. O'Brien, P. J.; Rahimtula, A., The possible involvement of a peroxidase in prostaglandin biosynthesis. *Biochem Biophys Res Commun* **1976,** 70, (3), 832-8.
6. Hemler, M. E.; Cook, H. W.; Lands, W. E., Prostaglandin biosynthesis can be triggered by lipid peroxides. *Arch Biochem Biophys* **1979,** 193, (2), 340-5.
7. Porter, N. A.; Funk, M. O., Letter: Peroxy radical cyclization as a model for prostaglandin biosynthesis. *J Org Chem* **1975,** 40, (24), 3614-5.
8. Gardner, H. W., Oxygen radical chemistry of polyunsaturated fatty acids. *Free Radic Biol Med* **1989,** 7, (1), 65-86.
9. Dietz, R.; Nastainczyk, W.; Ruf, H. H., Higher oxidation states of prostaglandin H synthase. Rapid electronic spectroscopy detected two spectral intermediates during the peroxidase reaction with prostaglandin G2. *Eur J Biochem* **1988,** 171, (1-2), 321-8.
10. Karthein, R.; Dietz, R.; Nastainczyk, W.; Ruf, H. H., Higher oxidation states of prostaglandin H synthase. EPR study of a transient tyrosyl radical in the enzyme during the peroxidase reaction. *Eur J Biochem* **1988,** 171, (1-2), 313-20.
11. Ohki, S.; Ogino, N.; Yamamoto, S.; Hayaishi, O., Prostaglandin hydroperoxidase, an integral part of prostaglandin endoperoxide synthetase from bovine vesicular gland microsomes. *J Biol Chem* **1979,** 254, (3), 829-36.
12. Samuelsson, B., *Journal of the American Chemical Society* **1965,** 87, 3011.
13. Smith, W. L.; Lands, W. E., Oxygenation of polyunsaturated fatty acids during prostaglandin biosynthesis by sheep vesicular gland. *Biochemistry* **1972,** 11, (17), 3276-85.
14. Miyamoto, T.; Ogino, N.; Yamamoto, S.; Hayaishi, O., Purification of prostaglandin endoperoxide synthetase from bovine vesicular gland microsomes. *J Biol Chem* **1976,** 251, (9), 2629-36.
15. Ogino, N.; Ohki, S.; Yamamoto, S.; Hayaishi, O., Prostaglandin endoperoxide synthetase from bovine vesicular gland microsomes. Inactivation and activation by heme and other metalloporphyrins. *J Biol Chem* **1978,** 253, (14), 5061-8.
16. Chen, W.; Pawelek, T. R.; Kulmacz, R. J., Hydroperoxide dependence and cooperative cyclooxygenase kinetics in prostaglandin H synthase-1 and -2. *J Biol Chem* **1999,** 274, (29), 20301-6.
17. von, E. U., Ueber die spezifische blutducksenkende Substanz des menschlichen Prostata-und Samenblasensekretes. *Klin. Wschr.* **1935,** 14, 1182-1183.

18. von, E. U., On the specific vaso-dilating substances from accessory genital glands in man and certain animals (prostaglandin and vesiglandin). *Journal of Physiology Lodon* **1936,** 88, 213-234.
19. Nugteren, D. H.; Van Dorp, D. A.; Bergstrom, S.; Hamberg, M.; Samuelsson, B., Absolute configuration of the prostaglandins. *Nature* **1966,** 212, (5057), 38-9.
20. Hamberg, M.; Samuelsson, B., Prostaglandin endoperoxides. Novel transformations of arachidonic acid in human platelets. *Proc Natl Acad Sci U S A* **1974,** 71, (9), 3400-4.
21. Hamberg, M.; Samuelsson, B., Detection and isolation of an endoperoxide intermediate in prostaglandin biosynthesis. *Proc Natl Acad Sci U S A* **1973,** 70, (3), 899-903.
22. Wlodawer, P.; Samuelsson, B., On the organization and mechanism of prostaglandin synthetase. *J Biol Chem* **1973,** 248, (16), 5673-8.
23. Nugteren, D. H.; van Dorp, D. A., The participation of molecular oxygen in the biosynthesis of prostaglandins. *Biochim Biophys Acta* **1965,** 98, (3), 654-6.
24. Anggard, E.; Samuelsson, B., Smooth Muscle Stimulating Lipids in Sheep Iris. the Identification of Prostaglandin F 2a. Prostaglandins and Related Factors 21. *Biochem Pharmacol* **1964,** 13, 281-3.
25. Bergstroem, S.; Danielsson, H.; Klenberg, D.; Samuelsson, B., The Enzymatic Conversion of Essential Fatty Acids into Prostaglandins. *J Biol Chem* **1964,** 239, PC4006-8.
26. Bergstroem, S.; Danielsson, H.; Samuelsson, B., The Enzymatic Formation of Prostaglandin E2 from Arachidonic Acid Prostaglandins and Related Factors 32. *Biochim Biophys Acta* **1964,** 90, 207-10.
27. Bygdeman, M.; Samuelsson, B., Quantitative Determination of Prostaglandins in Human Semen. *Clin Chim Acta* **1964,** 10, 566-8.
28. Samuelsson, B., Identification of Prostaglandin F3-Alpha in Bovine Lung: Prostaglandins and Related Factors 26. *Biochim Biophys Acta* **1964,** 84, 707-13.
29. Samuelsson, B., Prostaglandins and Related Factors. 28. Metabolism of Prostaglandin E1 in Guinea Pig Lung: the Structures of Two Metabolites. *J Biol Chem* **1964,** 239, 4097-102.
30. Samuelsson, B., Prostaglandins and Related Factors. 27. Synthesis of Tritium-Labeled Prostaglandin E1 and Studies on Its Distribution and Excretion in the Rat. *J Biol Chem* **1964,** 239, 4091-6.
31. Samuelsson, B., Identification of a Smooth Muscle-Stimulating Factor in Bovine Brain. Prostaglandins and Related Factors 25. *Biochim Biophys Acta* **1964,** 84, 218-9.
32. Bergstrom, S., Prostaglandins--a group of hormonal compounds of widespread occurrence. *Biochem Pharmacol* **1963,** 12, 413-4.
33. Bergstrom, S.; Carlson, L. A.; Weeks, J. R., The prostaglandins: a family of biologically active lipids. *Pharmacol Rev* **1968,** 20, (1), 1-48.
34. Bergstrom, S., Prostaglandins: members of a new hormonal system. These physiologically very potent compounds of ubiquitous occurrence are formed from essential fatty acids. *Science* **1967,** 157, (787), 382-91.
35. Malmsten, C.; Hamberg, M.; Svensson, J.; Samuelsson, B., Physiological role of an endoperoxide in human platelets: hemostatic defect due to platelet cyclo-oxygenase deficiency. *Proc Natl Acad Sci U S A* **1975,** 72, (4), 1446-50.

36. Samuelsson, B.; Granstrom, E.; Green, K.; Hamberg, M.; Hammarstrom, S., Prostaglandins. *Annu Rev Biochem* **1975,** 44, 669-95.
37. Bergstrom, S., The prostaglandins. *Recent Prog Horm Res* **1966,** 22, 153-75.
38. Bergstrom, S.; Carlson, L. A.; Oro, L., Effect of different doses of prostaglandin E on free fatty acids of plasma, blood glucose and heart rate in the nonanesthetized dog. Prostaglandin and related factors 53. *Acta Physiol Scand* **1966,** 67, (2), 185-93.
39. Bergstrom, S.; Carlson, L. A.; Oro, L., Effect of prostaglandin E on plasma free fatty acids and blood glucose in the dog. Prostaglandin and related factors 51. *Acta Physiol Scand* **1966,** 67, (2), 141-51.
40. Bergstrom, S.; Duner, H.; von, E. U.; Pernow, B.; Sjovall, J., Observations on the effects of infusion of prostaglandin E in man. *Acta Physiol Scand* **1959,** 45, 145-51.
41. Bergstrom, S.; Eliasson, R.; von, E. U.; Sjovall, J., Some biological effects of two crystalline prostaglandin factors. *Acta Physiol Scand* **1959,** 45, 133-44.
42. Hla, T.; Neilson, K., Human cyclooxygenase-2 cDNA. *Proc Natl Acad Sci U S A* **1992,** 89, (16), 7384-8.
43. Fu, J. Y.; Masferrer, J. L.; Seibert, K.; Raz, A.; Needleman, P., The induction and suppression of prostaglandin H2 synthase (cyclooxygenase) in human monocytes. *J Biol Chem* **1990,** 265, (28), 16737-40.
44. Kujubu, D. A.; Fletcher, B. S.; Varnum, B. C.; Lim, R. W.; Herschman, H. R., TIS10, a phorbol ester tumor promoter-inducible mRNA from Swiss 3T3 cells, encodes a novel prostaglandin synthase/cyclooxygenase homologue. *J Biol Chem* **1991,** 266, (20), 12866-72.
45. O'Banion, M. K.; Sadowski, H. B.; Winn, V.; Young, D. A., A serum- and glucocorticoid-regulated 4-kilobase mRNA encodes a cyclooxygenase-related protein. *J Biol Chem* **1991,** 266, (34), 23261-7.
46. Raz, A.; Wyche, A.; Fu, J.; Seibert, K.; Needleman, P., Regulation of prostanoids synthesis in human fibroblasts and human blood monocytes by interleukin-1, endotoxin, and glucocorticoids. *Adv Prostaglandin Thromboxane Leukot Res* **1990,** 20, 22-7.
47. Xie, W. L.; Chipman, J. G.; Robertson, D. L.; Erikson, R. L.; Simmons, D. L., Expression of a mitogen-responsive gene encoding prostaglandin synthase is regulated by mRNA splicing. *Proc Natl Acad Sci U S A* **1991,** 88, (7), 2692-6.
48. Smith, W. L.; DeWitt, D. L.; Garavito, R. M., Cyclooxygenases: structural, cellular, and molecular biology. *Annu Rev Biochem* **2000,** 69, 145-82.
49. Laneuville, O.; Breuer, D. K.; Xu, N.; Huang, Z. H.; Gage, D. A.; Watson, J. T.; Lagarde, M.; DeWitt, D. L.; Smith, W. L., Fatty acid substrate specificities of human prostaglandin-endoperoxide H synthase-1 and -2. Formation of 12-hydroxy-(9Z, 13E/Z, 15Z)- octadecatrienoic acids from alpha-linolenic acid. *J Biol Chem* **1995,** 270, (33), 19330-6.
50. Klenberg, D.; Samuelsson, B., The Biosynthesis of Prostaglandin E1 Studied with Specifically 3h-Labelled 8,11,14-Eicosatrienoic Acids. *Acta Chem Scand* **1965,** 19, 534-5.
51. Hemler, M. E.; Crawford, C. G.; Lands, W. E., Lipoxygenation activity of purified prostaglandin-forming cyclooxygenase. *Biochemistry* **1978,** 17, (9), 1772-9.
52. Needleman, P.; Minkes, M.; Raz, A., Thromboxanes: selective biosynthesis and distinct biological properties. *Science* **1976,** 193, (4248), 163-5.

53. Needleman, P.; Raz, A.; Minkes, M. S.; Ferrendelli, J. A.; Sprecher, H., Triene prostaglandins: prostacyclin and thromboxane biosynthesis and unique biological properties. *Proc Natl Acad Sci U S A* **1979,** 76, (2), 944-8.
54. Gerard, C. M.; Mollereau, C.; Vassart, G.; Parmentier, M., Molecular cloning of a human cannabinoid receptor which is also expressed in testis. *Biochem J* **1991,** 279 (Pt 1), 129-34.
55. Matsuda, L. A.; Lolait, S. J.; Brownstein, M. J.; Young, A. C.; Bonner, T. I., Structure of a cannabinoid receptor and functional expression of the cloned cDNA. *Nature* **1990,** 346, (6284), 561-4.
56. Stella, N.; Schweitzer, P.; Piomelli, D., A second endogenous cannabinoid that modulates long-term potentiation. *Nature* **1997,** 388, (6644), 773-8.
57. Burstein, S. H.; Audette, C. A.; Breuer, A.; Devane, W. A.; Colodner, S.; Doyle, S. A.; Mechoulam, R., Synthetic nonpsychotropic cannabinoids with potent antiinflammatory, analgesic, and leukocyte antiadhesion activities. *J Med Chem* **1992,** 35, (17), 3135-41.
58. Devane, W. A.; Hanus, L.; Breuer, A.; Pertwee, R. G.; Stevenson, L. A.; Griffin, G.; Gibson, D.; Mandelbaum, A.; Etinger, A.; Mechoulam, R., Isolation and structure of a brain constituent that binds to the cannabinoid receptor. *Science* **1992,** 258, (5090), 1946-9.
59. Nirodi, C. S.; Crews, B. C.; Kozak, K. R.; Morrow, J. D.; Marnett, L. J., The glyceryl ester of prostaglandin E2 mobilizes calcium and activates signal transduction in RAW264.7 cells. *Proc Natl Acad Sci U S A* **2004,** 101, (7), 1840-5.
60. Smith, W. L.; Langenbach, R., Why there are two cyclooxygenase isozymes. *J Clin Invest* **2001,** 107, (12), 1491-5.
61. Yu, Y.; Fan, J.; Hui, Y.; Rouzer, C. A.; Marnett, L. J.; Klein-Szanto, A. J.; FitzGerald, G. A.; Funk, C. D., Targeted cyclooxygenase gene (ptgs) exchange reveals discriminant isoform functionality. *J Biol Chem* **2007,** 282, (2), 1498-506.
62. Roth, G. J.; Siok, C. J.; Ozols, J., Structural characteristics of prostaglandin synthetase from sheep vesicular gland. *J Biol Chem* **1980,** 255, (4), 1301-4.
63. Van der Ouderaa, F. J.; Buytenhek, M.; Nugteren, D. H.; Van Dorp, D. A., Purification and characterisation of prostaglandin endoperoxide synthetase from sheep vesicular glands. *Biochim Biophys Acta* **1977,** 487, (2), 315-31.
64. Picot, D.; Loll, P. J.; Garavito, R. M., The X-ray crystal structure of the membrane protein prostaglandin H2 synthase-1. *Nature* **1994,** 367, (6460), 243-9.
65. Xiao, G.; Chen, W.; Kulmacz, R. J., Comparison of prostaglandin H synthase-1 and -2 structural stabilities. *Adv Exp Med Biol* **1999,** 469, 115-8.
66. Bhattacharyya, D. K.; Lecomte, M.; Rieke, C. J.; Garavito, M.; Smith, W. L., Involvement of arginine 120, glutamate 524, and tyrosine 355 in the binding of arachidonate and 2-phenylpropionic acid inhibitors to the cyclooxygenase active site of ovine prostaglandin endoperoxide H synthase-1. *J Biol Chem* **1996,** 271, (4), 2179-84.
67. Garavito, R. M.; Picot, D.; Loll, P. J., Preliminary X-Ray Investigations Into NSAID-Binding to Cyclooxygenase-1. *Am J Ther* **1995,** 2, (9), 611-615.
68. Garavito, R. M.; Picot, D.; Loll, P. J., The 3.1 A X-ray crystal structure of the integral membrane enzyme prostaglandin H2 synthase-1. *Adv Prostaglandin Thromboxane Leukot Res* **1995,** 23, 99-103.

69. Loll, P. J.; Picot, D.; Garavito, R. M., The structural basis of aspirin activity inferred from the crystal structure of inactivated prostaglandin H2 synthase. *Nat Struct Biol* **1995,** 2, (8), 637-43.
70. Garavito, R. M.; Picot, D.; Loll, P. J., Strategies for crystallizing membrane proteins. *J Bioenerg Biomembr* **1996,** 28, (1), 13-27.
71. Loll, P. J.; Picot, D.; Ekabo, O.; Garavito, R. M., Synthesis and use of iodinated nonsteroidal antiinflammatory drug analogs as crystallographic probes of the prostaglandin H2 synthase cyclooxygenase active site. *Biochemistry* **1996,** 35, (23), 7330-40.
72. Picot, D.; Loll, P. J.; Garavito, R. M., X-ray crystallographic study of the structure of prostaglandin H synthase. *Adv Exp Med Biol* **1997,** 400A, 107-11.
73. Luong, C.; Miller, A.; Barnett, J.; Chow, J.; Ramesha, C.; Browner, M. F., Flexibility of the NSAID binding site in the structure of human cyclooxygenase-2. *Nat Struct Biol* **1996,** 3, (11), 927-33.
74. Kiefer, J. R.; Pawlitz, J. L.; Moreland, K. T.; Stegeman, R. A.; Hood, W. F.; Gierse, J. K.; Stevens, A. M.; Goodwin, D. C.; Rowlinson, S. W.; Marnett, L. J.; Stallings, W. C.; Kurumbail, R. G., Structural insights into the stereochemistry of the cyclooxygenase reaction. *Nature* **2000,** 405, (6782), 97-101.
75. Rowlinson, S. W.; Crews, B. C.; Lanzo, C. A.; Marnett, L. J., The binding of arachidonic acid in the cyclooxygenase active site of mouse prostaglandin endoperoxide synthase-2 (COX-2). A putative L-shaped binding conformation utilizing the top channel region. *J Biol Chem* **1999,** 274, (33), 23305-10.
76. Kulmacz, R. J.; Palmer, G.; Wei, C.; Tsai, A. L., Reaction and free radical kinetics of prostaglandin H synthase with manganese protoporphyrin IX as the prosthetic group. *Biochemistry* **1994,** 33, (18), 5428-39.
77. Smith, W. L.; Garavito, R. M.; DeWitt, D. L., Prostaglandin endoperoxide H synthases (cyclooxygenases)-1 and -2. *J Biol Chem* **1996,** 271, (52), 33157-60.
78. Marnett, L. J.; Rowlinson, S. W.; Goodwin, D. C.; Kalgutkar, A. S.; Lanzo, C. A., Arachidonic acid oxygenation by COX-1 and COX-2. Mechanisms of catalysis and inhibition. *J Biol Chem* **1999,** 274, (33), 22903-6.
79. Shimokawa, T.; Kulmacz, R. J.; DeWitt, D. L.; Smith, W. L., Tyrosine 385 of prostaglandin endoperoxide synthase is required for cyclooxygenase catalysis. *J Biol Chem* **1990,** 265, (33), 20073-6.
80. Malkowski, M. G.; Ginell, S. L.; Smith, W. L.; Garavito, R. M., The productive conformation of arachidonic acid bound to prostaglandin synthase. *Science* **2000,** 289, (5486), 1933-7.
81. Malkowski, M. G.; Theisen, M. J.; Scharmen, A.; Garavito, R. M., The formation of stable fatty acid substrate complexes in prostaglandin H(2) synthase-1. *Arch Biochem Biophys* **2000,** 380, (1), 39-45.
82. Thuresson, E. D.; Lakkides, K. M.; Rieke, C. J.; Sun, Y.; Wingerd, B. A.; Micielli, R.; Mulichak, A. M.; Malkowski, M. G.; Garavito, R. M.; Smith, W. L., Prostaglandin endoperoxide H synthase-1: the functions of cyclooxygenase active site residues in the binding, positioning, and oxygenation of arachidonic acid. *J Biol Chem* **2001,** 276, (13), 10347-57.
83. Thuresson, E. D.; Malkowski, M. G.; Lakkides, K. M.; Rieke, C. J.; Mulichak, A. M.; Ginell, S. L.; Garavito, R. M.; Smith, W. L., Mutational and X-ray crystallographic

analysis of the interaction of dihomo-gamma -linolenic acid with prostaglandin endoperoxide H synthases. *J Biol Chem* **2001,** 276, (13), 10358-65.
84. Mancini, J. A.; Riendeau, D.; Falgueyret, J. P.; Vickers, P. J.; O'Neill, G. P., Arginine 120 of prostaglandin G/H synthase-1 is required for the inhibition by nonsteroidal anti-inflammatory drugs containing a carboxylic acid moiety. *J Biol Chem* **1995,** 270, (49), 29372-7.
85. Rieke, C. J.; Mulichak, A. M.; Garavito, R. M.; Smith, W. L., The role of arginine 120 of human prostaglandin endoperoxide H synthase-2 in the interaction with fatty acid substrates and inhibitors. *J Biol Chem* **1999,** 274, (24), 17109-14.
86. Kozak, K. R.; Crews, B. C.; Ray, J. L.; Tai, H. H.; Morrow, J. D.; Marnett, L. J., Metabolism of prostaglandin glycerol esters and prostaglandin ethanolamides in vitro and in vivo. *J Biol Chem* **2001,** 276, (40), 36993-8.
87. Smith, W. L.; Lands, W. E., Stimulation and blockade of prostaglandin biosynthesis. *J Biol Chem* **1971,** 246, (21), 6700-2.
88. Ferreira, S. H.; Moncada, S.; Vane, J. R., Indomethacin and aspirin abolish prostaglandin release from the spleen. *Nat New Biol* **1971,** 231, (25), 237-9.
89. Vane, J. R., Inhibition of prostaglandin synthesis as a mechanism of action for aspirin-like drugs. *Nat New Biol* **1971,** 231, (25), 232-5.
90. Rome, L. H.; Lands, W. E.; Roth, G. J.; Majerus, P. W., Aspirin as a quantitative acetylating reagent for the fatty acid oxygenase that forms prostaglandins. *Prostaglandins* **1976,** 11, (1), 23-30.
91. Roth, G. J.; Stanford, N.; Majerus, P. W., Acetylation of prostaglandin synthase by aspirin. *Proc Natl Acad Sci U S A* **1975,** 72, (8), 3073-6.
92. Lecomte, M.; Laneuville, O.; Ji, C.; DeWitt, D. L.; Smith, W. L., Acetylation of human prostaglandin endoperoxide synthase-2 (cyclooxygenase-2) by aspirin. *J Biol Chem* **1994,** 269, (18), 13207-15.
93. Greig, G. M.; Francis, D. A.; Falgueyret, J. P.; Ouellet, M.; Percival, M. D.; Roy, P.; Bayly, C.; Mancini, J. A.; O'Neill, G. P., The interaction of arginine 106 of human prostaglandin G/H synthase-2 with inhibitors is not a universal component of inhibition mediated by nonsteroidal anti-inflammatory drugs. *Mol Pharmacol* **1997,** 52, (5), 829-38.
94. Rowlinson, S. W.; Kiefer, J. R.; Prusakiewicz, J. J.; Pawlitz, J. L.; Kozak, K. R.; Kalgutkar, A. S.; Stallings, W. C.; Kurumbail, R. G.; Marnett, L. J., A novel mechanism of cyclooxygenase-2 inhibition involving interactions with Ser-530 and Tyr-385. *J Biol Chem* **2003,** 278, (46), 45763-9.
95. Kalgutkar, A. S.; Crews, B. C.; Rowlinson, S. W.; Marnett, A. B.; Kozak, K. R.; Remmel, R. P.; Marnett, L. J., Biochemically based design of cyclooxygenase-2 (COX-2) inhibitors: facile conversion of nonsteroidal antiinflammatory drugs to potent and highly selective COX-2 inhibitors. *Proc Natl Acad Sci U S A* **2000,** 97, (2), 925-30.
96. Kalgutkar, A. S.; Marnett, A. B.; Crews, B. C.; Remmel, R. P.; Marnett, L. J., Ester and amide derivatives of the nonsteroidal antiinflammatory drug, indomethacin, as selective cyclooxygenase-2 inhibitors. *J Med Chem* **2000,** 43, (15), 2860-70.
97. Kalgutkar, A. S.; Rowlinson, S. W.; Crews, B. C.; Marnett, L. J., Amide derivatives of meclofenamic acid as selective cyclooxygenase-2 inhibitors. *Bioorg Med Chem Lett* **2002,** 12, (4), 521-4.

98. Kalgutkar, A. S.; Crews, B. C.; Saleh, S.; Prudhomme, D.; Marnett, L. J., Indolyl esters and amides related to indomethacin are selective COX-2 inhibitors. *Bioorg Med Chem* **2005,** 13, (24), 6810-22.
99. Kozak, K. R.; Prusakiewicz, J. J.; Rowlinson, S. W.; Marnett, L. J., Enantiospecific, selective cyclooxygenase-2 inhibitors. *Bioorg Med Chem Lett* **2002,** 12, (9), 1315-8.
100. Harman, C. A.; Turman, M. V.; Kozak, K. R.; Marnett, L. J.; Smith, W. L.; Garavito, R. M., Structural basis of enantioselective inhibition of cyclooxygenase-1 by S-alpha-substituted indomethacin ethanolamides. *J Biol Chem* **2007,** 282, (38), 28096-105.
101. Moth, C. W.; Prusakiewicz, J. J.; Marnett, L. J.; Lybrand, T. P., Stereoselective binding of indomethacin ethanolamide derivatives to cyclooxygenase-1. *J Med Chem* **2005,** 48, (10), 3613-20.
102. Selinsky, B. S.; Gupta, K.; Sharkey, C. T.; Loll, P. J., Structural analysis of NSAID binding by prostaglandin H2 synthase: time-dependent and time-independent inhibitors elicit identical enzyme conformations. *Biochemistry* **2001,** 40, (17), 5172-80.
103. Shimokawa, T.; Smith, W. L., Expression of prostaglandin endoperoxide synthase-1 in a baculovirus system. *Biochem Biophys Res Commun* **1992,** 183, (3), 975-82.
104. DeWitt, D. L.; Smith, W. L., Cloning of sheep and mouse prostaglandin endoperoxide synthases. *Methods Enzymol* **1990,** 187, 469-79.
105. Smith, T.; Leipprandt, J.; DeWitt, D., Purification and characterization of the human recombinant histidine-tagged prostaglandin endoperoxide H synthases-1 and -2. *Arch Biochem Biophys* **2000,** 375, (1), 195-200.
106. Green, K.; Samuelsson, B., Prostaglandins and Related Factors: Xix. Thin-Layer Chromatography of Prostaglandins. *J Lipid Res* **1964,** 15, 117-20.
107. Houtzager, V.; Ouellet, M.; Falgueyret, J. P.; Passmore, L. A.; Bayly, C.; Percival, M. D., Inhibitor-induced changes in the intrinsic fluorescence of human cyclooxygenase-2. *Biochemistry* **1996,** 35, (33), 10974-84.
108. Johnson, A. R.; Marletta, M. A.; Dyer, R. D., Slow-binding inhibition of human prostaglandin endoperoxide synthase-2 with darbufelone, an isoform-selective antiinflammatory di-tert-butyl phenol. *Biochemistry* **2001,** 40, (25), 7736-45.
109. Cook, H. W.; Ford, G.; Lands, W. E., Instrumental improvements of rapid, detailed kinetic studies of oxygenase activity. *Anal Biochem* **1979,** 96, (2), 341-51.
110. Porter, N. A.; Nixon, J.; Isaac, R., Cyclic peroxides and the thiobarbituric assay. *Biochim Biophys Acta* **1976,** 441, (3), 506-12.
111. Gierse, J.; Kurumbail, R.; Walker, M.; Hood, B.; Monahan, J.; Pawlitz, J.; Stegeman, R.; Stevens, A.; Kiefer, J.; Koboldt, C.; Moreland, K.; Rowlinson, S.; Marnett, L.; Pierce, J.; Carter, J.; Talley, J.; Isakson, P.; Seibert, K., Mechanism of inhibition of novel COX-2 inhibitors. *Adv Exp Med Biol* **2002,** 507, 365-9.
112. Lands, W. E.; Cook, H. W.; Rome, L. H., Prostaglandin biosynthesis: consequences of oxygenase mechanism upon in vitro assays of drug effectiveness. *Adv Prostaglandin Thromboxane Res* **1976,** 1, 7-17.
113. Prusakiewicz, J. J.; Felts, A. S.; Mackenzie, B. S.; Marnett, L. J., Molecular basis of the time-dependent inhibition of cyclooxygenases by indomethacin. *Biochemistry* **2004,** 43, (49), 15439-45.

114. Timofeevski, S. L.; Prusakiewicz, J. J.; Rouzer, C. A.; Marnett, L. J., Isoform-selective interaction of cyclooxygenase-2 with indomethacin amides studied by real-time fluorescence, inhibition kinetics, and site-directed mutagenesis. *Biochemistry* **2002,** 41, (30), 9654-62.
115. Gierse, J. K.; Koboldt, C. M.; Walker, M. C.; Seibert, K.; Isakson, P. C., Kinetic basis for selective inhibition of cyclo-oxygenases. *Biochem J* **1999,** 339 (Pt 3), 607-14.
116. Walker, M. C.; Kurumbail, R. G.; Kiefer, J. R.; Moreland, K. T.; Koboldt, C. M.; Isakson, P. C.; Seibert, K.; Gierse, J. K., A three-step kinetic mechanism for selective inhibition of cyclo-oxygenase-2 by diarylheterocyclic inhibitors. *Biochem J* **2001,** 357, (Pt 3), 709-18.
117. Kurumbail, R. G.; Stevens, A. M.; Gierse, J. K.; McDonald, J. J.; Stegeman, R. A.; Pak, J. Y.; Gildehaus, D.; Miyashiro, J. M.; Penning, T. D.; Seibert, K.; Isakson, P. C.; Stallings, W. C., Structural basis for selective inhibition of cyclooxygenase-2 by anti-inflammatory agents. *Nature* **1996,** 384, (6610), 644-8.
118. Lanzo, C. A.; Beechem, J. M.; Talley, J.; Marnett, L. J., Investigation of the binding of isoform-selective inhibitors to prostaglandin endoperoxide synthases using fluorescence spectroscopy. *Biochemistry* **1998,** 37, (1), 217-26.
119. Lanzo, C. A.; Sutin, J.; Rowlinson, S.; Talley, J.; Marnett, L. J., Fluorescence quenching analysis of the association and dissociation of a diarylheterocycle to cyclooxygenase-1 and cyclooxygenase-2: dynamic basis of cyclooxygenase-2 selectivity. *Biochemistry* **2000,** 39, (20), 6228-34.
120. Wong, E.; Bayly, C.; Waterman, H. L.; Riendeau, D.; Mancini, J. A., Conversion of prostaglandin G/H synthase-1 into an enzyme sensitive to PGHS-2-selective inhibitors by a double His513 --> Arg and Ile523 --> val mutation. *J Biol Chem* **1997,** 272, (14), 9280-6.
121. Gierse, J. K.; McDonald, J. J.; Hauser, S. D.; Rangwala, S. H.; Koboldt, C. M.; Seibert, K., A single amino acid difference between cyclooxygenase-1 (COX-1) and -2 (COX-2) reverses the selectivity of COX-2 specific inhibitors. *J Biol Chem* **1996,** 271, (26), 15810-4.
122. Guo, Q.; Wang, L. H.; Ruan, K. H.; Kulmacz, R. J., Role of Val509 in time-dependent inhibition of human prostaglandin H synthase-2 cyclooxygenase activity by isoform-selective agents. *J Biol Chem* **1996,** 271, (32), 19134-9.
123. Piper, P. J.; Vane, J. R., Release of additional factors in anaphylaxis and its antagonism by anti-inflammatory drugs. *Nature* **1969,** 223, (5201), 29-35.
124. Palmer, M. A.; Piper, P. J.; Vane, J. R., The release of rabbit aorta contracting substance (RCS) from chopped lung and its antagonism by anti-inflammatory drugs. *Br J Pharmacol* **1970,** 40, (3), 581P-582P.
125. Palmer, M. A.; Piper, P. J.; Vane, J. R., Release of rabbit aorta contracting substance (RCS) and prostaglandins induced by chemical or mechanical stimulation of guinea-pig lungs. *Br J Pharmacol* **1973,** 49, (2), 226-42.
126. Nijkamp, F. P.; Moncada, S.; White, H. L.; Vane, J. R., Diversion of prostaglandin endoperoxide metabolism by selective inhibition of thromboxane A2 biosynthesis in lung, spleen or platelets. *Eur J Pharmacol* **1977,** 44, (2), 179-86.
127. Isakson, P. C.; Raz, A.; Denny, S. E.; Pure, E.; Needleman, P., A novel prostaglandin is the major product of arachidonic acid metabolism in rabbit heart. *Proc Natl Acad Sci U S A* **1977,** 74, (1), 101-5.

128. Blackwell, G. J.; Flower, R. J.; Parsons, M. F.; Vane, J. R., Factors influencing the turnover of prostaglandin synthetase. *Br J Pharmacol* **1975,** 53, (3), 467P-468P.
129. Needleman, P.; Moncada, S.; Bunting, S.; Vane, J. R.; Hamberg, M.; Samuelsson, B., Identification of an enzyme in platelet microsomes which generates thromboxane A2 from prostaglandin endoperoxides. *Nature* **1976,** 261, (5561), 558-60.
130. Hecker, M.; Haurand, M.; Ullrich, V.; Diczfalusy, U.; Hammarstrom, S., Products, kinetics, and substrate specificity of homogeneous thromboxane synthase from human platelets: development of a novel enzyme assay. *Arch Biochem Biophys* **1987,** 254, (1), 124-35.
131. Haurand, M.; Ullrich, V., Isolation and characterization of thromboxane synthase from human platelets as a cytochrome P-450 enzyme. *J Biol Chem* **1985,** 260, (28), 15059-67.
132. Ullrich, V.; Haurand, M., Thromboxane synthase as a cytochrome P450 enzyme. *Adv Prostaglandin Thromboxane Leukot Res* **1983,** 11, 105-10.
133. Hecker, M.; Baader, W. J.; Weber, P.; Ullrich, V., Thromboxane synthase catalyses hydroxylations of prostaglandin H2 analogs in the presence of iodosylbenzene. *Eur J Biochem* **1987,** 169, (3), 563-9.
134. Pryor, W. A.; Stanley, J. P., Letter: A suggested mechanism for the production of malonaldehyde during the autoxidation of polyunsaturated fatty acids. Nonenzymatic production of prostaglandin endoperoxides during autoxidation. *J Org Chem* **1975,** 40, (24), 3615-7.
135. Hecker, M.; Ullrich, V., On the mechanism of prostacyclin and thromboxane A2 biosynthesis. *J Biol Chem* **1989,** 264, (1), 141-50.
136. Eling, T. E.; Wilson, A. G.; Chaudhari, A.; Anderson, M. W., Covalent binding of an intermediate(s) in prostaglandin biosynthesis to guinea pig lung microsomal protein. *Life Sci* **1977,** 21, (2), 245-51.
137. Hecker, M.; Haurand, M.; Ullrich, V.; Terao, S., Spectral studies on structure-activity relationships of thromboxane synthase inhibitors. *Eur J Biochem* **1986,** 157, (1), 217-23.
138. Raychowdhury, M. K.; Yukawa, M.; Collins, L. J.; McGrail, S. H.; Kent, K. C.; Ware, J. A., Alternative splicing produces a divergent cytoplasmic tail in the human endothelial thromboxane A2 receptor. *J Biol Chem* **1994,** 269, (30), 19256-61.
139. Parise, L. V.; Venton, D. L.; Le Breton, G. C., Arachidonic acid-induced platelet aggregation is mediated by a thromboxane A2/prostaglandin H2 receptor interaction. *J Pharmacol Exp Ther* **1984,** 228, (1), 240-4.
140. Parise, L. V.; Venton, D. L.; Le Breton, G. C., Thromboxane A2/prostaglandin H2 directly stimulates platelet shape change independent of secreted ADP. *J Pharmacol Exp Ther* **1982,** 222, (1), 276-81.
141. Le Breton, G. C.; Venton, D. L., Thromboxane A2 receptor antagonism selectively reverses platelet aggregation. *Adv Prostaglandin Thromboxane Res* **1980,** 6, 497-503.
142. Le Breton, G. C.; Lipowski, J. P.; Feinberg, H.; Venton, D. L.; Ho, T.; Wu, K. K., Antagonism of thromboxane A2/prostaglandin H2 by 13-azaprostanoic acid prevents platelet deposition to the de-endothelialized rabbit aorta in vivo. *J Pharmacol Exp Ther* **1984,** 229, (1), 80-4.

143. Inoue, M.; Smith, W. L.; DeWitt, D. L., Molecular characterization of the prostacyclin synthase. *Adv Prostaglandin Thromboxane Leukot Res* **1987,** 17A, 29-33.
144. Dusting, G. J.; Moncada, S.; Vane, J. R., Prostacyclin (PGX) is the endogenous metabolite responsible for relaxation of coronary arteries induced by arachindonic acid. *Prostaglandins* **1977,** 13, (1), 3-15.
145. Moncada, S.; Bunting, S.; Mullane, K.; Thorogood, P.; Vane, J. R.; Raz, A.; Needleman, P., Imidazole: a selective inhibitor of thromboxane synthetase. *Prostaglandins* **1977,** 13, (4), 611-8.
146. Tanouchi, T.; Kawamura, M.; Ohyama, I.; Kajiwara, I.; Iguchi, Y.; Okada, T.; Miyamoto, T.; Taniguchi, K.; Hayashi, M.; Iizuka, K.; Nakazawa, M., Highly selective inhibitors of thromboxane synthetase. 2. Pyridine derivatives. *J Med Chem* **1981,** 24, (10), 1149-55.
147. Johnson, R. A.; Nidy, E. G.; Aiken, J. W.; Crittenden, N. J.; Gorman, R. R., Thromboxane A2 synthase inhibitors. 5-(3-Pyridylmethyl)benzofuran-2-carboxylic acids. *J Med Chem* **1986,** 29, (8), 1461-8.
148. Iizuka, K.; Akahane, K.; Momose, D.; Nakazawa, M.; Tanouchi, T.; Kawamura, M.; Ohyama, I.; Kajiwara, I.; Iguchi, Y.; Okada, T.; Taniguchi, K.; Miyamoto, T.; Hayashi, M., Highly selective inhibitors of thromboxane synthetase. 1. Imidazole derivatives. *J Med Chem* **1981,** 24, (10), 1139-48.
149. Coleman, R. A.; Humphrey, P. P.; Kennedy, I.; Levy, G. P.; Lumley, P., Comparison of the actions of U-46619, a prostaglandin H2-analogue, with those of prostaglandin H2 and thromboxane A2 on some isolated smooth muscle preparations. *Br J Pharmacol* **1981,** 73, (3), 773-8.
150. McAdam, B. F.; Byrne, D.; Morrow, J. D.; Oates, J. A., Contribution of cyclooxygenase-2 to elevated biosynthesis of thromboxane A2 and prostacyclin in cigarette smokers. *Circulation* **2005,** 112, (7), 1024-9.
151. McAdam, B. F.; Catella-Lawson, F.; Mardini, I. A.; Kapoor, S.; Lawson, J. A.; FitzGerald, G. A., Systemic biosynthesis of prostacyclin by cyclooxygenase (COX)-2: the human pharmacology of a selective inhibitor of COX-2. *Proc Natl Acad Sci U S A* **1999,** 96, (1), 272-7.
152. Renslo, A. R.; McKerrow, J. H., Drug discovery and development for neglected parasitic diseases. *Nat Chem Biol* **2006,** 2, (12), 701-10.
153. Control of Chagas disease. Report of a WHO Expert Committee. *World Health Organ Tech Rep Ser* **1991,** 811, 1-95.
154. Control of Chagas disease. *World Health Organ Tech Rep Ser* **2002,** 905, i-vi, 1-109, back cover.
155. Chagas, C., Neue Trypanosomen. *Vorlaufige Mittleilung. Archiv fur Schiffs- und Tropenhygiene* **1909,** 13, 120-122.
156. Chagas, C., Nova tripanozomiaze humana. *Memorias do Instituto Oswaldo Cruz* **1909,** 2, 159-218.
157. Chagas, C., Sobre a etiologia do bocio endemico no Estado de Minas Geraes. Nota preliminar. . *Brasil-Medico* **1910,** 24, (17), 3-4.
158. Teixeira, A. R.; Nascimento, R. J.; Sturm, N. R., Evolution and pathology in chagas disease--a review. *Mem Inst Oswaldo Cruz* **2006,** 101, (5), 463-91.
159. Gull, K., The biology of kinetoplastid parasites: insights and challenges from genomics and post-genomics. *Int J Parasitol* **2001,** 31, (5-6), 443-52.

160. Brener, Z., Biology of Trypanosoma cruzi. *Annu Rev Microbiol* **1973,** 27, 347-82.
161. Dujardin, J., Schofield, CJ, Panzera, F. , Les vecteurs de la maladie de Chagas: recherches taxonomiques, biologiques et genetiques. *Academie Royale des Science d'Utre-Mer.* **2000,** 241, 37-61.
162. Galvao, C., Carcavallo, R., da Silva Rorcha D., Jurberg, J., A checklist of the currenty valid species of the subfamily Triatominae, 1919 (Hemiptera, Reduviidae) and their geographical distribution, with nomenclatural and taxonomic notes. *Zootaxa* **2004,** 202, 1-36.
163. Dias, J. C., The indeterminate form of human chronic Chagas' disease A clinical epidemiological review. *Rev Soc Bras Med Trop* **1989,** 22, (3), 147-56.
164. Koberle, F., Chagas' disease and Chagas' syndromes: the pathology of American trypanosomiasis. *Adv Parasitol* **1968,** 6, 63-116.
165. Barrett, T. V.; Hoff, R. H.; Mott, K. E.; Miles, M. A.; Godfrey, D. G.; Teixeira, R.; Almeida de Souza, J. A.; Sherlock, I. A., Epidemiological aspects of three Trypanosoma cruzi zymodemes in Bahia State, Brazil. *Trans R Soc Trop Med Hyg* **1980,** 74, (1), 84-90.
166. Samuel, J.; Oliveira, M.; Correa De Araujo, R. R.; Navarro, M. A.; Muccillo, G., Cardiac thrombosis and thromboembolism in chronic Chagas' heart disease. *Am J Cardiol* **1983,** 52, (1), 147-51.
167. Croft, S. L.; Barrett, M. P.; Urbina, J. A., Chemotherapy of trypanosomiases and leishmaniasis. *Trends Parasitol* **2005,** 21, (11), 508-12.
168. Sosa Estani, S.; Segura, E. L.; Ruiz, A. M.; Velazquez, E.; Porcel, B. M.; Yampotis, C., Efficacy of chemotherapy with benznidazole in children in the indeterminate phase of Chagas' disease. *Am J Trop Med Hyg* **1998,** 59, (4), 526-9.
169. Murta, S. M.; Gazzinelli, R. T.; Brener, Z.; Romanha, A. J., Molecular characterization of susceptible and naturally resistant strains of Trypanosoma cruzi to benznidazole and nifurtimox. *Mol Biochem Parasitol* **1998,** 93, (2), 203-14.
170. Wilkinson, S. R.; Taylor, M. C.; Horn, D.; Kelly, J. M.; Cheeseman, I., A mechanism for cross-resistance to nifurtimox and benznidazole in trypanosomes. *Proc Natl Acad Sci U S A* **2008,** 105, (13), 5022-7.
171. Urbina, J. A.; Docampo, R., Specific chemotherapy of Chagas disease: controversies and advances. *Trends Parasitol* **2003,** 19, (11), 495-501.
172. Lepesheva, G. I.; Zaitseva, N. G.; Nes, W. D.; Zhou, W.; Arase, M.; Liu, J.; Hill, G. C.; Waterman, M. R., CYP51 from Trypanosoma cruzi: a phyla-specific residue in the B' helix defines substrate preferences of sterol 14alpha-demethylase. *J Biol Chem* **2006,** 281, (6), 3577-85.
173. Buckner, F. S., Sterol 14-demethylase inhibitors for Trypanosoma cruzi infections. *Adv Exp Med Biol* **2008,** 625, 61-80.
174. Cazzulo, J. J., Proteinases of Trypanosoma cruzi: patential targets for the chemotherapy of Changas desease. *Curr Top Med Chem* **2002,** 2, (11), 1261-71.
175. Garzoni, L. R.; Waghabi, M. C.; Baptista, M. M.; de Castro, S. L.; Meirelles Mde, N.; Britto, C. C.; Docampo, R.; Oldfield, E.; Urbina, J. A., Antiparasitic activity of risedronate in a murine model of acute Chagas' disease. *Int J Antimicrob Agents* **2004,** 23, (3), 286-90.
176. Garzoni, L. R.; Caldera, A.; Meirelles Mde, N.; de Castro, S. L.; Docampo, R.; Meints, G. A.; Oldfield, E.; Urbina, J. A., Selective in vitro effects of the farnesyl

pyrophosphate synthase inhibitor risedronate on Trypanosoma cruzi. *Int J Antimicrob Agents* **2004,** 23, (3), 273-85.
177. Schmidt, A.; Krauth-Siegel, R. L., Enzymes of the trypanothione metabolism as targets for antitrypanosomal drug development. *Curr Top Med Chem* **2002,** 2, (11), 1239-59.

CHAPTER II

A CONSERVATIVE SUBSTITUTION IN A SECOND-SHELL RESIDUE ALTERS LOCAL DYNAMICS AND DIMINISHES CYCLOOXYGENASE-2 INHIBITION BY INDOMETHACIN AMIDES

Introduction

Structural and functional analysis is a powerful combination for probing the molecular basis of protein-ligand interactions. Such studies provide the basis for computational modeling, drug design, lead optimization, etc. A striking example of the fruits of combined structure-function analysis is provided by the study of cyclooxygenase (COX) enzymes. COX-1 and COX-2 play important roles in a range of physiological and pathophysiological responses and are the molecular targets for non-steroidal anti-inflammatory drugs (NSAIDs) and COX-2-selective inhibitors (COXIBs)[1-3]. COX proteins from different vertebrate species are approximately 60% identical in amino acid sequence and virtually superimposable in three-dimensional structure[4-7].The COX active sites have approximately 85% identity, which might lead to the impression that ligand recognition and inhibitor binding to these isoforms should be identical[8]. Yet, structurally similar inhibitors exhibit significantly different binding modes [9,10].

For any small molecule to bind in the COX active site, it must first enter through the membrane into an open area termed the "lobby" composed of the four-helix membrane-binding domain[5]. The lobby is separated from the active site by a constriction comprised of the conserved residues, Arg-120, Tyr-355, and Glu-524 (Fig. 1). The active site is located in a hydrophobic channel that runs from the constriction site to the catalytic tyrosine (Tyr-385) then bends sharply and terminates in an alcove near Gly-533 [11]. Site-

directed mutagenesis has been very useful in defining critical interactions between inhibitors and residues in the active site and, in some cases, has predicted novel binding modes in advance of the solution of protein-inhibitor structures[12].

The molecular basis for selectivity of inhibition of the individual COX enzymes has been of special interest from a biochemical and pharmacological point of view. Several years ago, our laboratory reported that neutral derivatives of certain arylcarboxylic acid-containing NSAIDs, such as indomethacin (INDO), are highly selective COX-2 inhibitors. Inhibition by the various ester and amide derivatives contrasts sharply with that of their parent carboxylic acids, which are frequently more potent inhibitors of COX-1 than COX-2. Site-directed mutagenesis indicates that the constriction residues, Tyr-355 and Glu-524, are important for neutral NSAID derivative binding but these residues cannot account for COX-2 selectivity because they are conserved in both proteins. Mutagenesis of the few divergent residues in the active site that account for the selectivity of the diarylheterocycle class of COX-2 selective inhibitors does not alter the selectivity of NSAID amides [13,14].

The generality of COX-2-selective inhibition by INDO-amides or esters implies the existence of novel selectivity determinants outside the cyclooxygenase active site. To search for such determinants, we scanned a number of divergent amino acids by making COX-2 → COX-1 substitutions in regions likely to either contact the amide portion of the inhibitors or in the second shell adjacent to this area. Our investigation uncovered a subtle substitution of a second shell residue that makes a significant contribution to the COX-2 selectivity of INDO-amides. Mutation of this residue alters the selectivity of INDO-amides in a kinetically unique way that is consistent with a model developed by

molecular dynamic analysis. These findings underscore the dynamic nature of protein-ligand interactions that can only be elucidated by a combination of structural, functional, and computational analysis.

Materials and Methods

Materials - Arachidonic acid was purchased from Nu Check Prep (Elysian, MN). [1-C^{14}]Arachidonic acid was purchase from NEN Dupont (Boston, MA). Mouse COX-2 and mutant enzymes were purified as previously described[11] Materials for cloning and protein expression was purchased from Invitrogen (Carlsbad, CA)

Free-enzyme COX Inhibition Screening Assay - Reactions were run with reconstituted protein at final concentrations adjusted to give approximately 30% substrate consumption. Time-dependent inhibition reactions were performed by preincubating the inhibitor and enzyme for 17 min at 25 °C, followed by 3 min at 37 °C prior to the addition of 50 μM [1-^{14}C]-AA for 30 s at 37 °C. Assays were terminated and analyzed for substrate consumption by thin-layer chromatography as previously described. All inhibitor concentrations for 50% enzyme activity (IC_{50}) were determined graphically and were the average of two independent determinations.

Time-Dependent COX Inhibition Assays - Enzymes at the concentrations listed above, were preincubated at 37 °C for varying lengths of time (0 s, 15 s, 30 s, 45 s, 1 min, 3 min, 5 min, 15 min, and 30 min) with various concentrations of inhibitor. All reactions were performed with for [1-^{14}C]-AA for 30 s at 37 °C; reactions were terminated and analyzed

as previously described[13]. The values of kinetic parameters were the average of at least two independent determinations.

Reverse Mutant Cloning and Transfection - A 2599 nucleotide cDNA containing the 1800 base pair open reading frame encoding wild type human COX-1 was ligated into the *NheI* and *NotI* restriction sites of the expression vector pcDNA3.1 Hygro(+). Site directed mutagenesis of codon 472 from methionine (wild type) to leucine (mutant; M472L) was performed by PCR using the primers: 5'-GAGGTTTGGCCTGAAACCCTACACC-3' and 5'-GCCAAACCTCTTGCGGTACTCATTG-3'. PCR was performed for 30 cycles using LA Taq, then digested with *DpnI* prior to transformation into XL1-Blue competent *E. coli* . To obtain stable transfectants, HEK293t/17 cells (ATCC) were grown to 70% confluence in DMEM supplemented with 10% fetal bovine serum in 10 cm plates and transfected with 5 μg plasmid DNA using Lipofectamine 2000 according to manufacturer's protocol. After transfection, cells were selected using 200 μg/ml Hygromycin B for four passages, and plated at 70% confluence in 6-well plates or 10 cm dishes for cyclooxygenase activity assays.

Mutagenesis Methods - Site-directed mutagenesis was performed on a mCOX-2 pBS(+) vector (Stratagene, La Jolla, CA) using the Quick Change site-directed mutagenesis kit (Stratagene). Mutant containing regions were subcloned into the mCOX-2 pVL1393 baculovirus expression vector (PharMingen, San Diego, CA) using the StuI restriction site in mCOX-2 and the XbaI restriction site present in both the pBS(+) and pVL1393 vectors. The subcloned region was fully sequenced to ensure that no accidental mutations

were incorporated. Mutant enzyme expression and purification was performed as previously reported.[4]

Synthesis and Characterization of INDO-Amides - Synthesis of Compounds 1, 2, 3, 6, and 7 (Table 1) was accomplished similarly to previously reported and according to the scheme below. The synthesis of Compounds 4, 5, and 8 were previously reported[1-3]. 2-(1-(4-chlorophenylcarbonyl)-5-methoxy-2-methyl-1H-indol-3-yl)-N-(4-(trifluoromethyl)benzyl)ethanamide (**Compound 1**): A reaction mixture containing indomethacin (300 mg, 0.84 mmol) in 6 mL of anhydrous CH2Cl2 was treated with dicyclohexylcarbodiimide (192 mg,0.92 mmol), dimethylaminopyridine (10 mg, 84 mmol), and 4-trifluoromethylbenzyl amine (0.13 mL,0.92 mmol). After stirring at room temperature for 5 h, the reaction mixture was filtered and the filtrate was concentrated in vacuo. The residue was diluted with water (2x15 mL) and extracted with methylene chloride (3x15 mL). The combined organic solution was washed with brine (2x15 mL), dried over MgSO4, and filtered, and concentrated in vacuo. The crude product was purified by trituration with a minimal amount of methylene chloride and one equivalent of hexanes to give a white precipitate. The solid was collected in a fritted funnel (301 mg, 69%). ^{1}H NMR :(300 MHz, $CDCl_3$, ppm) δ 7.58 (m, 2H), 7.49 (m, 4H), 7.26 (s, 2H), 6.86 (m, 1H), 6.81 (s, 1H), 6.69 (dd, J = 3.4, 9.0 Hz, 1H), 6.12 (br s, 1H), 4.43 (d, J = 6.2 Hz, 2H), 3.76 (s, 3H), 3.71 (s, 2H), 2.37 (s, 3H) 13C: (400 MHz, CDCl3, ppm) 170.44, 168.04, 156.17,142.24, 139.58, 136.35, 133.31, 130.82, 130.17,129.62, 129.12, 127.52, 125.38, 125.35, 115.00,112.53,112.15, 57.98, 55.58, 42.86, 31.97, 18.12, 13.13 mp = 174 ^{o}C ESI-MS (positive) 536 $[C_{27}H_{22}ClF_3N_2O_3 + Na]^+$

Analysis (calcd, found): C (62.98, 63.02), H (4.31, 4.39), N (5.44, 5.40) Hi-Res MS: Theoretical $(M+H)^+$ = 515.1349 Found $(M+H)^+$ 515.1356 HPLC: rt= 21.9 min, >99%

N-(4-bromobenzyl)-2-(1-(4-chlorophenylcarbonyl)-5-methoxy-2-methyl-1H-indol-3-yl)ethanamide(**Compound 2**) This compound was prepared in a similar manner as described for Compound 1.Compound 3 was obtained as an off-white solid (260 mg, 79%)1H NMR :(300 MHz, CDCl3, ppm) δ 7.52(d, J = 9.0 Hz, 2H), 7.48 (d, J = 9.0 Hz, 2H), 7.38 (d, J = 9.0 Hz, 2H), 7.03 (d, J = 9.0 Hz, 2H), 6.86 (m, 2H), 6.81, 6.69 (dd, J = 3.0, 9.0 Hz, 1H), 5.99 (br s, 1H), 4.36 (d, J = 6.0 Hz, 2H), 3.80 (s, 3H), 3.71 (s, 2H), 2.38 (s, 3H) 13C: (400 MHz, CDCl3, ppm) 170.84, 168.34, 156.12, 142.34, 139.56, 133.32, 130.86, 130.17,129.64, 129.12, 127.54, 125.40, 125.35, 115.02,112.54, 112.20, 57.98, 55.58, 42.88, 31.99, 18.13, 13.11 mp = 154 ^oC ESI-MS (positive) 525 $[C_{26}H_{22}BrClN_2O_3]^+$ Analysis (calcd, found): C (59.39, 59.42), H (4.22, 4.39), N (5.33, 5.30)Hi-Res MS: Theoretical $(M+H)^+$ =525.0581 Found $(M+H)^+$ 525.0589 HPLC: rt= 21.6 min, 98.9%

2-(1-(4-chlorophenylcarbonyl)-5-methoxy-2-methyl-1H-indol-3-yl)-N-((6-(trifluoromethyl)pyridin-3-yl)methyl)ethanamide (**Compound 3**) This compound was prepared in a similar manner as describedfor Compound 1. Compound was obtained as an off-white solid (264 mg, 69%) 1H NMR (CDCl3) δ 8.54 (s, 1H), 7.60 (m, 4H), 7.49 (m, 2H), 6.85 (m, 2H), 6.70 (d, J = 8.7 Hz, 1H), 6.12 (br s, 1H), 4.47 (s, 2H), 3.79 (s, 3H), 3.72 (s, 2H), 2.39 (s, 3H) 13C: (400 MHz, CDCl3, ppm) 170.74, 168.43, 156.16,148.94, 146.77, 139.59, 137.45,136.67, 136.35, 133.28, 131.07, 130.82, 130.20, 129.13,

120.22,114.97, 112.47, 111.99, 100.92, 57.98, 55.60, 40.54, 31.86, 18.12, 13.15 mp = 183 ^{o}C ESI-MS (positive) 516 $[C_{26}H_{21}ClF_3N_3O_3]^+$ Analysis (calcd, found): C (60.53, 60.59), H (4.10, 4.27), N (8.14, 8.12) Hi-Res MS: Theoretical $(M+H)^+$ = 516.1302 Found $(M+H)^+$ 516.1306 HPLC: rt=20.0 min, >99%

N-(4-chlorobenzyl)-2-(1-(4-chlorophenylcarbonyl)-5-methoxy-2-methyl-1H-indol-3-yl)ethanamide (**Compound 6**) This compound was prepared in a similar manner as described for Compound 1. Compound 6 was obtained as an off-white solid (210 mg, 52%) 1H NMR: (300 MHz, CDCl3, ppm) δ 7.58 (dd, J = 6.3, 13.1 Hz, 4H), 7.13 (dd, J = 6.3, 13.1 Hz, 4H), 7.26 (s, 2H), 6.84 (m, 2H), 6.69 (m, 1H), 6.00 (br s, 1H), 4.35 (s, 2H), 3.77 (s, 3H), 3.70 (s, 2H), 2.35 (s, 3H) 13C: (400 MHz, CDCl3, ppm)169.82, 168.23, 156.25, 139.58, 136.62, 136.29, 133.40, 131.09, 130.82,130.08, 129.16, 128.72,128.66, 115.09, 112.50, 112.37, 100.67, 55.63, 42.70, 33.80, 32.16, 25.51, 24.83, 13.19 mp = 167 ^{o}C ESI-MS(positive) 503 $[C_{26}H_{22}Cl_2N_2O_3$+ Na$]^+$ Analysis (calcd, found): C (64.87, 64.92), H (4.61, 4.81), N (5.82, 5.80) Hi-Res MS: Theoretical $(M+H)^+$ = 481.1086 Found $(M+H)^+$483.1080 HPLC: rt= 21.333 min, >99%

2-(1-(4-chlorophenylcarbonyl)-5-methoxy-2-methyl-1H-indol-3-yl)-N-((6-chloropyridin-3-yl)methyl)ethanamide(**Compound 7**) This compound was prepared in a similar manner as described for Compound 1. Compound 7 was obtained as an off-white solid (250 mg, 59%) 1H NMR (300 MHz,$CDCl_3$,ppm) δ 8.15 (d, 1H, J = 2.1 Hz), 7.50 (m, 5H), 7.422 (d, 1H, J = 8.4 Hz), 6.83 (m, 2H),6.69 (dd, J1 = 9 Hz, J2 =2.4 Hz 1H), 6.19 (br t, J = 6 Hz, 1H), 4.37 (d, J = 6Hz, 2H), 3.79 (s, 3H), 3.71(s, 2H), 2.36 (s, 3H) 13C: (400 MHz,

$CDCl_3$, ppm) 170.61, 168.39, 156.16, 150.15, 148.52, 139.54,138.48, 136.32, 133.28, 133.12, 130.80, 124.10, 124.06, 114.97, 112.50, 100.90, 55.63, 40.12, 31.89, 18.13, 13.16 mp = 177 ^oC ESI-MS (positive) 482 $[C_{25}H_{21}Cl_2N_3O_3]^+$ Analysis (calcd, found): C (62.25, 62.42), H (4.39, 4.49), N (8.71, 8.43) Hi-Res MS: Theoretical $(M+H)^+$ = 482.1038 Found $(M+H)^+$ 482.1033 HPLC: rt= 19.1 min, >99%

Cellular Inhibition Assay - The medium was removed and cells washed with PBS and replaced with 900 μL of SF-DMEM. The cells were allowed to equilibrate for 1 h prior to the addition of either Compound **2** or DMSO. Substrate was subsequently added and allowed to metabolize for 6 min. A portion of the medium (600 μL) was removed and added to an equal volume of acidified EtOAc containing deuterated internal standards of prostaglandins. The organic layer was extracted, dried down, and reconstituted in 1:1 MeOH:water and analyzed by LC/MS/MS. Samples were run in negative mode with the aqueous solution containing 10 mM ammonium acetate. The organic solvent used was acetonitrile containing 10% of the aqueous solution. An isocratic method was used containing 70% aqueous and 30% organic on a C18 column with a flow rate of 350 μL/min. Selective reaction monitoring was used to identify the appropriate products and percent inhibition determined by normalization against internal standards and DMSO control.

Steady-State Quenching of COX Intrinsic Fluorescence - Fluorescence quenching experiments with inhibitors were performed with a Spex Fluorolog-3 spectrofluorometer. The compounds were dissolved in DMSO before further dilution into buffer. The organic

component in the buffer was below 0.4%. The excitation (280 nm) and emission (327 nm) bandwidths were 4 and 6 nm, respectively. Steady-state measurements were performed at 37 °C in a 3.5 mL fluorescence cuvette with continuous stirring. All *apo*-proteins were diluted to 200 nM and displayed less than 2% activity of an equivalent amount of holoenzyme. Data were collected over 240 or 360 s with 2 s integration times. Proteins were mixed with inhibitors until a plateau was reached (240-1200 s), and binding was monitored by intrinsic fluorescence quenching of COX. Incubations were normalized to the DMSO control and fit to a single exponential. The dependence of k_{obs} on the inhibitor concentrations (0.05 to 4 mM) was graphed in a secondary plot for the forward reaction (k_{obs}). The k_{obs} data were analyzed by nonlinear regression with eq. 2

Stopped Flow Analysis of Compound 1 Binding - Reactions were performed with an Applied Photophysics SX.18MV stopped-flow unit with a 100 μL cuvette and an auto stop assembly. For the on-rates, the enzyme (100 nM) was loaded in a separate syringe from the inhibitors and the quenching was monitored for either 200 or 500 s. Excitation for all experiments was at 280 nm. Slits were set to 2-4 mm on the stopped flow instrument. Emission was detected through a 320 nm long pass filter for the stopped flow using a Hamamatsu emission photomultiplier with high voltage. All experiments were performed at 37 °C. The kinetic results are averages of at least 4 independent determinations and the vehicle control subtracted. The results were globally fit to a two-phase exponential decay and each exponential plotted against concentration to extract the individual rates.

Computational Methods - An uninhibited COX-2 homodimer was extracted from the *4COX* pdb file and solvated with SPC/E water through a Grand Canonical ensemble Monte Carlo simulation implemented in the program MMC (http://inka.mssm.edu/~mezei/mmc/)[34]. MD Simulation of the explicitly hydrated system was conducted with AMBER, using standard AMBER99 all-atom potential functions [35]. The mCOX-2 trajectory energies and structural fluctuations stabilized completely after 4.5 ns, and we extracted a configuration snapshot at 4.5 ns to generate the starting configuration for the L472M simulation. We collected 20 ns of data from both the mutant and wild type trajectories for subsequent analysis. Quasiharmonic vibrational modes and energies were calculated by the PTRAJ module in AMBER 9 [35,36]. Main channel radius analysis was performed with our Channel_Finder utilities[21].

Derivation of Kinetic Analysis - Each exponential obtained (λ_1 and λ_2) was plotted against concentration of inhibitor for each enzyme. The graph of λ_1 plotted against compound 1 concentration give a linear fit where the slope is equal to k_1 (the forward rate constant of the first step) and the y-intercept is equal to the sum of all other rate constants ($k_{-1}+k_2+k_{-2}$). The second exponential, λ_2, plotted against concentration of compound 1 yields a hyberbolic fit where the plateau is equal to the sum of the rate constants of the second step (k_2+k_{-2}). In this case, the y-intercept of the line ($k_{-1}+k_2+k_{-2}$) was equivalent to the plateau of the hyperbola (k_2+k_{-2})such that k_{-1} is negligible. As such, we can consider the slope of the concentration-dependence of λ_1 to be equal to k_1 and λ_2 (max) equal to (k_2+k_{-2}).[5]

Results

Design and Expression of COX-2 Mutants - The structure of the complex of INDO with COX-2 (*4COX*) reveals that INDO fills a significant portion of the active site (Fig. 1)[6]. The *para*-chlorobenzoyl moiety is close to Tyr-385 and Trp-387 near the top of the cyclooxygenase active site and the carbonyl of the *para*-chlorobenzoyl group is hydrogen-bonded to Ser-530. The 2'-methyl of the indole ring is inserted into a hydrophobic depression in the side of the active site. Insertion of the methyl group into this region is responsible for the slow, pseudo-irreversible, step of INDO binding[15]. The carboxylate of INDO is situated at the constriction site near Tyr-355, Arg-120, and Glu-524, where it is hydrogen-bonded to Tyr-355 and ion-paired to Arg-120.

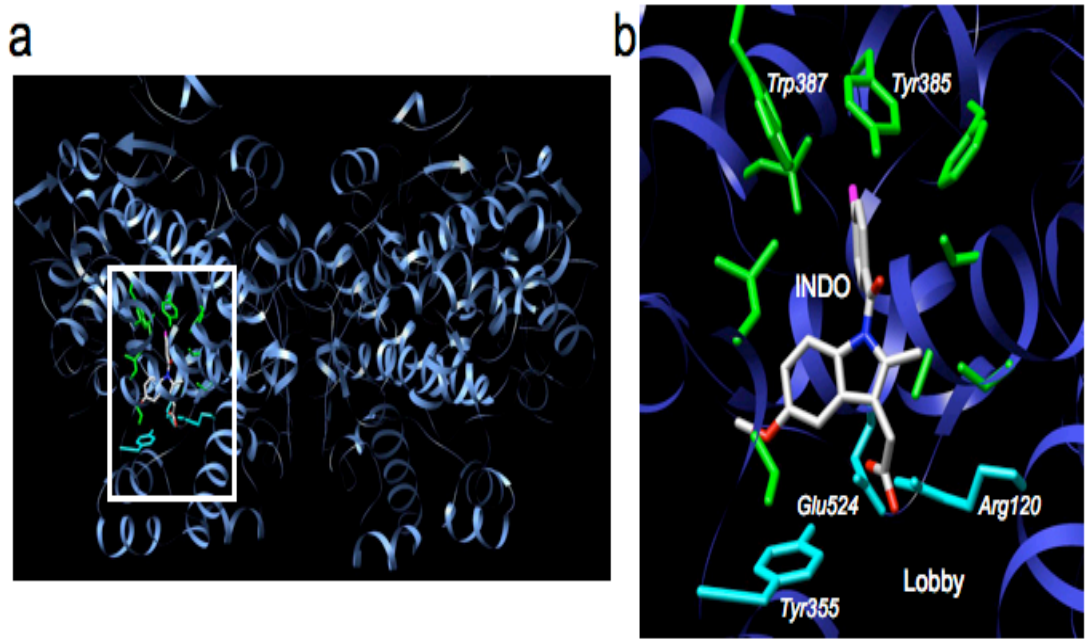

Figure 1. COX dimer structure with insert of the cyclooxygenase active site
(a). COX dimer with a cyclooxygenase site highlighted; (b). Insert from panel a showing INDO (stick, carbon;gray, oxygen;red, nitrogen;blue, chlorine;magenta), active site residues (stick, green), and constriction site residues (stick, turquoise). The lobby region is below Glu-524, Arg-120, and Tyr-355 as indicated. Structure from *4COX*

The binding interactions between COX-2 and the INDO portion of INDO-amides or esters appear to be similar to those between COX-2 and INDO, which leaves no room in the active site for the amide or ester functionality[14]. Thus, we expect these compounds to breach the constriction site and project into the lobby, a region that has remained largely uncharacterized in terms of possible interactions between protein residues and small molecules. To explore the role that divergent non-active site residues have in conferring selectivity, we constructed a series of site-directed mCOX-2 mutants. We focused our selection on residues near the constriction site and in the lobby. Residues within 7 Å of the cyclooxygenase active site that were divergent between COX-1 and COX-2 were mutated from the mCOX-2 residue to the corresponding oCOX-1 residue in a mCOX-2 background. The mutants constructed were V89I, I112L, Y115L, S119V, D125P, A151I, S471M, and L472M (rendered as stick, Fig. 2). The mutant proteins were expressed, purified, and assayed for activity as previously described[10]. All mutant enzymes metabolized arachidonic acid with similar efficiency to wild-type enzyme, indicating that these point mutations did not induce significant conformational alterations in the enzyme.

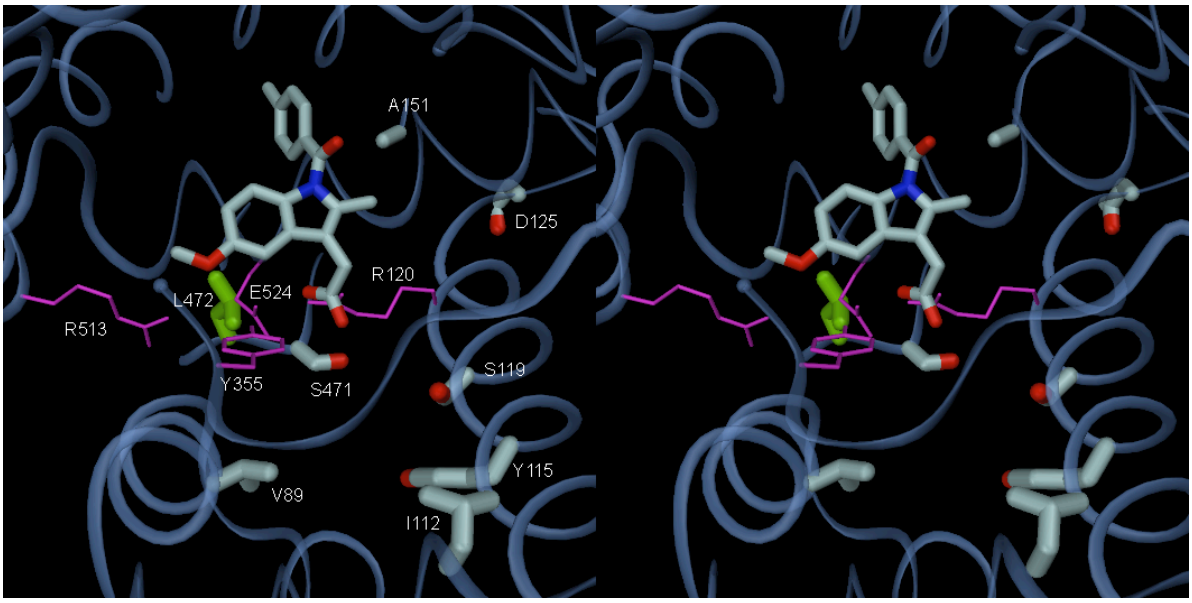

Figure 2. Location of Mutated Second-Shell Residues Relative to the COX Active Site Model illustrating the location of mutated second shell residues (V89I, I112L, Y115L, S119V, D125P, A151I, S471M, and L472M) using the *4COX* crystal structure. L472 is highlighted in green. INDO and remaining second-shell residues are shown using the same color scheme as INDO in Fig. 1 and the constriction site residues (Arg-120, Glu-524, and Tyr-355) are shown with wire in magenta.

L472M Emerges as Key Residue - Each mutant was screened for altered inhibitor binding by fluorescence quenching. 2-(1-(4-Chlorophenylcarbonyl)-5-methoxy-2-methyl-1*H*-indol-3-yl)-*N*-(4-(trifluoromethyl)benzyl)ethanamide, (**1) ,** with a trifluoromethyl group as a *para*-substituent in the amide portion, is an extremely potent and selective inhibitor of COX-2 (IC_{50}-COX-2 = 17 nM; IC_{50}-COX-1 > 4000 nM) (Table 1). Compound **1** forms a pseudo-irreversible complex with COX-2 in a time-dependent manner and no residual enzyme activity remains. The loss of activity parallels the loss of intrinsic enzyme fluorescence. Mutants were screened for the rate and extent of fluorescence loss following incubation with 2.5 µM **1**. The only mutant that showed a significantly attenuated binding rate compared to mCOX-2 was L472M (Figure 3.).

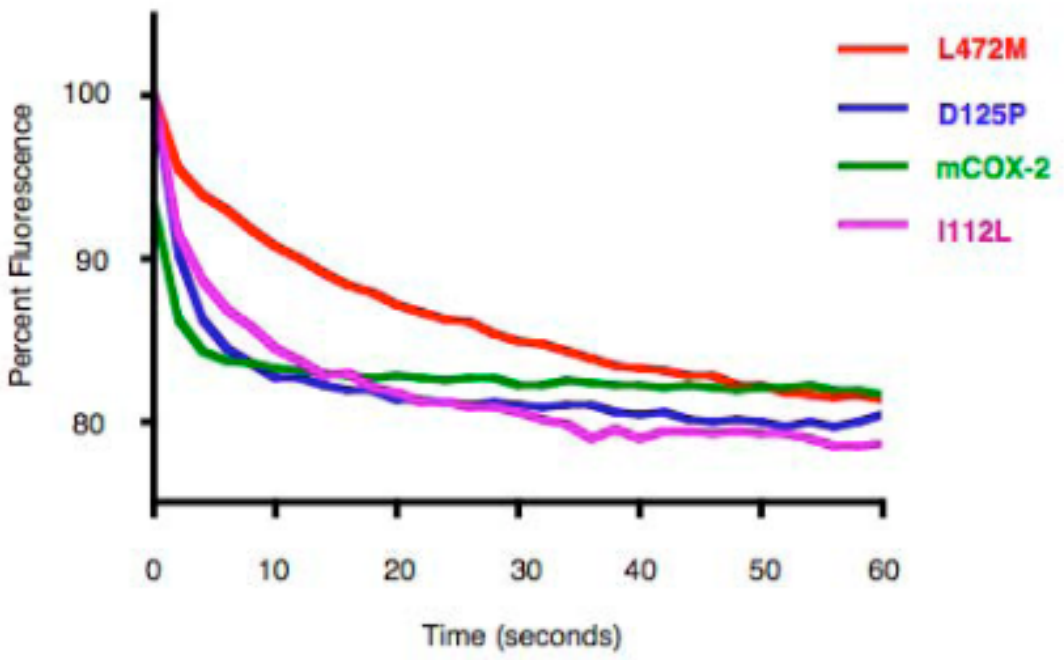

Figure 3. Fluorescence quenching of mCOX-2 and second-shell mutant enzymes

A series of COX-2-selective INDO-amides were screened at 2.5 μM against L472M and were found to have rates of association (k_{obs}) up to 48-fold slower compared to mCOX-2 (Table 1.). To quantify the effect of the L472M mutation on inhibitor potency, compounds were screened using a radiochemical assay that directly monitors arachidonic acid conversion to products. In all cases, the neutral INDO derivatives were less potent against L472M. The extent of potency loss (IC_{50}(L472M)/ IC_{50}(mCOX-2)) ranged from 3 to 92 (Table 1).

Table 1. Potency and selectivity of INDO-amides.

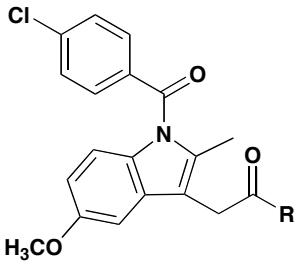

Compound	R	k_{obs} (s^{-1})		k_{obs} (L472M) / k_{obs} (COX-2)†	IC_{50}* (nM)		IC_{50} (L472M) / IC_{50} (COX-2)†
		mCOX-2	L472M		mCOX-2	L472M	
1	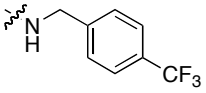	0.462	0.023	0.050	17	101	5
2	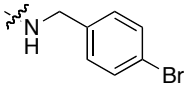	0.291	0.041	0.141	54	214	4
3	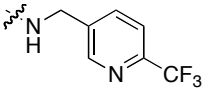	0.030	0.006	0.200	29	2600	92
4	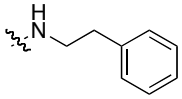	0.481	0.022	0.046	60	4400	73
5	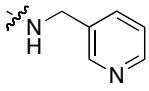	0.237	0.070	0.295	100	302	3
6	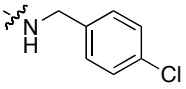	0.060	0.013	0.217	160	>1000	>6
7	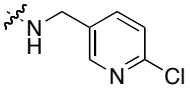	0.209	0.004	0.019	57	>10000	>175

*All IC_{50} data are in nM. †Ratio of kinetic constant values or potency values to give a selectivity index. P values <0.005 for all values.

Reverse Mutant Design - The complementary mutation of M472L in a COX-1 background was constructed to produce the reverse mutant. This COX-1 mutant was subsequently evaluated for its effect on INDO-amide inhibitor potency. Although most neutral NSAID derivatives do not inhibit COX-1, a series of INDO ethanolamides have been reported to exhibit moderate COX-1 inhibitory activity [16,17]. Thus, (*R*)-2-(1-(4-chlorophenylcarbonyl)-5-methoxy-2-methyl-1*H*-indol-3-yl)-*N*-(1-hydroxybutan-2-yl)ethanamide (**8**) was chosen as a probe for the impact of the M472L mutation in a COX-1 background. The human COX-1 mutant was expressed in HEK293T cells and stably transfected cells evaluated for sensitivity to **8** compared to wild-type protein expressed from the same vector. Compound **8** displayed a 14-fold higher potency against the M472L mutant than hCOX-1 (Fig. 4). Interestingly, the potency of the parent drug, INDO, was not affected by the reverse mutation.

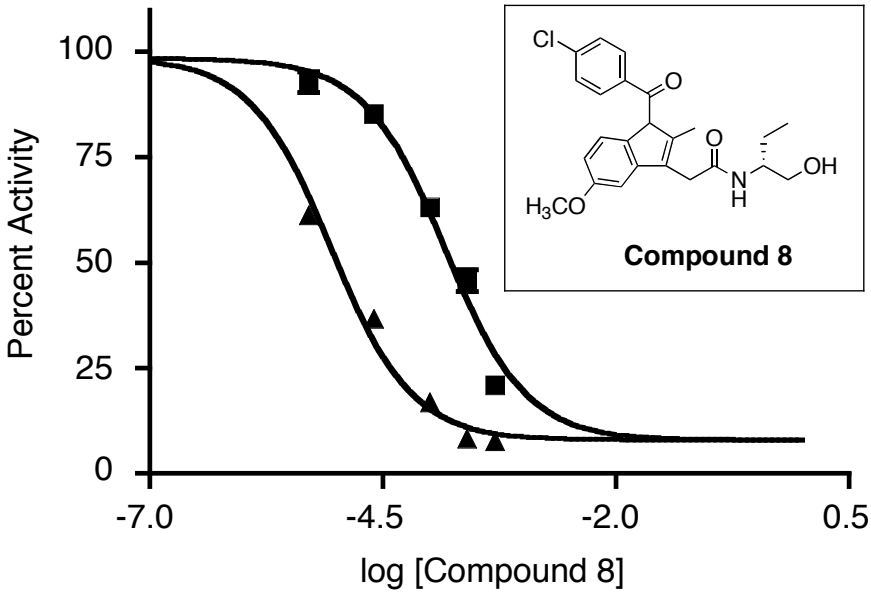

Figure 4. Potency of Compound **8** against hCOX-1 (IC_{50} = 20.1 μM) and M472L (IC_{50} = 1.5 μM) expressed in HEK293T cells with hCOX-1 (squares); M472L (triangles). Experimental errors are s.e.m.

Structural Analysis of L472M - Residue 472 is located in a turn that links two alpha helices comprised of residues 463-470 and 478-482. This turn is stabilized by a network of backbone hydrogen bonds that includes, in all COX crystal structures: 471N-468O, 472N-467O, and 470N-466O. Over the residue range 463-482, no pair of COX-2 X-ray structures exhibits a backbone RMSD greater than 0.4 Å and the 4COX structure we used for model construction has a backbone RMSD of 0.36 Å vs. the 2.0 Å COX-1 structures (2AYL and 1Q4G)[18,19]. In all COX crystal structures, Leu-472 and Met-472 are packed similarly, with a χ_1 dihedral angle of -60 ± 15°, and χ_2 of 180 ± 25°. Residue 472 is adjacent to the constriction site residue, Glu-524. The invariant backbone and side chain geometry seen in this region of the enzyme allows easy superposition of all COX crystal structures. However, visual and numerical analysis of superimposed COX-1 and COX-2 crystal structures reveals no significant structural differences in the region around residue 472.

Molecular Dynamic Analysis - Since the COX crystal structures do not exhibit any meaningful structural differences near residue 472, we postulated that the L472M mutation in COX-2 might induce a change in local dynamical behavior, and we performed 20 ns molecular dynamics simulations and quasi-harmonic analysis for both wild-type and L472M mutant proteins to explore this possibility. The RMSD for binding site residue backbone atoms (vs. the *4COX* reference crystal structure) is less than 1.3 Å for each monomer in both mCOX-2 and L472M simulations. Typical COX hydrogen-bonding interactions among constriction site residues and transient bridging waters are preserved as seen in the crystal structures. The backbone atom RMSD for residues 463-

482, which includes the helices flanking residue 472, is less than 1.0 Å, relative to the 4COX crystal structure. Simple distance analysis shows that the hydrogen bonds that stabilize the turn (residues 471-477 discussed above) are present greater than 90% of the time during the simulations. Leu and Met side chains maintain the same χ_1 and χ_2 torsion angles as seen in crystal structures, varying only ± 30°. Side chain packing analysis shows that residue 472 is well-packed over the entire trajectories for both mCOX-2 and L472M mutant[20].

We performed quasi-harmonic analyses of both trajectories to examine more carefully possible changes in local dynamics conferred by the mutant. The lowest frequency quasi-harmonic modes show clearly that L472M strongly impacts local dynamics in the constriction site region, as can be seen in the online Supplemental Movies. In mutant enzyme, the lowest frequency modes manifest themselves as concerted motions of Glu-524 and Arg-120 side chains. In the mCOX-2 enzyme, these motions are, by comparison, much less strongly coupled. To explore the structural effect these differential motions might have, we used our Channel_Finder utility to conduct a frame-by-frame analysis of the width of the main channel that runs from the lobby region, through the constriction site, and into the active site[21]. The results, shown in Fig. 5, demonstrate that the constriction site opens much more widely and frequently in mCOX-2 compared to the L472M protein. Thus, these channel width measurements reflect, structurally, the motions observed in the quasi-harmonic analyses.

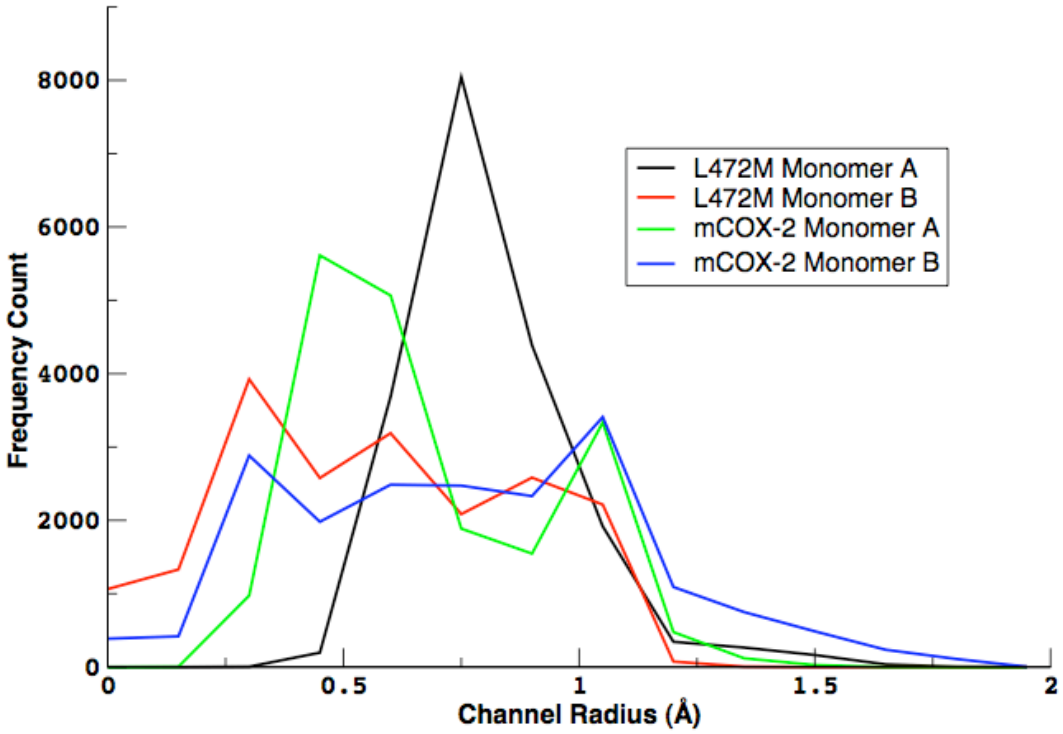

Figure 5. Main channel radii histograms for the mCOX-2 and L472M mutant MD trajectories. Radii values are computed every picosecond over the final 19 ns of each trajectory. While all radii values are displayed here, the channel is considered closed if the channel radius is smaller than 0.7 Å (the minimum navigable radius for a water molecule).

The quasi-harmonic analyses and Channel_Finder results suggest that the L472M substitution alters local dynamics which, in turn, leads to further stabilization of the tightly bound constriction site residues and reduces the frequency of transient constriction site opening.

As noted above, the L472M mutation causes no statistically significant structural displacements in the protein backbone around residue 472 or any nearby residue side chains. Indeed, the local protein geometry, including the residue 472 side chain orientation and packing, is highly conserved throughout both wild-type and mutant

simulations, as well as in all published COX-1 and COX-2 crystal structures, and one can therefore easily superimpose all trajectory configurations onto a common backbone reference structure. We then projected the low-frequency vibrational modes computed in the quasi-harmonic analyses onto this common backbone reference structure to examine the structural effects of the altered local dynamics. The L472M substitution decreases the Glu-524 side chain fluctuations anisotropically by 0.2 - 0.3 Å, along an axis that projects from the residue 472 side chain through the Glu-524 side chain to the Arg-120 side chain. The Glu-524 side chain fluctuations in the orthogonal directions are unaltered between mCOX-2 and L472M mutant simulations. This anisotropic reduction in Glu-524 side chain fluctuation effectively reinforces the Glu-524/Arg-120 hydrogen- bonding interaction, by diminishing the normal thermal fluctuation that would lengthen, or even transiently break, the Glu-524/Arg-120 hydrogen bond. The mechanistic explanation for this effect is quite simple: the Met-472 side chain is slightly longer than Leu-472, as seen in Fig. 6, and thus physically reduces the range of motion possible for the Glu-524 side chain along the Met-472/Glu-524/Arg-120 axis described above. The 'reinforced' Glu-524/Arg-120 hydrogen bond in turn stabilizes the constriction site network and reduces the constriction site opening frequency and open-state diameter.

Figure 6. Leu-472 superimposed on Monomer A from a typical snapshot of the COX-2 Met-472 trajectory.The constriction site residues are labeled. Double-headed arrows display the change in anisotropic fluctuations of Glu-524, relative to the helices flanking position 472. Along this axis, Glu-524 sidechain atoms fluctuate 0.2 to 0.3 Å less (yellow arrow) when adjacent to Met-472 (white), vs. mCOX-2 Leu-472 (white arrow).

Kinetic Analysis of L472M COX-2-Inhibitor Association and Dissociation - The computational analysis suggests differential constriction site dynamics between mCOX-2 and L472M contributes to their differential sensitivity to inhibition by indomethacin-amides. To test this hypothesis, we performed a series of experiments to compare the kinetics of inhibitor association and dissociation to mCOX-2 and L472M enzymes. INDO and INDO-esters and amides are slow, tight-binding inhibitors that exhibit a two-step kinetic mechanism for inhibition (eq 1)[13,22-24].

$$E + I \underset{k_{-1}}{\overset{k_1}{\rightleftharpoons}} E - I \underset{k_{-2}}{\overset{k_2}{\rightleftharpoons}} E - I^* \qquad K_I = k_{-1}/k_1$$

Concentration-dependent binding experiments were performed using *N*-(4-bromobenzyl)-2-(1-(4-chlorophenylcarbonyl)-5-methoxy-2-methyl-1*H*-indol-3-yl)ethanamide (**2**) to compare the kinetics of inhibition for mCOX-2 and L472M more closely. The selection of **2** was based upon its relatively slow rate of binding to mCOX-2 as well as its measurable binding to L472M. The other INDO-amides in Table 1 associated with L472M so slowly that reliable kinetic measurements were not possible across a range of concentrations at which they were soluble. The rate constants (k_{obs}) were measured by monitoring the quenching of intrinsic protein fluorescence at increasing concentrations of **2** against both enzymes. The k_{obs} values were calculated for each concentration time-course by fitting to a single exponential decay. A plot of k_{obs} vs the concentration of **2** (Fig. 7) fit to a hyperbola described by equation 2:

$$k_{obs} = \frac{k_2\,[I]}{K_D + [I]} + k_{-2}$$

Figure 7. a) Concentration dependence of the observed rate of association by Compound **2** with both mCOX-2 and L472M with mCOX-2 (squares); L472M (triangles).b) Dissociation of compound **2** from L472M (black) and mCOX-2 (red) measured with arachidonic acid as the competitor by monitoring the return of intrinsic protein fluorescence. Experimental errors are s.e.m.

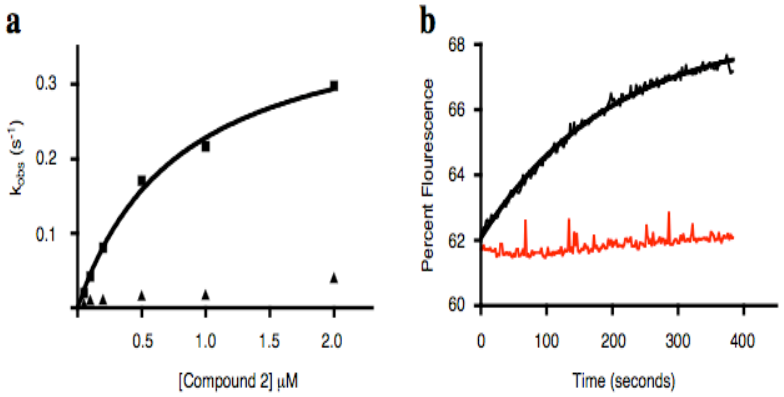

The k_{obs} values for L472M were dramatically reduced compared to those from mCOX-2, which is consistent with reduced dynamics of inhibitor binding. The K_D values calculated from these data were 0.34 ± 0.04 μM and 1.5 ± 0.09 μM for mCOX-2 and L472M respectively. These values corresponded closely to the K_I's for inhibition by **2** determined by radiochemical analysis (0.32 ± 0.03 μM and 1.8 ± 0.3 μM, respectively). The value of the forward rate constant of the second-step, k_2, was determined to be 0.414 $\pm$ 0.021 s^{-1} for mCOX-2 but could not be determined within experimental error for L472M by this method because it was so low.

A non-zero intercept on the y-axis of the plot of k_{obs} vs. [**2**] indicated reversible binding to L472M. The value appeared to by greater than that of mCOX-2 but neither value could be reliably determined. We addressed the question of the effect of the L472M mutation on reversibility, *via* modulation of k_{-2}, more directly through steady-state fluorescence experiments using the substrate AA as a competitor. After a pre-incubation time sufficient to ensure equilibrium for the binding of **2** to each enzyme, the recovery of intrinsic protein fluorescence was monitored after the addition of AA at a final concentration of 25 μM. An increase in intrinsic enzyme fluorescence was only observed for L472M that exhibited a rate constant of $0.0056 \pm 0.0003\ s^{-1}$. No increase in fluorescence was observed for mCOX-2.

Considering the result of **2**, we undertook experiments to determine the reversibility of other INDO-amides (**3, 4,** and **7** in Table 1) whose association to L472M was so slow that they could not be reliably measured by fluoroscopy over a range of concentrations at which they were soluble. Compounds were incubated with mCOX-2 or L472M enzymes for 120 minutes to ensure equilibrium was reached for both systems. Then a saturating concentration of AA (50 μM) was added and the percentage of product production relative to the DMSO control was determined at different time points (15 s - 300 s) by LC/MS/MS quantification of PGE_2/PGD_2. The time course of AA oxygenation corresponds to the rate of dissociation of the inhibitor from the enzyme. In each case the L472M mutation did hasten dissociation but only between 2-3 fold. These results indicate that the while the L472M mutation has an effect on the k_{off} of INDO-amides as compared to mCOX-2, the magnitude of this change alone is not sufficient to explain the large diminishment of potency (Fig. 8).

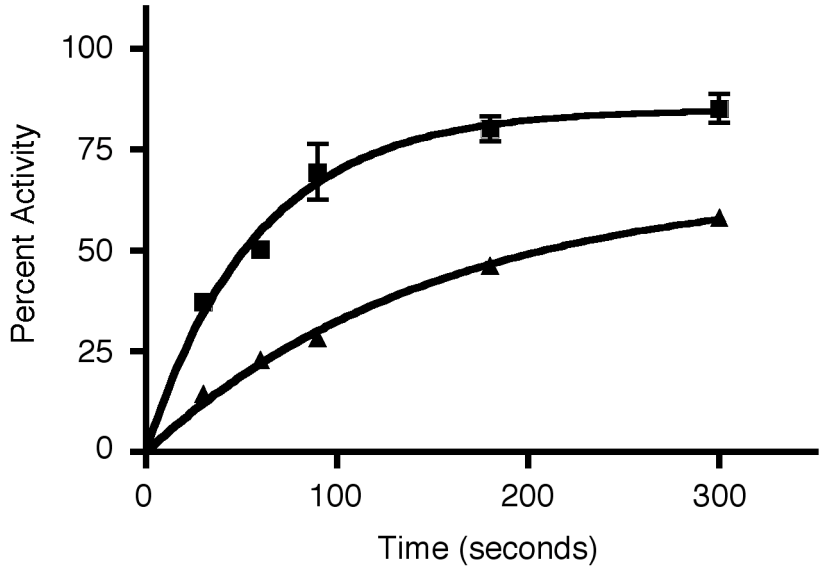

Figure 8. Kinetics of dissociation of compound **4** from both L472M (squares) and mCOX-2 (triangles) after pre-equilibration for 120 minutes to ensure equilibria had been reached for each system.

Pre-steady-state analysis of fluorescence quenching by compound **1** was conducted on a stopped-flow instrument to more clearly determine the effect of the L472M mutation on each individual rate constants. The curve obtained from each concentration fit better to a two-phase exponential decay (first exponent, λ_1, and second exponent, λ_2), than to a single-exponential decay. By using an analysis described by Anderson et. al, we determined that the slope of the line obtained by graphing the concentration-dependence of the first exponent (λ_1) and the plateau of the hyperbola obtained by graphing the concentration of the second exponent (λ_2) are equivalent to k_1 and k_2+k_{-2} respectively (eq 1) (full derivation described in Materials and Methods)[25]. The plot of k_1 vs. the concentration of compound **1** for each enzyme clearly showed a reduced rate constant for L472M compared to mCOX-2 (Fig. 9).

a

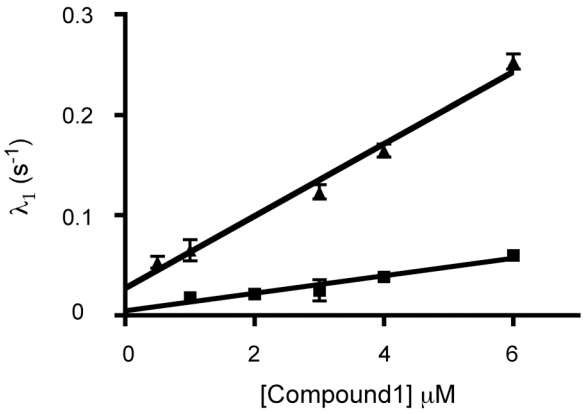

b

	mCOX-2	L472M	mCOX-2/L472M
k_1	0.0360 ± 0.002	0.009 ± 0.001	4.00 ± 0.2
k_2+ k_{-2}	0.0270 ± 0.008	0.005 ± 0.004	5.40 ± 3.5

Figure 9. (A) Concentration dependence of k_1 for binding of Compound **1** to both mCOX-2 (triangles) and L472M (squares). The slope of the lines are equivalent to k_1. (B) presents the rate constants (k_1 and k_2+k_{-2}) for binding of Compound **1** to both mCOX-2 and L472M (* - $\mu M^{-1}s^{-1}$); († - s^{-1}).

This is the first report of a COX mutation that slows the initial phase of inhibitor binding as reflected by k_1. Since k_1 is slower than the diffusion-controlled limit, it reflects both the bimolecular association of inhibitor with enzyme and its movement on the enzyme. In addition to a reduced k_1, the sum of k_{-2}+k_2 is reduced by approximately the same magnitude as k_1 for L472M.

In summary of the results from kinetic analysis of association and dissociation of INDO-amides to mCOX-2 and L472M, we have determined that at least two rate constants are slowed by this mutation; k_1 and k_{-2}. We could not rule out impact on the forward rate constant of the second step, k_2. Additionally, we can infer from stopped-flow experiments that the increase in K_d is due predominantly through altering k_1. It is clear that in order for the potency of an INDO-amide to be substantially attenuated, even a very

modest increase in k_{off} leads to an increase in the portion of EI complex The impact of this effect is subsequently amplified in IC_{50} assays due to the rapid equilibrium back to empty E. Confirmation of this model is that the time-dependence of INDO itself is increased by the L472M mutation, but the IC_{50} is not measurably altered due to the lack of an effect of L472M mutation of reversibility. Additionally, other NSAIDs (celecoxib, diclofenac, piroxicam, and meclofenamic acid) whose potency is not dependent on the second step did not exhibit a change in potency against L472M relative to mCOX-2. It is noteworthy that all of these inhibitors bind entirely in the cyclooxygenase site and do not breach the constriction site.

Discussion

The present study identifies a subtle difference between COX-1 and COX-2 that makes a significant contribution to the sensitivity of COX-2 to inhibition by neutral derivatives of INDO. Conversion of the second-shell Leu residue at position 472 of COX-2 to the Met residue that is present in COX-1 decreases the inhibitory potency of a series of INDO amides relative to wild-type enzyme, decreases the rate of association, and increases the rate of dissociation from the enzyme. The reverse mutation of Met-472 in COX-1 to Leu increases the sensitivity of COX-1 to inhibition by INDO amide, **2**. Although the impact of the L472M mutation in COX-2 is dramatic for some INDO amides, its impact on others is less so, and it is clearly not the sole determinant of the COX-2 selectivity of this class of compounds. Nevertheless, it is the first residue of COX-2 in which a change to a COX-1 residue has any impact on binding and inhibition by INDO amides. This includes a number of conserved first-shell residues that directly contact the inhibitors either in the active site or the lobby beneath it.

Examination of the crystal structures of COX-1 and COX-2 in the region of Leu-472 reveals no detectable differences in backbone configuration or side chain packing. Thus, structural analysis alone is unable to shed light on the mechanism by which this conserved substitution alters inhibitor binding. To probe the origin of this subtle but significant effect, we employed molecular dynamic simulations. Our analyses suggest that the L472M mutation alters low-frequency dynamical motions in the constriction site region, in a manner that effectively reduces the frequency and magnitude of constriction site opening. We propose that this altered dynamical behavior reduces inhibitor binding to the enzyme.

Kinetic analysis of inhibitor binding to wild-type enzyme and L472M is consistent with the results of the molecular dynamics simulations. The L472M mutation slows the rates of both the first and second steps of inhibitor-COX-2 binding that leads to tight association with the enzyme. This is the first example of a mutation that has an effect on the first step of inhibitor binding, a step believed to represent a combination of the initial binding of the inhibitor to the enzyme and its movement through the constriction that separates the lobby from the active site. This first step is normally much faster than the second step, which yields the final, tightly bound E-I* complex. In the case of INDO, the second step is related to insertion of the 2'-methyl group of the indole ring into the hydrophobic depression in the side of the active site. The fact that the L472M mutant exhibits a significantly reduced initial step of both INDO and INDO amide binding implies that it has an effect on the movement of the inhibitor into the active site and is consistent with alterations in constriction site dynamics. The drastic deacrease in potency

is found for INDO amides for which the L472M mutation not only effects the first step, but also the dissociation from the enzyme.

Our results are certainly unanticipated in light of the numerous COX crystal structures, which show clearly that either leucine or methionine can be accommodated at position 472 with no effect on equilibrium structure. Substitution of Met for Leu is one of the most conservative observed in protein families (based on Blossum62 and PAM-250 scoring matrices [26,27]), and it is rather striking that this conservative substitution could cause a nearly 100-fold decrease in potency for some of these COX-2 selective inhibitors. However, the possibility that non-local effects, such as a point mutation, can impact ligand binding and/or enzyme function is not unreasonable. Conformational gating due to fluctuating constriction site opening and closing events has been reported previously for enzyme-ligand binding reactions and there are recent reports that point mutations distal to the enzyme active site can have a notable impact on reaction rates, often due to alteration of equilibrium conformational fluctuations that increase the activation free energy barrier [28-33]. In light of these previous studies, our computational results and mechanistic hypothesis are quite plausible. The specific details of our mechanistic hypothesis are novel, but it is likely that this type of behavior will be observed in many other gated ligand binding reactions as more enzyme complexes are analyzed.

Previous X-ray studies of COX-inhibitor complexes have not provided full rationalizations for analogous differential binding kinetics. For example, flurbiprofen and methyl-flurbiprofen exhibit drastically different binding kinetics and time-dependence of inhibition[9]. Yet, cocrystals of these inhibitors with COX-1 revealed virtually identical structures[9]. Active-site mutagenesis studies have revealed some functional aspects of

COX-2 selective inhibition, but have not previously yielded insights into COX-2 inhibition by INDO-amides. Our work here shows that the synergistic combination of crystallography, functional analysis, and computational techniques is required to tease out critical dynamical details from complicated systems, which currently challenge rational drug design. Other examples of second-shell residues impacting ligand binding are an emerging trend. Our approach should be extensible to the study of these systems, and should provide a sophisticated strategy with which to address this important, expanding, area of scientific study.

References

1. Smith, J.B. & Willis, A.L. Aspirin selectively inhibits prostaglandin production in human platelets. *Nat. New Biol.* **231**, 235-237 (1971).
2. Ferreira, S.H., Moncada, S. & Vane, J.R. Indomethacin and aspirin abolish prostaglandin release from the spleen. *Nat. New Biol.* **231**, 237-239 (1971).
3. Simmons, D.L., Botting, R.M. & Hla, T. Cyclooxygenase isozymes: the biology of prostaglandin synthesis and inhibition. *Pharmacol. Rev.* **56**, 387-437 (2004).
4. Kujubu, D.A., Fletcher, B.S., Varnum, B.C., Lim, R.W. & Herschman, H.R. TIS10, a phorbol ester tumor promoter-inducible mRNA from Swiss 3T3 cells, encodes a novel prostaglandin synthase/cyclooxygenase homologue. *J. Biol. Chem.* **266**, 12866-12872 (1991).
5. Picot, D., Loll, P.J. & Garavito, R.M. The X-ray crystal structure of the membrane protein prostaglandin H2 synthase-1. *Nature* **367**, 243-249 (1994).
6. Kurumbail, R.G. et al. Structural basis for selective inhibition of cyclooxygenase-2 by anti-inflammatory agents. *Nature* **384**, 644-648 (1996).
7. Luong, C. et al. Flexibility of the NSAID binding site in the structure of human cyclooxygenase-2. *Nat. Struct. Biol.* **3**, 927-933 (1996).
8. Smith, W.L., DeWitt, D.L. & Garavito, R.M. Cyclooxygenases: structural, cellular, and molecular biology. *Annu. Rev. of Biochem.* **69**, 145-182 (2000).
9. Selinsky, B.S., Gupta, K., Sharkey, C.T. & Loll, P.J. Structural analysis of NSAID binding by prostaglandin H2 synthase: time-dependent and time-independent inhibitors elicit identical enzyme conformations. *Biochemistry* **40**, 5172-5180 (2001).
10. Rowlinson, S.W. et al. A novel mechanism of cyclooxygenase-2 inhibition involving interactions with Ser-530 and Tyr-385. *J. Biol. Chem.* **278**, 45763-45769 (2003).
11. Rowlinson, S.W., Crews, B.C., Lanzo, C.A. & Marnett, L.J. The binding of arachidonic acid in the cyclooxygenase active site of mouse prostaglandin endoperoxide synthase-2 (COX-2). A putative L-shaped binding conformation utilizing the top channel region. *J. Biol. Chem.* **274**, 23305-23310 (1999).
12. Blobaum, A.L. & Marnett, L.J. Structural and functional basis of cyclooxygenase inhibition. *J. Med. Chem.* **50**, 1425-1441 (2007).
13. Kalgutkar, A.S. et al. Biochemically based design of cyclooxygenase-2 (COX-2) inhibitors: facile conversion of nonsteroidal antiinflammatory drugs to potent and highly selective COX-2 inhibitors. *Proc. Natl. Acad. Sci. U S A* **97**, 925-930 (2000).
14. Kalgutkar, A.S., Marnett, A.B., Crews, B.C., Remmel, R.P. & Marnett, L.J. Ester and amide derivatives of the nonsteroidal antiinflammatory drug, indomethacin, as selective cyclooxygenase-2 inhibitors. *J. Med. Chem.* **43**, 2860-2870 (2000).
15. Prusakiewicz, J.J., Felts, A.S., Mackenzie, B.S. & Marnett, L.J. Molecular basis of the time-dependent inhibition of cyclooxygenases by indomethacin. *Biochemistry* **43**, 15439-15445 (2004).
16. Kozak, K.R., Prusakiewicz, J.J., Rowlinson, S.W. & Marnett, L.J. Enantiospecific, selective cyclooxygenase-2 inhibitors. *Bioorg. Med. Chem. Lett.* **12**, 1315-1318 (2002).

17. Harman, C.A. et al. Structural basis of enantioselective inhibition of cyclooxygenase-1 by S-alpha-substituted indomethacin ethanolamides. *J. Biol. Chem.* **282**, 28096-28105 (2007).
18. Gupta, K., Selinsky, B.S. & Loll, P.J. 2.0 angstroms structure of prostaglandin H2 synthase-1 reconstituted with a manganese porphyrin cofactor. *Acta Crystallogr.* **62**, 151-156 (2006).
19. Gupta, K., Selinsky, B.S., Kaub, C.J., Katz, A.K. & Loll, P.J. The 2.0 A resolution crystal structure of prostaglandin H2 synthase-1: structural insights into an unusual peroxidase. *J. Mol. Biol.* **335**, 503-518 (2004).
20. Gregoret, L.M. & Cohen, F.E. Novel method for the rapid evaluation of packing in protein structures. *J. Mol. Biol.* **211**, 959-974 (1990).
21. Furse, K.E., Pratt, D.A., Porter, N.A. & Lybrand, T.P. Molecular dynamics simulations of arachidonic acid complexes with COX-1 and COX-2: insights into equilibrium behavior. *Biochemistry* **45**, 3189-3205 (2006).
22. Rome, L.H. & Lands, W.E. Structural requirements for time-dependent inhibition of prostaglandin biosynthesis by anti-inflammatory drugs. *Proc. Natl. Acad. Sci. U S A* **72**, 4863-4865 (1975).
23. Thuresson, E.D. et al. Prostaglandin endoperoxide H synthase-1: the functions of cyclooxygenase active site residues in the binding, positioning, and oxygenation of arachidonic acid. *J. Biol. Chem.* **276**, 10347-10357 (2001).
24. Greig, G.M. et al. The interaction of arginine 106 of human prostaglandin G/H synthase-2 with inhibitors is not a universal component of inhibition mediated by nonsteroidal anti-inflammatory drugs. *Mol. Pharmacol.* **52**, 829-838 (1997).
25. Anderson, K.S., Miles, E.W. & Johnson, K.A. Serine modulates substrate channeling in tryptophan synthase. A novel intersubunit triggering mechanism. *J. Biol. Chem* **266**, 8020-8033 (1991).
26. Gonnet, G.H., Cohen, M.A. & Benner, S.A. Exhaustive matching of the entire protein sequence database. *Science* **256**, 1443-1445 (1992).
27. Henikoff, S. & Henikoff, J.G. Amino acid substitution matrices from protein blocks. *Proc. Natl. Acad. Sci. U S A* **89**, 10915-10919 (1992).
28. Zhou, H.-X., Wong, K.-Y. & Vijayakumar, M. Design of fast enzymes by optimizing interaction potential in active†site. *Proc. Natl. Acad. Sci. U S A* **94**, 12372-12377 (1997).
29. Billeter, S.R., Webb, S.P., Agarwal, P.K., Iordanov, T. & Hammes-Schiffer, S. Hydride Transfer in Liver Alcohol Dehydrogenase: Quantum Dynamics, Kinetic Isotope Effects, and Role of Enzyme Motion. *J. Am. Chem. Soc.* **123**, 11262-11272 (2001).
30. Rod, T.H., Radkiewicz, J.L. & Brooks, C.L., III. Correlated motion and the effect of distal mutations in dihydrofolate reductase. *Proc. Natl. Acad. Sci. U S A* **100**, 6980-6985 (2003).
31. Thorpe, I.F. & Brooks, C.L., 3rd. The coupling of structural fluctuations to hydride transfer in dihydrofolate reductase. *Proteins* **57**, 444-457 (2004).
32. Wong, K.F., Selzer, T., Benkovic, S.J. & Hammes-Schiffer, S. Impact of distal mutations on the network of coupled motions correlated to hydride transfer in dihydrofolate reductase. *Proc. Natl. Acad. Sci. U S A* **102**, 6807-6812 (2005).

33. Sergi, A., Watney, J.B., Wong, K.F. & Hammes-Schiffer, S. Freezing a single distal motion in dihydrofolate reductase. *J. Phys. Chem.* **110**, 2435-2441 (2006).
34. Berendsen, H.J.C., Grigera, J.R. & Straatsma, T.P. The missing term in effective pair potentials. *J. Phys. Chem.* **91**, 6269-6271 (1987).
35. Case, D.A. et al. AMBER 9. (University of California, San Francisco, 2006).
36. Levy, R.M., Srinivasan, A.R., Olson, W.K. & McCammon, J.A. Quasi-harmonic method for studying very low frequency modes in proteins. *Biopolymers* **23**, 1099-1112 (1984).

CHAPTER III

SPECIES DIFFERENCE BETWEEN MURINE AND HUMAN CYCLOOXYGENASES INFLUENCES 2-ARACHIDONOYL GLYCEROL METABOLISM

Introduction

The two isoforms of cyclooxygenase (COX), COX-1 and COX-2, are very similar in structure with 60% global sequence identity and nearly superimposable three-dimensional structure. However, they are divergent in some functional aspects. COX-1 is constitutively expressed in nearly all tissues and is thought to be responsible for mainly homeostatic functions such as stomach cytoprotection and regulation of platelet function. In contrast, COX-2 expression is inducible in most tissues and is thought to be involved in the regulation of cell proliferation and the inflammatory response[1-18].

COX isoforms have comparable kinetic values for conversion of the substrate arachidonic acid (AA) to prostaglandin H_2 (PGH_2). In contrast, neutral derivatives of AA such as the endocannabinoids, such as 2-arachidonoyl glycerol (2-AG) and arachidonoyl ethanolamide (AEA) have been reported to be COX-2-selective substrates. They are oxygenated by COX-2 into the corresponding prostaglandin endoperoxides which are converted into prostaglandin glyceryl esters (PG-Gs) or prostaglandin ethanolamides (PG-EA)[19-21].

To clarify the molecular determinants of COX-2 oxygenation of 2-AG, experiments using purified site-directed mutant enzymes of mCOX-2 have been reported. It was hypothesized that 2-AG was oriented similarly to AA in the cyclooxyenase active site of COX-2 because the products produced had analogous positional and

stereospecificity [19, 20]. This hypothesis was confirmed through mutagenesis studies on residues key for oxygenation (the catalytic Tyr-385) and binding (constriction site residues) of AA. The Y385F mutant severely attenuated oxygenation of 2-AG. The constriction site residues, Tyr-355, Glu-524, and Arg-120, participate in a hydrogen-bonding network that divides the cyclooxygenase active site from the lobby region of the membrane-binding domain. Mutation of Arg-120 to Gln diminished 2-AG oxygenation 9-fold. Additionally, the mutation of Glu-524 to leucine diminished 2-AG turnover by 66% relative to wt enzyme [19, 20, 22]. The identity of constriction site residues are conserved across all known sequences of both COX-1 and COX-2. As such, these residues cannot account for varying abilities across isoforms, and now homologues, of cyclooxygenases to metabolize 2-AG.

Other studies using site-directed mutagenesis were focused around the region of the COX-2 cyclooxygenase active know as the side-pocket that is not readily available in COX-1 due to the change from a valine in COX-2 to a bulkier isoleucine in COX-1. Two other residues that are divergent between COX-2 and COX-1 are R513H/Q and V434I respectively. The mutagenesis of R513H and V434I in a mCOX-2 background had the greatest impact on the capacity of these enzymes to metabolize 2-AG [19, 20].

In addition to mutagenesis studies, recently reported experiments using freshly harvested murine resident peritoneal macrophage (RPM) cells, which contain a high basal level of mCOX-1, showed that production of PG-Gs due to zymosan treatment did not increase concomitantly with the induction of mCOX-2 expression from pre-treatment with lipopolysaccharide (LPS). It is noteworthy that the production of PGs from exogenous AA was much higher than the production of PGGs from exogenous 2-AG

from zymosan treated RPM cells. The administration of the COX-2-selective inhibitor SC236 only decreased PG-G production by 60% [Rouzer, Marnett, JBC, 2005]. Additionally, the RPM cells harvested from COX-1 (-/-) animals produced 15% as much PG-Gs after LPS and zymosan treatment as compared to cells from wt animals [23-27].

These results give indirect evidence that COX-2 is not solely responsible for PG-G synthesis in murine macrophages challenged with inflammatory stimuli. Since the majority of animal models used for testing therapeutics and studying endocannabinoid signaling are established in the mouse, we directly investigated whether species differences would affect the ability of COX-1 to metabolize 2-AG.

Experimental Procedures

Materials 2-AG and PGE_2-d_4 was purchased from Cayman Chemical (Ann Arbor, MI). AA was obtained from NuChek Prep (Elysian, MN). All mutagenesis primers were purchased from Operon Technologies (Alameda, CA). Mammalian cell lines were purchased from ATCC. Lipofectamine, molecular biology enzymes, vectors, and cell media was purchased from Invitrogen Corporation (Carlsbad, CA).

Construction of M472L/hCOX-1 - A 2599 nucleotide cDNA containing the 1800 base pair open reading frame encoding wild type human COX1 was ligated into the *NheI* and *NotI* restriction sites of the expression vector pcDNA3.1 Hygro(+) (Invitrogen, Carlsbad, CA). Site directed mutagenesis of codon 471 from methionine (wild type) to leucine (mutant; M472L) was performed by PCR using the primers: 5'-GAGGTTTGGCCTGAAACCCTACACC-3' and 5'-

GCCAAACCTCTTGCGGTACTCATTG-3'. PCR was performed for 30 cycles using LA Taq, then digested with *DpnI* prior to transformation into XL1-Blue competent *E. coli* . To obtain stable transfectants, 293t/17 cells (ATCC) were grown to 70% confluence in DMEM supplemented with 10% fetal bovine serum in 10 cm plates and transfected with 5 μg plasmid DNA using Lipofectamine 2000 according to manufacturer's protocol. After transfection, cells were selected using 200 μg/ml Hygromycin B for four passages, and plated at 70% confluence in 6-well plates for cyclooxygenase activity assays.

Cyclooxygenase Activity Assays - The cells (HEK293T for COX-1, CHOK1 for COX-2) transfected with the appropriate enzyme were plated at 70% confluence in 6-well plates and 900 μL serum-free media applied (DMEM and F-12 respectively). Each enzyme was treated with either arachidonic acid (AA) or 2-arachidonoyl glycerol (2-AG) at 25 μM for 6 minutes at 37^{o} C with 5% CO_2. Media (600 μL) was removed and added to an equal volume of acidified ethyl acetate containing deuterated internal standards (PGE_2-d_4 and PGE_2-G-d_5). The organic layer was extracted, evaporated, and reconstituted in 1:1 methanol:water for LC/MS/MS analysis.

LC/MS/MS Analysis - The analytes were separated chromatographically by reverse-phase HPLC using a 3μ C18(2) Luna column (50 x 2.0 mm) from Phenomenex. The elution was accomplished by an isocratic method of 66% A, 34% B (component A = 5 mM ammonium acetate at pH 3.3 and component B = acetonitrile with 10% component A) with a flow rate of 0.375 mL/minute. The non-enzymatic degradation products of

unstable PGH_2 (from AA turnover), PGE_2 (rt = 3.6 min)and PGD_2 (rt = 3.8 min), were resolved chromatographically and assessed using electrospray ionization in positive mode (ESI^+) with selective reaction monitoring (370.13 → 317.13). The non-enzymatic degradation products of unstable PGH_2-G (from 2-AG turnover), PGE_2-G (1-isomer rt = 2.3, 2-isomer = 2.4) and PGD_2-G (1-isomer = 2.5, 2-isomer = 2.6), were resolved chromatographically and assessed using ESI^+ ionization with selective reaction monitoring (444.13 → 391.13)[28].

Quantitation of Substrate Turnover - Quantitation of AA turnover was accomplished by dividing the sum of the area under the curve for PGE_2 and PGD_2 by the area under the curve for PGE_2-d_4 (374.13 → 321.13) to give $(PGs)_{response}$. Similarly, quantitation of 2-AG turnover was accomplished by dividing the sum of the area under the curve for both the 1 and 2-isomer of PGE_2-G and PGD_2-G by the area under the curve for PGE_2-G-d_5 (449.13 → 396.13) to give $(PGGs)_{response}$. The substrate selectivity ratio was determined by dividing the $(PGGs)_{response}$ by $(PGs)_{response}$.

Results and Discussion

Mutation of Residue 472 – Residue 472 is positioned behind the constriction site residue Glu-524, which has already been reported as a key for 2-AG oxygenation by COX-2. However, residue 472 is not in the active site and is assumed to make no direct contact with either 2-AG or AA. In considering all cyclooxygenases, the identity of residue 472 is either leucine or methionine. However, residue 472 is not categorically conserved by isoform but rather is leucine in all COX-2 homologues as well as rodent COX-1 homologues but is methionine in human and ovine COX-1 (Figure 1).

	465							472				
mCOX-1	E	Y	R	K	R	F	G	L	K	P	Y	T	S
rCOX-1	E	Y	R	K	R	F	G	L	K	P	Y	T	S
hCOX-1	E	Y	R	K	R	F	G	M	K	P	Y	T	S
oCOX-1	E	Y	R	K	R	F	G	M	K	P	Y	T	S
mCOX-2	E	Y	R	K	R	F	S	L	K	P	Y	T	S
rCOX-2	E	Y	R	K	R	F	S	L	K	P	Y	T	S
hCOX-2	E	Y	R	K	R	F	M	L	K	P	Y	E	S
oCOX-2	E	Y	R	K	R	F	L	L	K	P	Y	E	S

Figure 1. Portion of a sequence alignment of rodent, human, and ovine cyclooxygenases highlighting resiude 472

We constructed a M472L mutant in an hCOX-1 background (designated M472L/hCOX-1) to investigate if the identity of residue 472 is a determinant for neutral substrate turnover. Additionally, we cloned L472M in a mCOX-1 background (designated L472M/mCOX-1) in an attempt to make a mCOX-1 identical to its human homologue at position 472.

2-AG Metabolism by COX-1 Enzymes – Cellular assays can simulate *in vivo* activity better than purified enzyme activity assays. The vectors of the four COX-1 enzymes were (mCOX-1, L472M/mCOX-1, M472L/hCOX-1, hCOX-1) were transfected into HEK293T cells and treated with either AA or 2-AG. The non-selective substrate AA was used to ensure enzyme viability and to estimate transfection levels. Culture medium removed after 6 minutes of metabolism and lipid products extracted with acidified ethyl acetate containing deuterated internal standards (PGE_2-d_4 and PGE_2-G-d_5). The amount of the unstable PGH_2 or PGH_2-G produced was assessed by monitoring the non-enzymatic degradation products (PGE_2 /PGD_2 or PGE_2-G/PGD_2-G respectively) using LC/MS/MS analysis by employing selective reaction monitoring (Figure 2.)

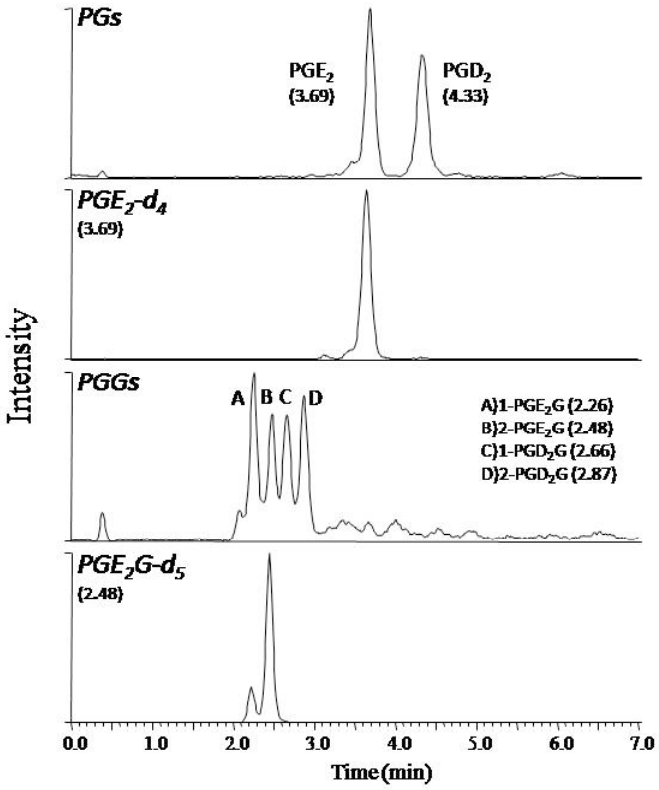

Figure 2. Sample chromatogram of PGs and PGGs with their respective internal Standards. The glycerol head group of PGE_2-G and PGD_2-G can Undergo acyl-migration in aqueouse media giving rise to both the 1 and 2 isomer of each PGG.

Quantification of AA turnover was accomplished by dividing the sum of the area under the curve for PGE_2 and PGD_2 by the area under the curve for PGE_2-d_4 to give $(PGs)_{response}$. Similarly, quantification of 2-AG turnover was accomplished by dividing the sum of the area under the curve for both the 1 and 2-isomer of PGE_2-G and PGD_2-G by the area under the curve for PGE_2-G-d_5 to give $(PGGs)_{response}$.

As anticipated, hCOX-1 treated with 2-AG did not produce any detectable amount of PG-Gs. Strikingly, the wild-type mCOX-1 produced 100 pmol of PG-Gs from 2-AG. The M472L/hCOX-1 point mutation was able to confer the capacity to metabolize 2-AG to produce 106 pmol of PG-Gs. We hypothesized that L472M/mCOX-1 point mutant

would eliminate 2-AG metabolism by the mCOX-1 enzyme. The L472M/mCOX-1 point mutation did diminish the amount of PG-Gs produced by 58% (42 pmol) compared to wild-type mCOX-1 (100 pmol), but did not make it equivalent to hCOX-1 (no PG-Gs produced) (Figure 3). Although the amounts of 2-AG oxygenation varied between the individual enzymes, all these enzymes exhibited AA metabolism comparable to that of the wild-type COX-1 enzymes.

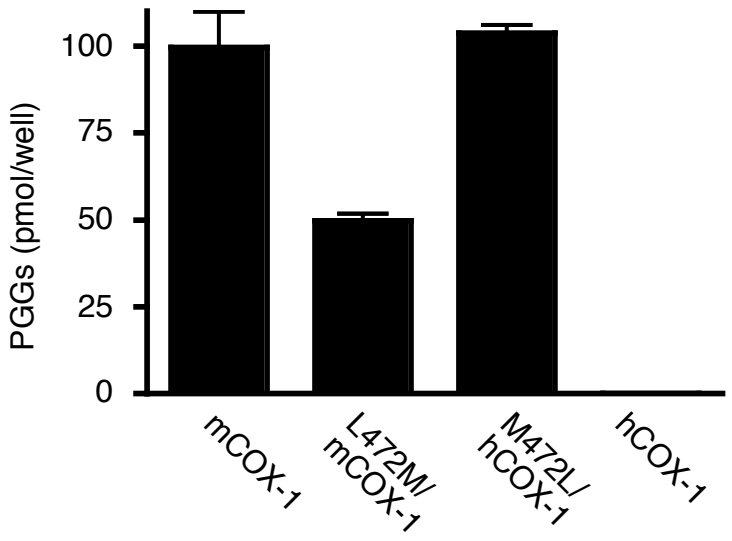

Figure 3. PGGs (pmol/well) produced from 2-AG by COX-1 enzymes wt mCOX-1, L472M/mCOX-1, M472L/hCOX-1, and wt hCOX-1

Substrate Selectivity of COXs - We transfected hCOX-2 and mCOX-2 into CHO-K1 cells to compare the substrate selectivity of 2-AG vs. AA of the COX-2 enzymes relative to COX-1 enzymes. The substrate selectivity ratio for each enzyme was determined by dividing the $(PGGs)_{response}$ /$(PGs)_{response}$ (Figure 4). As such, a substrate selectivity ratio of 1.0 would indicate a given enzyme was equally efficient at oxygenating 2-AG and AA whereas a substrate selectivity ration near zero would indicate 2-AG is a very poor substrate for a given enzyme relative to AA. The substrate selectivity ratio for the COX-2 enzymes, mCOX-2 and hCOX-2, were comparable at approximately 0.36. The substrate selectivity ratio for the 2-AG-metabolizing COX-1 enzymes mCOX-1 and M472L/hCOX-1 was 0.045, nearly 8-fold lower than COX-2 enzymes. The L472M/mCOX-1 enzyme exhibited an even lower substrate selectivity ratio of 0.020.

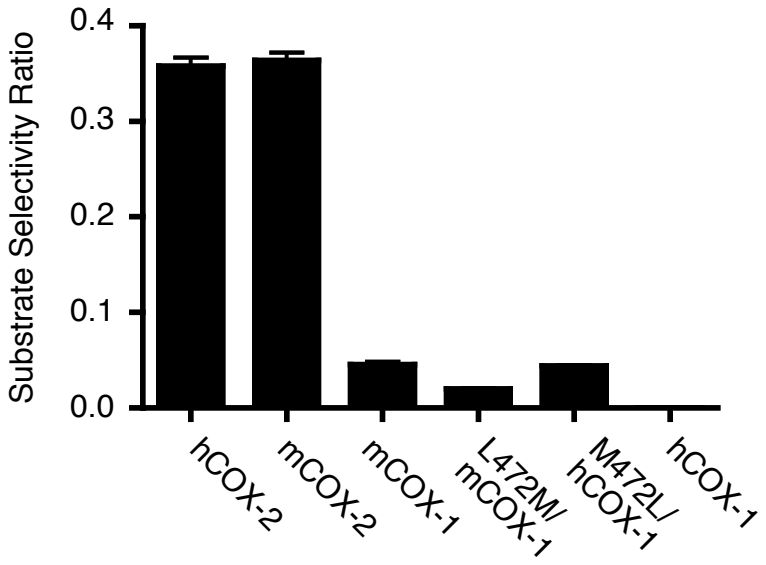

Figure 4. Comparison of substrate selectivity ratio ($(PGGs)_{response}/(PGs)_{repnse}$) by COX enzymes wt hCOX-2, wt mCOX-2, mCOX-1, L472M/mCOX-1, M472L/hCOX-1, hCOX-1

While these experiments indicate that no studied COX-1 enzyme was as efficient at 2-AG turnover as COX-2 enzymes, there are several other factors that may come to bear in an *in vivo* setting. The levels and timing of expression of COX-1 and COX-2 enzymes in a given mouse tissue would have an impact on the contribution of each enzyme to the production of PG-Gs by changing the relative amounts of enzymes. Additionally, the accessibility of each enzyme to each substrate in a cellular system is still poorly understood. However there is increasing evidence that multiple and separate pools of each of these lipids exist in cells.

In this report we have shown that wt mCOX-1, in stark contrast to hCOX-1 has the capacity to produce PG-Gs from exogenous 2-AG in a cellular system. We have also shown that the identity of a second-shell residue, 472, is one of the molecular determinants in 2-AG metabolism. Mutating residue 472 from a methionine to a leucine

in hCOX-1 was able to confer the ability to metabolize 2-AG. Similarly, changing leucine to methionine in mCOX-1 diminished this capacity.

The ability of COX enzymes to selectively oxygenate endocannabinoids raises the exciting possibility that the ultimate products of the oxygenation exert a range of biological effects analogous to prostaglandin metabolites of arachidonic acid[29, 30]. Additionally, the ability of rodent COX-1 to oxygenate 2-AG needs to be carefully considered when designing model systems to study the biology and pharmacology of these interesting molecules.

References

1. Hla, T.; Neilson, K., Human cyclooxygenase-2 cDNA. *Proc Natl Acad Sci U S A* **1992,** 89, (16), 7384-8.
2. Fu, J. Y.; Masferrer, J. L.; Seibert, K.; Raz, A.; Needleman, P., The induction and suppression of prostaglandin H2 synthase (cyclooxygenase) in human monocytes. *J Biol Chem* **1990,** 265, (28), 16737-40.
3. Kujubu, D. A.; Fletcher, B. S.; Varnum, B. C.; Lim, R. W.; Herschman, H. R., TIS10, a phorbol ester tumor promoter-inducible mRNA from Swiss 3T3 cells, encodes a novel prostaglandin synthase/cyclooxygenase homologue. *J Biol Chem* **1991,** 266, (20), 12866-72.
4. O'Banion, M. K.; Sadowski, H. B.; Winn, V.; Young, D. A., A serum- and glucocorticoid-regulated 4-kilobase mRNA encodes a cyclooxygenase-related protein. *J Biol Chem* **1991,** 266, (34), 23261-7.
5. Raz, A.; Wyche, A.; Fu, J.; Seibert, K.; Needleman, P., Regulation of prostanoids synthesis in human fibroblasts and human blood monocytes by interleukin-1, endotoxin, and glucocorticoids. *Adv Prostaglandin Thromboxane Leukot Res* **1990,** 20, 22-7.
6. Xie, W. L.; Chipman, J. G.; Robertson, D. L.; Erikson, R. L.; Simmons, D. L., Expression of a mitogen-responsive gene encoding prostaglandin synthase is regulated by mRNA splicing. *Proc Natl Acad Sci U S A* **1991,** 88, (7), 2692-6.
7. Smith, W. L.; DeWitt, D. L.; Garavito, R. M., Cyclooxygenases: structural, cellular, and molecular biology. *Annu Rev Biochem* **2000,** 69, 145-82.
8. Xiao, G.; Chen, W.; Kulmacz, R. J., Comparison of prostaglandin H synthase-1 and -2 structural stabilities. *Adv Exp Med Biol* **1999,** 469, 115-8.
9. Bhattacharyya, D. K.; Lecomte, M.; Rieke, C. J.; Garavito, M.; Smith, W. L., Involvement of arginine 120, glutamate 524, and tyrosine 355 in the binding of arachidonate and 2-phenylpropionic acid inhibitors to the cyclooxygenase active site of ovine prostaglandin endoperoxide H synthase-1. *J Biol Chem* **1996,** 271, (4), 2179-84.
10. Garavito, R. M.; Picot, D.; Loll, P. J., Preliminary X-Ray Investigations Into NSAID-Binding to Cyclooxygenase-1. *Am J Ther* **1995,** 2, (9), 611-615.
11. Garavito, R. M.; Picot, D.; Loll, P. J., The 3.1 A X-ray crystal structure of the integral membrane enzyme prostaglandin H2 synthase-1. *Adv Prostaglandin Thromboxane Leukot Res* **1995,** 23, 99-103.
12. Loll, P. J.; Picot, D.; Garavito, R. M., The structural basis of aspirin activity inferred from the crystal structure of inactivated prostaglandin H2 synthase. *Nat Struct Biol* **1995,** 2, (8), 637-43.
13. Garavito, R. M.; Picot, D.; Loll, P. J., Strategies for crystallizing membrane proteins. *J Bioenerg Biomembr* **1996,** 28, (1), 13-27.
14. Loll, P. J.; Picot, D.; Ekabo, O.; Garavito, R. M., Synthesis and use of iodinated nonsteroidal antiinflammatory drug analogs as crystallographic probes of the prostaglandin H2 synthase cyclooxygenase active site. *Biochemistry* **1996,** 35, (23), 7330-40.
15. Picot, D.; Loll, P. J.; Garavito, R. M., X-ray crystallographic study of the structure of prostaglandin H synthase. *Adv Exp Med Biol* **1997,** 400A, 107-11.

16. Luong, C.; Miller, A.; Barnett, J.; Chow, J.; Ramesha, C.; Browner, M. F., Flexibility of the *NSAID binding site in the structure of human cyclooxygenase-2. Nat Struct Biol* **1996,** 3, (11), 927-33.
17. Picot, D.; Loll, P. J.; Garavito, R. M., The X-ray crystal structure of the membrane protein prostaglandin H2 synthase-1. *Nature* **1994,** 367, (6460), 243-9.
18. Kiefer, J. R.; Pawlitz, J. L.; Moreland, K. T.; Stegeman, R. A.; Hood, W. F.; Gierse, J. K.; Stevens, A. M.; Goodwin, D. C.; Rowlinson, S. W.; Marnett, L. J.; Stallings, W. C.; Kurumbail, R. G., Structural insights into the stereochemistry of the cyclooxygenase reaction. *Nature* **2000,** 405, (6782), 97-101.
19. Kozak, K. R.; Crews, B. C.; Morrow, J. D.; Wang, L. H.; Ma, Y. H.; Weinander, R.; Jakobsson, P. J.; Marnett, L. J., Metabolism of the endocannabinoids, 2-arachidonylglycerol and anandamide, into prostaglandin, thromboxane, and prostacyclin glycerol esters and ethanolamides. *J Biol Chem* **2002,** 277, (47), 44877-85.
20. Kozak, K. R.; Crews, B. C.; Ray, J. L.; Tai, H. H.; Morrow, J. D.; Marnett, L. J., Metabolism of prostaglandin glycerol esters and prostaglandin ethanolamides in vitro and in vivo. *J Biol Chem* **2001,** 276, (40), 36993-8.
21. Yu, M.; Ives, D.; Ramesha, C. S., Synthesis of prostaglandin E2 ethanolamide from anandamide by cyclooxygenase-2. *J Biol Chem* **1997,** 272, (34), 21181-6.
22. Rieke, C. J.; Mulichak, A. M.; Garavito, R. M.; Smith, W. L., The role of arginine 120 of human prostaglandin endoperoxide H synthase-2 in the interaction with fatty acid substrates and inhibitors. *J Biol Chem* **1999,** 274, (24), 17109-14.
23. Rouzer, C. A.; Marnett, L. J., Non-redundant functions of cyclooxygenases: oxygenation of endocannabinoids. *J Biol Chem* **2008,** 283, (13), 8065-9.
24. Rouzer, C. A.; Tranguch, S.; Wang, H.; Zhang, H.; Dey, S. K.; Marnett, L. J., Zymosan-induced glycerylprostaglandin and prostaglandin synthesis in resident peritoneal macrophages: roles of cyclo-oxygenase-1 and -2. *Biochem J* **2006,** 399, (1), 91-9.
25. Rouzer, C. A.; Marnett, L. J., Structural and functional differences between cyclooxygenases: fatty acid oxygenases with a critical role in cell signaling. *Biochem Biophys Res Commun* **2005,** 338, (1), 34-44.
26. Rouzer, C. A.; Marnett, L. J., Glycerylprostaglandin synthesis by resident peritoneal macrophages in response to a zymosan stimulus. *J Biol Chem* **2005,** 280, (29), 26690-700.
27. Rouzer, C. A.; Ghebreselasie, K.; Marnett, L. J., Chemical stability of 2-arachidonylglycerol under biological conditions. *Chem Phys Lipids* **2002,** 119, (1-2), 69-82.
28. Kingsley, P. J.; Rouzer, C. A.; Saleh, S.; Marnett, L. J., Simultaneous analysis of prostaglandin glyceryl esters and prostaglandins by electrospray tandem mass spectrometry. *Anal Biochem* **2005,** 343, (2), 203-11.
29. Yu, Y.; Fan, J.; Hui, Y.; Rouzer, C. A.; Marnett, L. J.; Klein-Szanto, A. J.; FitzGerald, G. A.; Funk, C. D., Targeted cyclooxygenase gene (ptgs) exchange reveals discriminant isoform functionality. *J Biol Chem* **2007,** 282, (2), 1498-506.
30. Nirodi, C. S.; Crews, B. C.; Kozak, K. R.; Morrow, J. D.; Marnett, L. J., The glyceryl ester of prostaglandin E2 mobilizes calcium and activates signal transduction in RAW264.7 cells. *Proc Natl Acad Sci U S A* **2004,** 101, (7), 1840-5.

CHAPTER IV

DESIGN AND SYNTHESIS OF DUAL INHIBITORS OF CYCLOOXYGENASE-2 AND THROMBOXANE SYNTHASE

Introduction

Cyclooxygenase (COX) performs the committed step in the arachidonic acid cascade by catalyzing the conversion of ararchidonic acid to prostaglandin H_2 (PGH_2) [1-3]. PGH_2 serves as the key intermediate for all downstream prostaglandins, including prostacyclin (PGI_2). and thromboxane A_2 (TXA_2)(Figure 1). TXA_2 is an unstable and potent mediator of vasoconstriction and inducer of platelet aggregation [4-6] produced by thromboxane synthase (TXAS), a cytochrome P450 enzyme [7]. Though also produced by a cytochrome P450 enzyme (prostaglandin I synthase) and similarly unstable, PGI_2 chiefly prevents platelet aggregation and acts as a vasodilator (Figure 1) [8-10].

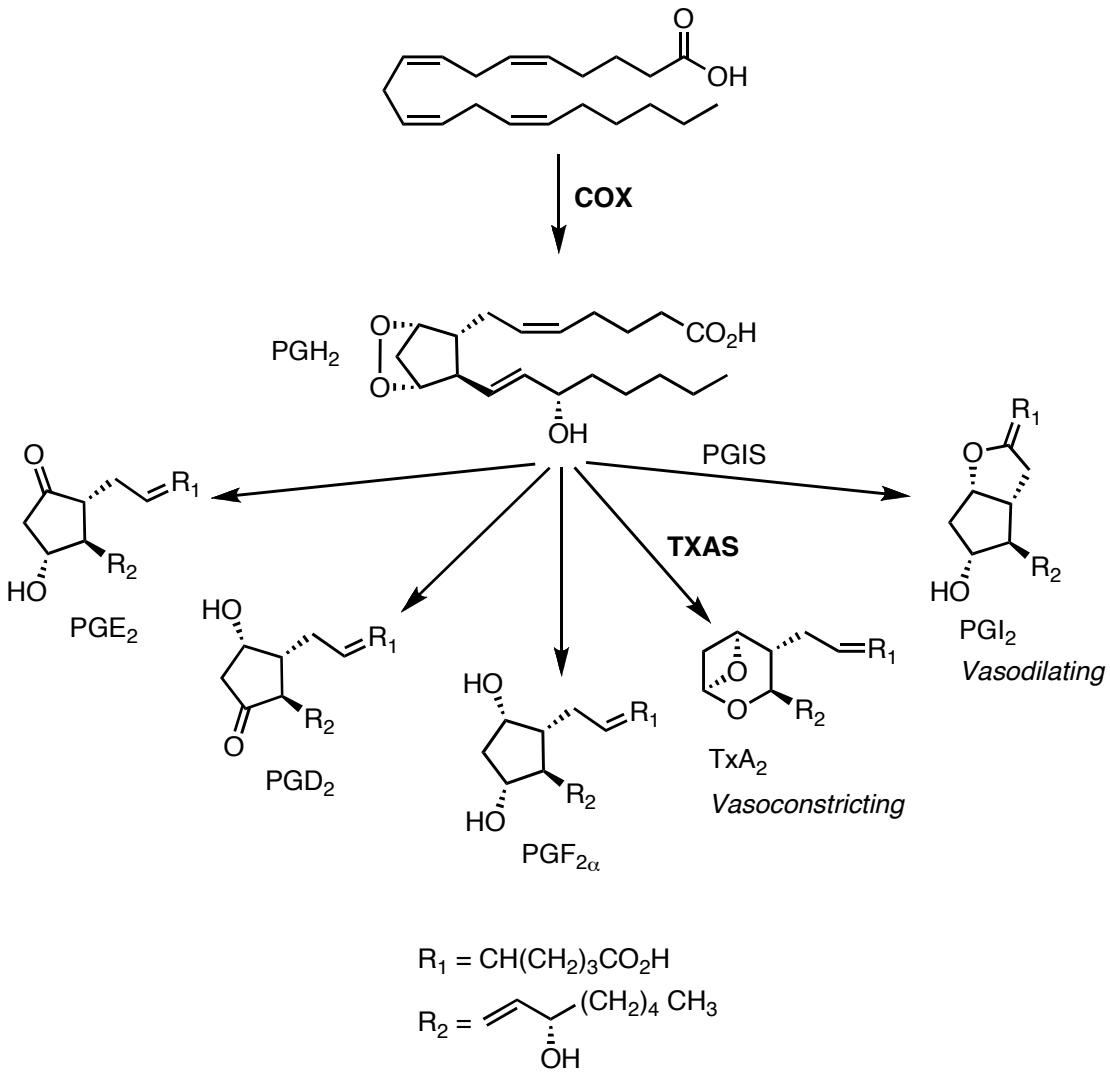

Figure 1. Metabolic pathway for the formation of the vasoactive eicosanoids PGI_2 and TXA_2 from the lipid arachidonic acid through the enzymatic action COX

Inhibition of COX isoforms, COX-1 and COX-2, by aspirin and other non-steroidal anti-inflammatory drugs (NSAIDs), including indomethacin (INDO) has been a therapeutic strategy for treating pain and inflammation since 1899[11-13]. Unfortunately, long-term use of these drugs led to ulcerogenecity caused by inhibition of the COX-1 isoform. Subsequently, the strategy was undertaken to design COX-2 selective inhibitors

(COXIBs) and was proven to be successful with the commercial launch of both rofecoxib and celecoxib. It was also found that chemical neutralization of carboxylic acid-containing NSAIDs, such as INDO, to an ester or amide would afford a COXIB (Figure 2.) [14-17].

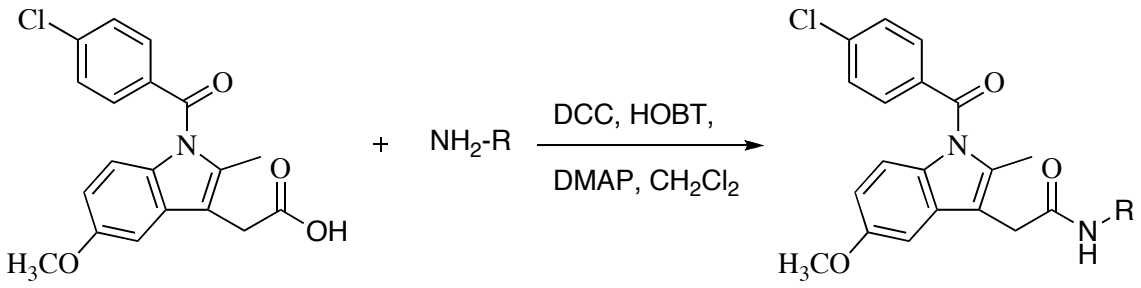

Indomethacin
Non-selective

Indomethacin Amide
Selective for COX-2

Figure 2. Transformation of the non-selective NSAID Indomethacin to a COX-2 selective inhibitor can be accomplished through facile chemistry such as amidation

Unexpectedly, unanticipated cardiovascular side effects resulted in rofecoxib being pulled from the market and led to an FDA black-box warning on celecoxib. The cause of the cardiovascular toxicity is still unclear, though it has been shown that administration of both rofecoxib and celecoxib decreases the level of vasodilating PGI_2 while having no effect on production of vasoconstricting TXA_2. Currently, the hypothesis is that restoration of the balance between these two vasoactive metabolites would eliminate cardiotoxicity of the, otherwise very effective, COXIBs. We report the design and synthesis of dual inhibitors of COX-2 and TXAS that we propose as proof-of-concept for cardio-protective COXIBs.

Experimental Procedures

Reagents and Solvents - HPLC grade solvents obtained from Fischer (Pittsburgh, PA) were used as for both reactions and purification. Reagent grade chemicals were obtained from Aldrich (Milwaukee, WI), Sigma (St. Louis, MO), Matrix Scientific (Columbia, SC), and Cayman Chemicals (Ann Arbor, MI). All chemicals were used without further purification. Thin layer chromatography was performed on silica plates obtained from Analtech (Newark, DE). The plates were read by UV fluorescence (254 nm). Column chromatography was performed using silica gel 200-300 mesh from Fischer (Pittsburgh, PA).

Instrumental Analysis.- Mass spectra were obtained by electrospray ionization (ESI-MS) on a Finnigan TSQ 7000 triple-quadrupole spctrometer. ^{1}H-NMR were obtained on a Bruker AC 300 MHz NMR spectrometer using $CDCl_3$ from Cambridge Isotopes (Andover, MA) with tetramethyl silane (TMS) as the internal standard. All chemical shifts are reported in ppm downfield from TMS and coupling constants (*J* values) are reported in Hertz (Hz). Chiral HPLC was done on a Waters 2695 Separation Module with UV detection at 254 nm by a Chiral Pak AD 00CE-AB003 column at 35 ^{O}C. An isocratic method of 60% hexanes and 40% isopropanol was used for separation.

TXAS Vector Construction - Thromboxane synthase (TXAS) ampicillin-resistant cDNA plasmid in the PCW vector (obtained from M. Waterman) was mutated by PCR to extend the His-tag with primer of ccg cca tca cca tca cca cca ctg aga tct. The P195A vector was converted to wild-type by PCR with primers gat gtg gtt gcc agc gtc ccg ttt ccg acc. Vectors were expressed in competent *E. coli* BL21(DE3) cells containing the chloramphenicol-resistant plasmid pT-groE, All cDNAs were sequenced prior to use.

TXAS Expression – Transformation of BL21(DE3) cells were transformed by heat shock and grown on plates containing ampicilin and chloramphenicol. A starter culture of 10 mL of LB medium was inoculated with a single colony and grown overnight at 37 ^{o}C at

250 rpm with antibiotics. The starter culture was added to a 1L of LB media containing antibiotics and gamma-aminolevulinic acid (0.3 mM) at 30 ^{o}C and 200 rpm. When the OD_{600} reached 0.5 a subsequent dose of gmma-aminolevulinic acid was added. When the OD_{600} reached 0.9, IPTG (1 mM) was added to induce expression under the *lac* operon. The culture was allowed to grow for 3 days. The cells were subsequently harvested by centrifugation and sonicated by 10 s (6 bursts) bursts on ice (for 60 s between each burst) in the presence of protease inhibitors. The detergent CHAPS was added to 1% (v/v) to the homogenate and incubated for 2 hours. Subsequently, sodium chloride was added to a final concentration of 0.7 M and incubated for an additional 30 min. The homogenate was centrifuged and the lysate used for TXAS inhibition assay.

Western Blotting - Protein lysates were made in 20 mM potassium phoshate, 0.5 M sodium chloride, 5 mM DTT, 0.5% sodium cholate, and 15% glycerol. The protein was electrophoresed on 7.5% SDS-polyacrylamide gels then transferred to PVDF membranes. Membranes were blocked in 5% Blotto milk powder (Santa Cruz) in 0.1% Tween-TBS (TTBS), probed with anti-His tag antibodies in 1% Blotto milk powder with shaking at 4 ^{O}C. The protein was then stained with anti-rabbit secondary antibody, washed, treated with a chemiluminescence detection agent, and exposed to film.

TXAS Inhibition Assay PGH_2 was generated from the incubation of arachidonic acid (50 uM) with OCX-1 isolated from ram seminal vesicles. The mixture was distribute in aliquots of 100 uLto tubes of TXAS lysate (10 uL TXAS lysate added to 90 uL of 100 uM Tris buffer) that varying concentrations of inhibitor or vehicle (TXAS) had been previously added. The reactionwas allowed to proceed for 1 minute before termination with acidified EtOAc containg TXB_2-d_4 as an internal standard. The organic layer was

extracted and evaporated. The residue was then reconstituted in 1:1 MeOH/H_2O for LC/MS/MS analysis.

Chemical Synthesis and Characterization – **Compound 1** A reaction mixture containing indomethacin (300 mg, 1.0 equivalent, 0.84 mmol) in 6 mL of anhydrous CH_2Cl_2 was treated with dicyclohexylcarbodiimide (192 mg, 1.1 equivalent 0.92 mmol), dimethylaminopyridine (10 mg, 0.1 equivalent, 0.084 mmol), and the appropriate amine (1.1 equivalent, 0.92 mmol). After stirring at room temperature for 5 h, the reaction mixture was filtered and the filtrate was concentrated in vacuo. The residue was diluted with water (2x15 mL) and extracted with CH_2Cl_2 (3x15 mL). The combined organic solution was washed with brine (2x15 mL), dried over $MgSO_4$, and filtered, and concentrated *in vacuo*. The crude product was purified by trituration with ethanol to give a yellow precipitate. The solid was collected in a fritted funnel. Compound was obtained as a yellow solid (280 mg, 59%) ^{1}H NMR (300 MHz,$CDCl_3$,ppm) mp = 188 ^{o}C δ 8.40 (d, J = 1.4 Hz, 1H), 8.32 (dd, J_1 = 4.7 Hz, J_2 = 1.4 Hz, 1H), 8.06 (m, 1H), 7.65 (d, J = 8.6, 2H), 7.48 (d, J = 8.6, 2H), 7.24 (m, 1H), 6.94 (d, J = 2.5 Hz, 1H), 6.86 (d, J = 9.0 Hz, 1H), 6.72 (dd, J_1 = 9.0, j_2 = 2.5, 1H), 5.61 (br s, 1H), 3.81 (s, 3H), 3.59 (s, 2H), 3.45 (m, 2H),2.70 (t, J = 6.7 Hz, 2H), 2.04 (s, 3H) ESI-MS (positive) 462 $[C_{26}H_{24}ClN_3O_3+H]^+$ HPLC: rt= 15.1 min, >99%

Compound 2 This compound was prepared in a similar manner as described for **Compound 1.** Compound was obtained as an off-white solid (204 mg , 55%). mp = 178 ^{o}C ^{1}H NMR ($CDCl_3$) δ 8.47 (dd, J = 1.8, 4.3 Hz, 2H), 7.63 (d, J = 13.1 Hz, 2H), 7.47 (d, J = 13.1 Hz, 2H), 7.05 (dd, J = 1.8, 4.3 Hz, 2H), 6.89 (d, J = 2.4 Hz, 1H), 6.84 (d, J = 9.0

Hz, 1H), 6.70 (dd, *J* = 2.4, 9.0 Hz, 1H), 4.40 (d, *J* = 6.3 Hz, 2H), 3.80 (s, 3H), 3.74 (s, 2H), 2.41 (s, 3H) ESI 469 $[C_{25}H_{22}ClN_3O_3 + Na]^+$ HPLC: rt= 17.2 min, >99%

Compound 3 This compound was prepared in a similar maner as described for **Compound 1.** This compound was obtained as a yellow solid (310 mg, 85%). mp = 163 ^oC ^1H NMR ($CDCl_3$) δ 8.24 (d, *J* = 8.4 Hz, 1H), 8.10 (d, *J* = 5.9 Hz, 1H), 7.95 (s, 1H), 7.51 (d, *J* = 13.1 Hz, 2H), 7.08 (m, 1H), 6.94 (d, *J* = 2.4 Hz, 1H), 6.87(d, *J* = 9.0 Hz, 1H), 3.87 (s, 2H), 3.82 (s, 3H), 2.45 (s, 3H) ESI 455 $[C_{24}H_{20}ClN_3O_3 + Na]^+$ HPLC: rt= 17.1 min, >99%

Compound 4 This compound was prepared in a similar manner as described for **Compound 1.** Compound was obtained as an off-white solid (53 mg, 13%) mp = 181 ^oC ^1H NMR ($CDCl_3$) δ 8.48 (dd, *J* = 1.6, 4.4 Hz, 2H), 7.65 (d, *J* = 13.1 Hz, 2H), 7.49 (d, *J* = 13.1 Hz, 2H), 7.04 (dd, *J* = 1.6, 4.4 Hz, 2H), 6.85 (m, 1H), 6.72 (dd, *J* = 2.5, 9.0 Hz, 1H), 5.83 (d, *J* = 7.8 Hz, 1H), 5.10 (quint, *J* = 7.4 Hz, 1H), 3.78 (s, 3H), 3.68 (s, 2H), 2.40 (s, 3H), 1.35 (d, *J* = 7.4 Hz, 3H) ESI 483 $[C_{26}H_{24}ClN_3O_3 + Na]^+$ HPLC: rt= 16.2 min, >99%

Compound 5 This compound was prepared in a similar manner as described for **Compound 1.** Compound was obtained as a yellow solid (60 mg, 16%) mp = 167 ^oC ^1H NMR ($CDCl_3$) δ 8.61 (d, *J* = 4.9 Hz, 2H), 8.41 (br s, 1H), 7.69 (d, *J* = 13.1 Hz, 2H), 7.47 (d, *J* = 13.1 Hz, 2H), 7.02 (t, *J* = 3.2 Hz, 1H), 6.96 (d, *J* = 2.4 Hz, 1H), 6.87(d, *J* = 9.0 Hz, 1H), 6.69 (dd, *J* = 2.4, 9.0 Hz, 1H), 4.03 (s, 2H), 3.80 (s, 3H), 2.44 (s, 3H) ESI 456 $[C_{23}H_{19}ClN_4O_3 + Na]^+$ HPLC: rt= 18.9 min, 98.0%

Compound 6 This compound was prepared in a similar manner as described for **Compound 1.** Compound was obtained as an off-white solid (264 mg, 69%) mp = 183 ^{o}C ^{1}H NMR (300 MHz,$CDCl_3$, ppm) δ 8.54 (s, 1H), 7.60 (m, 4H), 7.49 (m, 2H), 6.85 (m, 2H), 6.70 (d, J = 8.7 Hz, 1H), 6.12 (br s, 1H), 4.47 (s, 2H), 3.79 (s, 3H), 3.72 (s, 2H), 2.39 (s, 3H) ESI-MS (positive) 516 $[C_{26}H_{21}ClF_3N_3O_3]^+$ HPLC: rt=20.0 min, >99%

Compound 9 This compound was prepared in a similar manner as described for **Compound 1.** This compound was obtained as a yellow solid(60 mg, 15%). mp = 171 ^{o}C ^{1}H NMR ($CDCl_3$) δ 7.67 (d, *J* = 13.1 Hz, 2H), 7.46 (d, *J* = 13.1 Hz, 2H), 6.97 (d, *J* = 2.4 Hz, 1H), 6.82 (d, *J* = 9.0 Hz, 1H), 6.64 (dd, *J* = 2.4, 9.0 Hz, 1H), 4.02 (m, 2H), 3.82 (s, 5H), 3.63 (m, 1H), 3.46 (m, 1H), 2.38 (s, 3H) ESI 472 $[C_{24}H_{23}ClN_4O_3+ Na]^+$ HPLC: rt= 16.8 min, 98.7%

Compound 8 This compound was prepared in a similar manner as described for **Compound 1.** Compound was obtained as an off-white solid (320 mg, 69%)^{1}H NMR (300 MHz,$CDCl_3$,ppm) mp = 183 ^{o}C δ 8.40 (d, *J* = 1.4 Hz, 1H) 8.32 (dd, J_1 = 4.7 Hz, J_2 = 1.4 Hz, 1H), 8.06 (m, 1H,), 7.65 (d, J = 8.6 Hz, 2H), 7.50 (m, 3H), 7.25 (m, 1H), 6.94 (d, J= 2.4 Hz, 1H), 6.86 (d, J = 9.0 Hz, 1H), 6.71 (dd, J_1 = 9.0 Hz, J_2 = 2.4 Hz, 1H), 3.84 (s, 2H), 3.81(s, 3H), 2.46 (s, 3H) ESI-MS (positive) 434 $[C_{24}H_{20}ClN_3O_3+H]^+$ HPLC: rt= 18.1 min, 98.7%

Compound 10 This compound was prepared in a similar manner as described for **Compound 1.** Compound was obtained as an off-white solid (250 mg, 59%) mp = 177

^{o}C ^{1}H NMR (300 MHz,$CDCl_3$,ppm) δ 8.15 (d, 1H, J = 2.1 Hz), 7.50 (m, 5H), 7.422 (d, 1H, J = 8.4 Hz), 6.83 (m, 2H),6.69 (dd, J1 = 9 Hz, J2 =2.4 Hz 1H), 6.19 (br t, J = 6 Hz, 1H), 4.37 (d, J = 6Hz, 2H), 3.79 (s, 3H), 3.71(s, 2H), 2.36 (s, 3H) ESI-MS (positive) 482 $[C_{25}H_{21}Cl_2N_3O_3]^+$ HPLC: rt= 19.1 min, >99%

Compound 11 This compound was prepared in a similar manner as described for **Compound 1.**. Compound was obtained as a yellow solid (120 mg, 32%) mp = 181 ^{o}C ^{1}H NMR ($CDCl_3$) δ 8.39 (d, *J* = 4.3 Hz, 1H), 7.68 (d, *J* = 13.1 Hz, 2H), 7.62 (dt, *J* = 1.8, 7.7 Hz, 1H), 7.47 (d, *J* = 13.1 Hz, 2H), 7.15 (m, 2H), 6.92 (d, *J* = 2.4 Hz, 2H), 6.88 (s, 1H), 6.69 (dd, *J* = 2.4, 9.0 Hz, 1H), 4.52 (d, *J* = 5.1 Hz, 2H), 3.79 (s, 3H), 3.72 (s, 2H), 3.39 (s, 3H) ESI 469 $[C_{25}H_{22}ClN_3O_3+ Na]^+$ HPLC: rt= 18.6 min, >99%

Results and Discussion

INDO-Amides as TXAS Inhibitors - Structure-activity relationships (SAR) for TXAS inhibitors emerged from drug discovery efforts in the 1970's and 1980's that were based, in part, by considering the structural requirements for binding substrate and in part from evaluating newly synthesized small molecules. The main SAR garnered from analyzing the substrate was the requirement of a free carboxylate. The requirement for a specific nitrogen heterocycle, either a 3-pyridyl or l-imidazolyl, a certain distance from the carboxylate (6.8-8.0 A) was the SAR that has, until recently, been assumed to be required[18]. Programs in medicinal chemistry were very successful at producing extremely potent inhibitors such as ozagrel (IC_{50} = 10 nM) and furegrelate (IC_{50} = 500 nM) (Figure 12.)[19, 20].

In this study, we chose to further investigate the use of a pyridyl moiety as the pendant group of INDO-amides. In this small library, we utilized pyridyl-containing amines where the nitrogen was located at the 2, 3, or 4 position of the heterocyclic ring relative to the alkyl linker. While the reported requisite SAR for pyridyl-containing TXAS inhibitors is a 3-pyridyl moiety, we found that the position of the nitrogen in the pyrdiyl ring did not correlate with potency against TXAS. The most potent TXAS inhibitors in our library (**Compound 1-4**) with IC_{50} < 100 nM are comprised of INDO-amides containing 2, 3, and 4-pyridyl moieties (Figure 3). Of additional note, none of these potent TXAS inhibitors contain a free-carboxylate group which has also been previously reported as requirement for TXAS inhibition. We also tested whether additional substitution at the 4-position of a 3-pyridyl containing INDO-amide would be tolerated by TXAS. A trifluormethyl group at the 4-position (**Compound 6**) improved potency of it unsubstituted counterpart (**Compound 7**) against TXAS, whereas a chloro substitution at the 4 position (**Compound 10**) eliminated all measurable potency against TXAS.

In addition to varying the location of the nitrogen atom in the pendant heterocyclic ring, we varied the length of the alkyl tether between the pendant ring and the amide nitrogen. Since there is little structural information on this membrane-bound P450 enzyme, we hope to discover important features of this mostly unknown active site by changing the length between carbonyls of the INDO scaffold and the nitrogen in the pyridyl pendant ring and monitoring the effect this modulation has on potency. We used tether links of 0-2 methylene groups. A tether link of 0 methylenes created an aniline-type amide. By extending the alkyl linker, we introduced additional rotation into this

mostly constricted INDO-scaffold. However, we could find no correlation between changing the linker from 0 to 1 methylene groups. The most potent TXAS inhibitor, **Compound 1**, is the only inhibitor in the library that has a 2 methylene linker. Future studies could be developed in this direction to investigate whether this result is meaningful. Substitutions on the linker (methlylene length of 1) by a methyl group did diminish potency against TXAS relative to the corresponding unsubstituted counter part as was the case for **Compounds 2** and **4** as well as **Compounds 7** and **9**. These substitutions do introduce a new chiral center. However, when **Compound 4** was resolved using chiral HPLC each enantiomer had similar potency to that obtained when testing the racemic mixture.

Indo-Amides as COX-2 Inhibitors When designing inhibitors for two separate enzymes, it is a medicinal chemistry balancing act. There is never a guarantee that a compound that is very potent at one enzyme target will be tolerated by the other target. One strategy to circumvent this pitfall is to start with a molecular scaffold where liberal substitutions are well-tolerated against one of the targeted enzymes. This was the case with INDO and COX-2. The only known restriction to retaining potency against COX-2 by amidation of INDO is that the amine used to couple to the acid of INDO cannot be a secondary amine (which would make the tertiary amide). It is key for hydrogen-bonding interactions with the COX-2 active site residues that the INDO-amide be a secondary amide.

The amide portion of INDO-amides are assumed to extend through the constriction site of the COX site into the open lobby region. While INDO-amides were

reported to be COXIBs eight years ago, very little structural information about the interactions of the amide R group with lobby residues is available. The most potent compounds against COX-2 (IC_{50} < 100 nM) in this library are **Compounds 12, 6,** and **10** are all 4-substituted by halogen-containing groups. Additionally, the alkyl linker for each of these compounds is 1 methylene in length. However, including that length of an alkyl linker to the pendant ring does not guarantee potency as **Compound 11** is not a COX-2 inhibitor. Compounds **6** and **10** also contain a 3-pyridyl moiety. Most of the compounds in this library are moderately potent (IC_{50} = 100 – 400 nM) against COX-2 Only **Compounds 2** and **11** are poor COX-2 inhibitors.

As anticipated, the rank order of potency of this small library is not the same for TXAS and COX-2. In the case of inhibition of COX-2 activity, **Compound 12** was the most potent compound against TXAS. It was included in this library as a negative control for TXAS inhibition as it does not contain a nitrogen heterocycle. The other very potent COX-2 inhibitors (IC_{50} < 100), **Compounds 10** and **6,** were not potent or moderately potent respectively against TXAS. Simlarly, the most potent TXAS inhibitor, **Compound 1,** is only moderately potent against COX-2. The ratio of IC_{50}(TXAS)/IC_{50}(COX-2) indicates the selectivity ratio each compound has for the two target enzymes, TXAS and COX-2. In this small library we have been able to design inhibitors with selectivity ratios ranging from 0.06 to 88. These dual inhibitors serve not only as proof-of concept compounds for cardioprotective NSAIDS, but may also serve as novel probes for investigating further the mechanism of COXIB cardiotoxicity.

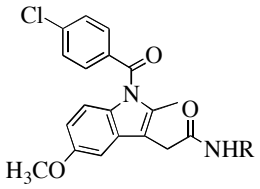

Compound	R	IC_{50}*		IC_{50} (TXAS) / IC_{50} (COX-2)
		mCOX-2	TXAS	
1	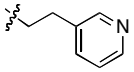	240	53	0.22
2	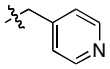	1000	63	0.06
3		210	90	0.43
4	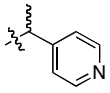	172	92	0.54
5		361	213	0.59
6	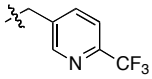	28	293	11
7	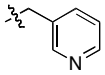	167	340	2.0
8		210	6800	32
9	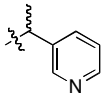	137	12000	88
10	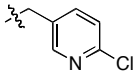	57	>12000	>210
11	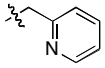	>4000	>12000	n.d.
12	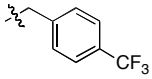	16	>12000	>750

Figure 3. Potency of INDO-amides for COX-2 and TXAS. * All IC_{50}values reported in nM

References

1. Hemler, M. E.; Lands, W. E., Evidence for a peroxide-initiated free radical mechanism of prostaglandin biosynthesis. *J Biol Chem* **1980,** 255, (13), 6253-61.
2. Hamberg, M.; Samuelsson, B., Oxygenation of unsaturated fatty acids by the vesicular gland of sheep. *J Biol Chem* **1967,** 242, (22), 5344-54.
3. Schreiber, J.; Mason, R. P.; Eling, T. E., Carbon-centered free radical intermediates in the hematin- and ram seminal vesicle-catalyzed decomposition of fatty acid hydroperoxides. *Arch Biochem Biophys* **1986,** 251, (1), 17-24.
4. Gryglewski, R.; Vane, J. R., Rabbit-aorta contracting substance (RCS) may be a prostaglandin precursor. *Br J Pharmacol* **1971,** 43, (2), 420P-421P.
5. Palmer, M. A.; Piper, P. J.; Vane, J. R., The release of rabbit aorta contracting substance (RCS) from chopped lung and its antagonism by anti-inflammatory drugs. *Br J Pharmacol* **1970,** 40, (3), 581P-582P.
6. Piper, P. J.; Vane, J. R., Release of additional factors in anaphylaxis and its antagonism by anti-inflammatory drugs. *Nature* **1969,** 223, (5201), 29-35.
7. Needleman, P.; Moncada, S.; Bunting, S.; Vane, J. R.; Hamberg, M.; Samuelsson, B., Identification of an enzyme in platelet microsomes which generates thromboxane A2 from prostaglandin endoperoxides. *Nature* **1976,** 261, (5561), 558-60.
8. Dusting, G. J.; Moncada, S.; Vane, J. R., Prostacyclin (PGX) is the endogenous metabolite responsible for relaxation of coronary arteries induced by arachindonic acid. *Prostaglandins* **1977,** 13, (1), 3-15.
9. Whittaker, N.; Bunting, S.; Salmon, J.; Moncada, S.; Vane, J. R.; Johnson, R. A.; Morton, D. R.; Kinner, J. H.; Gorman, R. R.; McGuire, J. C.; Sun, F. F., The chemical structure of prostaglandin X (prostacyclin). *Prostaglandins* **1976,** 12, (6), 915-28.
10. Moncada, S.; Gryglewski, R.; Bunting, S.; Vane, J. R., An enzyme isolated from arteries transforms prostaglandin endoperoxides to an unstable substance that inhibits platelet aggregation. *Nature* **1976,** 263, (5579), 663-5.
11. Smith, W. L.; Lands, W. E., Stimulation and blockade of prostaglandin biosynthesis. *J Biol Chem* **1971,** 246, (21), 6700-2.
12. Ferreira, S. H.; Moncada, S.; Vane, J. R., Indomethacin and aspirin abolish prostaglandin release from the spleen. *Nat New Biol* **1971,** 231, (25), 237-9.
13. Vane, J. R., Inhibition of prostaglandin synthesis as a mechanism of action for aspirin-like drugs. *Nat New Biol* **1971,** 231, (25), 232-5.
14. Kalgutkar, A. S.; Crews, B. C.; Rowlinson, S. W.; Marnett, A. B.; Kozak, K. R.; Remmel, R. P.; Marnett, L. J., Biochemically based design of cyclooxygenase-2 (COX-2) inhibitors: facile conversion of nonsteroidal antiinflammatory drugs to potent and highly selective COX-2 inhibitors. *Proc Natl Acad Sci U S A* **2000,** 97, (2), 925-30.
15. Kalgutkar, A. S.; Marnett, A. B.; Crews, B. C.; Remmel, R. P.; Marnett, L. J., Ester and amide derivatives of the nonsteroidal antiinflammatory drug, indomethacin, as selective cyclooxygenase-2 inhibitors. *J Med Chem* **2000,** 43, (15), 2860-70.
16. Kalgutkar, A. S.; Rowlinson, S. W.; Crews, B. C.; Marnett, L. J., Amide derivatives of meclofenamic acid as selective cyclooxygenase-2 inhibitors. *Bioorg Med Chem Lett* **2002,** 12, (4), 521-4.

17. Kalgutkar, A. S.; Crews, B. C.; Saleh, S.; Prudhomme, D.; Marnett, L. J., Indolyl esters and amides related to indomethacin are selective COX-2 inhibitors. *Bioorg Med Chem* **2005,** 13, (24), 6810-22.
18. Tanouchi, T.; Kawamura, M.; Ohyama, I.; Kajiwara, I.; Iguchi, Y.; Okada, T.; Miyamoto, T.; Taniguchi, K.; Hayashi, M.; Iizuka, K.; Nakazawa, M., Highly selective inhibitors of thromboxane synthetase. 2. Pyridine derivatives. *J Med Chem* **1981,** 24, (10), 1149-55.
19. Johnson, R. A.; Nidy, E. G.; Aiken, J. W.; Crittenden, N. J.; Gorman, R. R., Thromboxane A2 synthase inhibitors. 5-(3-Pyridylmethyl)benzofuran-2-carboxylic acids. *J Med Chem* **1986,** 29, (8), 1461-8.
20. Iizuka, K.; Akahane, K.; Momose, D.; Nakazawa, M.; Tanouchi, T.; Kawamura, M.; Ohyama, I.; Kajiwara, I.; Iguchi, Y.; Okada, T.; Taniguchi, K.; Miyamoto, T.; Hayashi, M., Highly selective inhibitors of thromboxane synthetase. 1. Imidazole derivatives. *J Med Chem* **1981,** 24, (10), 1139-48.

CHAPTER V

INDOMETHACIN AMIDES AS A NOVEL MOLECULAR SCAFFOLD FOR TARGETING *TRYPANOSOMA CRUZI* STEROL 14α-DEMETHYLASE

Introduction

Chagas disease is an insect-borne parasitic disease threatening millions of lives in Latin America and spreading worldwide as a result of migration (mammalian hosts and insect vectors), HIV-co-infection, blood transfusion and organ transplantation. For example, a recent American Red Cross study indicates that approximately one of 4,700 blood donors in the United States in 2007 tested positive for Chagas [1]. Victims often do not experience specific symptoms during the early stages of the disease, which can either pass unnoticed or be deadly, depending on their immune status to the protozoan parasite *Trypanosoma cruzi* (TC). At the chronic stage, when TC infects human tissues and exists predominantly as the intracellular amastigote, the disease is commonly fatal. Serious cardiac and/or intestinal symptoms develop in 20-40% of infected individuals 10 to 20 years later, the probability increasing up to 70% in immunocompromised patients [2].

Only acute TC infection can be cured with the two currently available drugs, nifurtimox and benznidazole [3]. The drugs are nonspecific, have severe side effects and induce resistance. The demand for new drug candidates has given rise to multiple attempts to use the progress in understanding TC physiology and biochemistry for the development of more specific treatments for Chagas disease[4, 5]. Inhibition of the TC sterol biosynthetic pathway is currently amongst the most promising approaches[6]. Similar to fungi or plants, TC produces 24-methylated/alkylated (ergosterol-like) sterols which

are necessary for membrane formation and cannot be replaced in the parasite membranes by the host cholesterol [7].

We are focusing our attention on sterol 14α-demethylase (CYP51). In TC, this cytochrome P450 enzyme catalyzes a three-step reaction of oxidative removal of the 14α-methyl group from 24-methylene dihydrolanosterol [8]. We have shown recently that specific inhibition of TCCYP51 with imidazole derivatives is highly effective in killing the parasite [9]. In good correspondence with the fact that TCCYP51 has only about 25% amino acid identity to the orthologous fungal enzymes, the structure of the lead compounds we have used differs significantly from the structures of the antifungal imidazole and triazole drugs. However, the compounds still belong to the same class of CYP51 inhibitors, and it is known that azoles currently used as clinical and agricultural fungicides can cause resistance [10]. This may be especially crucial for immunocompromised (especially HIV-infected) patients with Chagas as it is very likely for many of them to also have fungal co-infections and to be treated with azoles for a long time.

In order to investigate other options for the development of alternative sets of potential anti-chagastic drugs, optical high throughput screening of TCCYP51 for binding ligands other than azoles has been undertaken. Several compounds producing type 1 (substrate-like) or type 2 (azole-like) spectral responses in the cytochrome P450 Soret band were identified. Following high throughput screening, a web-database search for similar structures revealed additional TCCYP51 ligands, some of them of higher inhibitory potency. The strongest TCCYP51 inhibitor from this search (more than two-fold decrease in activity at equimolar ratio inhibitor/enzyme ($I/E_2<1$ [9])) demonstrated a

clear antiparasitic effect in the TC cells and was found to have significant structural similarity to indomethacin amide derivatives (COX-2 inhibitors).

Indomethacin (INDO) is a classic non-steroidal anti-inflammatory drug (NSAID) that has been available commercially to treat rheumatoid arthritis since 1963. INDO exerts its anti-inflammatory effect by non-selective inhibition of both cyclooxygenase isoforms, COX-1 and COX-2. Despite the high global sequence homology (>66%) between the COX isoforms, it was discovered that INDO could be converted to a COX-2-selective inhibitor by neutralization of the carboxylic-acid to an ester or amide (INDO-amides) [11, 12]. Additionally, it was found that removing the 2'-methyl group of the INDO scaffold eliminated potency of INDO against both isoforms of COX[13]. INDO is an attractive scaffold for drug development because it is relatively inexpensive, readily converted to amide derivatives, and has a long clinical history. We have synthesized a number of amide derivatives of INDO and find that several of them are potent inhibitors of TCCYP51.

Experimental Procedures

Molecular Cloning - The TCCYP51 gene subcloned into the pCW vector (Nde I/Hind III cloning sites) was expressed in *E. coli* and purified as previously described[8]. The protein was electrophoretically pure, had spectrophotometric index of OD_{417}/OD_{278} of 1.55 and specific heme content of 17 nmol/mg. P450 concentration was determined from the difference spectra of the reduced carbon monoxide complexes using the extinction coefficient of $91 mM^{-1}\ cm^{-1}$ (450-490 nm) [14] or from the absolute absorbance spectra of

the ferric water-coordinated TCCYP51 in the Soret band maximum (417 nm) using the extinction coefficient of 117 mM^{-1} cm^{-1} [8].

High throughput screening (HTS) and web search for similar structures - HTS of the FMP library of small organic molecules (20,000-compounds selected from ChemDiv, San Diego, CA) was performed using a pipetting robot (Sciclone 3000; Caliper Lifesciences), a plate reader for absorbance scanning (Safire; Tecan), and various robots for washing and dispensing. Compounds were dissolved in DMSO at 10 mM stock concentrations and distributed in 0.4-µl aliquots into 384-well microtiter plates. Buffer (40 µl of 50 mM potassium-phosphate buffer, pH 7.4, containing 100 mM NaCl) was added to each well to achieve a 100 µM concentration of the tested compounds. Plates were incubated for 15 min at 37°C and then sonicated for 5 min to allow solubilization of suspensions of the most hydrophobic compounds. Compound-specific changes in absorption spectra (350 to 450 nm) were recorded automatically after adding 10 µl of 5 µM TCCYP51 in 50 mM potassium-phosphate buffer, pH 7.4 containing 100 mM NaCl and 0.1 mM EDTA, optical path length 7 mm, and then validated manually by spectral titration. Search for similar structures was done using the ChemDiv database (http://chemdiv.emolecules.com). The examples of TCCYP51 ligands (shown in Figure 1) identified by HTS are: **1,** 1-(3-amino-4-chlorophenyl)(thien-2-yl)methanone ; **2,** 3-(4-aminophenyl)-2H-chromen-2-one; **3,** [5-(4-Fluoro-benzylidene)-4-oxo-2-thioxo-thiazolidin-3-yl]-acetic acid; **4,** 3-thien-2-yl-5,6-dihydroimidazo[2,1-b][1,3]thiazole; **5**, 3-(2-furyl)-5,6-dihydroimidazo[2,1-b][1,3]thiazole; **6,** 2-phenyl-N-pyridin-4-

ylbutanamide. Compound **5**-like ligands found via web search, ChemDiv numbers: 5556-0480 (**7**); 6903-0018 **(8)**; C155-0123 **(9)**; 3124-0167 **(10)**; 000L-5707 **(11)**.

Synthesis of INDO-amide derivatives **-** Materials and instrumentation were as previously described [12]. A reaction mixture containing indomethacin (300 mg, 1.0 eq, 0.84 mmol) in 6 mL of anhydrous CH_2CL_2 was treated with dicyclohexylcarbodiimide (192 mg, 1.1 eq 0.92 mmol), dimethylaminopyridine (10 mg, 0.1 eq, 0.084 mmol), and the appropriate amine (1.1 eq, 0.92 mmol). After stirring at room temperature for 5 h, the reaction mixture was filtered and the filtrate was concentrated *in vacuo*. The residue was diluted with water (2 x 15 mL) and extracted with CH_2CL_2 (3 x 15 mL). The combined organic solution was washed with brine (2 x 15 mL), dried over MgSO4, filtered, and concentrated *in vacuo*. The crude product was purified by trituration with ethanol to give a precipitate. The solid was collected in a fritted funnel. The HPLC analysis was done using a C18 column with UV detection at 235 nm using a gradient of 90:10 A:B to 100% B over 30 min with solvent A= water with 0.05% TFA and B = acetonitrile with 0.05% TFA. NMR and ESI-MS were performed as described [15]. The details of the chemical characterization of each compound are provided in Supplemental Data.

Spectral titration of TCCYP51 - The apparent affinities of ligand binding were evaluated by the spectral changes they induced in the TCCYP51 [9]. The titration experiments were carried out at 24^{o} C in 2 ml tandem cuvettes, containing 2 μM TCCYP51 in buffer A in the wavelength range 350-500 nm using a Shimadzu UV-2401PC spectrophotometer. The tested compounds (1 or 10 mM stock solutions in DMSO, depending on the affinity

of the interaction) were added in 1-µl aliquots to the test cuvette until the maximum in the TCCYP51 spectral response was reached. Equal volumes of DMSO were added to the reference cuvette. The apparent K_d's were determined from the equilibrium titration curves by plotting absorbance changes against the concentration of free ligand and fitting the data to a rectangular hyperbola using SigmaPlot Statistics [16].

ESI-MS analysis of non-covalent interactions in TCCYP51 - The experiments were conducted with an ESI-oaTOF mass spectrometer (micrOTOF, Bruker Daltonics, Inc., Billirica, MA) which has been modified for enhanced collisional cooling in the source for the analysis of non-covalent protein complexes. This was completed by the addition of a valve in turbo pump line restricting vacuum. The standard instrument parameters were used with the exception of the following: capillary voltage 3.5 kV, capillary exit 250 V, fore pressure 4.99 mbar, and TOF pressure 6.29 X 10^{-7} mbar. TCCYP51 was buffer exchanged into 50 mM ammonium acetate, pH 7.0; **20**-HCl was dissolved in ethanol and added to the protein solution to give the final concentration of 100 µM. The ESI flow rate was 180 µLh-1. Spectra were acquired in positive polarity mode, externally calibrated, and processed using DataAnalysis software (Bruker Daltonics, Inc.) by smoothing and base-line subtracting.

Reconstitution of enzymatic activity and inhibition assay - Sterol 14α-demethylase activity of TCCYP51 *in vitro* was reconstituted with cytochrome P450 reductase (CPR) from *Trypanosoma brucei* as an electron donor partner [17] and 24-methylenedihydrolanosterol (MDL) as a substrate [8]. The concentrated proteins were pre-

incubated for 10 min at room temperature with dilauroyl-α-phosphatidylcholine (DLPC) at molar ratio TCCYP51:CPR:DLPC=1:2:50. The final reaction mixture contained 1 μM TCCYP51 and 50 μM substrate (unlabeled and [^{3}H]-MDL were mixed to give ~2,000 cpm/nmol and added from 1 mM stock solution in 45%, 2-hydroxypropyl-β-cyclodextrin) in 20 mM MOPS (pH 7.4), 50 mM KCl, 5 mM $MgCl_2$, 10% glycerol , 0.4 mg/ml isocitrate dehydrogenase and 25 mM sodium isocitrate. For the inhibition assay, the reaction was performed in the presence of the increasing concentrations of the compounds tested as TCCYP51 inhibitors (concentration range 1-100 μM). After 5 min of pre-incubation with the inhibitors at 37ºC, the reaction was initiated with the addition of NADPH (5 μM). Sterols were extracted with ethyl acetate and analyzed by reverse phase HPLC in the linear gradient of methanol: acetonitrile: H_2O=9:9:2 (solution A) and methanol (solution B) (0-100%) using Waters C18 column and β-RAM radioactivity detector. The inhibitory potency was estimated as molar ratio inhibitor/enzyme at which the activity decreased 2-fold (I/E_2) [9]. Inhibitory effect of the compounds on COX-2 enzyme was determined at 100 nM final concentration of mouse cyclooxygenase 2 as previously described [12] and the potency was expressed as I/E_2 to correspond to the way it is expressed for TCCYP51.

Cell culture and growth inhibition assay in TC cells - Trypomastigotes (10^6 organisms) were pre-exposed to the CYP51 inhibitors dissolved in DMSO at several concentrations (1-50 μM) or to control DMSO for 30 min. Exposure of different concentrations of CYP51 inhibitors to trypomastigotes for 30 min did not affect their motility. The parasites were then exposed in triplicate to rat cardiomyocyte monolayers at the ratio 10 parasites/cell in Lab Tech chambers for 2h as described [18]. To verify that the inhibitory

effect was on trypanosomaes and not on cardiomyocytes, in additional experiments excess compound was removed from the trypanosomes prior to infection, producing similar results. After removing the unbound parasites, monolayers were incubated with DMEM supplemented with 10% FBS for 72 hr to allow parasite intracellular multiplication and the number of *T. cruzi* per 200 cells and the percent of infection were microscopically determined in Giemsa stained monolayers [18].

TC cellular sterol analysis - Epimastigotes (plating density 10^7 cells/ml) were cultured in brain heart infusion supplemented with hemin and 10% calf serum for 120 hours without an inhibitor and in the presence of **20**. The inhibitor was added daily to maintain 50 μM concentration. The cell pellet was washed with Hanks' balanced salt solution without phenol red to remove excess cholesterol from the serum and saponified using 10% KOH in 98% aqueous methanol at reflux temperature for 1 hour. The TC sterols were extracted with hexane and analyzed by silica gel TLC in hexane:ethyl acetate (8:2) as described previously [9].

Characterization of INDO-amide derivatives - **Compound 12** was obtained as an off-white solid (320 mg, 69% isolated yield). Melting point = 183 ^{o}C, ^{1}H NMR (300 MHz,$CDCl_3$,ppm) δ 8.40 (d, J = 1.4 Hz, 1H) 8.32 (dd, J_1 = 4.7 Hz, J_2 = 1.4 Hz, 1H), 8.06 (m, 1H,), 7.65 (d, J = 8.6 Hz, 2H), 7.50 (m, 3H), 7.25 (m, 1H), 6.94 (d, J= 2.4 Hz, 1H), 6.86 (d, J = 9.0 Hz, 1H), 6.71 (dd, J_1 = 9.0 Hz, J_2 = 2.4 Hz, 1H), 3.84 (s, 2H), 3.81(s, 3H), 2.46 (s, 3H); ESI-MS *m/z* (positive) 434 $[C_{24}H_{20}ClN_3O_3+H]^+$, HPLC: retention time= 18.1 min, 99% pure.

Compound 13 was obtained as a yellow solid (120 mg, 32% isolated yield). Melting point = 181 ^{o}C, ^{1}H NMR ($CDCl_3$) δ 8.39 (d, *J* = 4.3 Hz, 1H), 7.68 (d, *J* = 13.1 Hz, 2H), 7.62 (dt, *J* = 1.8, 7.7 Hz, 1H), 7.47 (d, *J* = 13.1 Hz, 2H), 7.15 (m, 2H), 6.92 (d, *J* = 2.4 Hz, 2H), 6.88 (s, 1H), 6.69 (dd, *J* = 2.4, 9.0 Hz, 1H), 4.52 (d, *J* = 5.1 Hz, 2H), 3.79 (s, 3H), 3.72 (s, 2H), 3.39 (s, 3H) ESI-MS *m/z* 469 $[C_{25}H_{22}ClN_3O_3+ Na]^+$, HPLC: retention time = 18.6 min, >99% pure.

Compound 14 was obtained as an off-white solid (204 mg , 55% isolated yield). Melting point = 178 ^{o}C, ^{1}H NMR ($CDCl_3$) δ 8.47 (dd, *J* = 1.8, 4.3 Hz, 2H), 7.63 (d, *J* = 13.1 Hz, 2H), 7.47 (d, *J* = 13.1 Hz, 2H), 7.05 (dd, *J* = 1.8, 4.3 Hz, 2H), 6.89 (d, *J* = 2.4 Hz, 1H), 6.84 (d, *J* = 9.0 Hz, 1H), 6.70 (dd, *J* = 2.4, 9.0 Hz, 1H), 4.40 (d, *J* = 6.3 Hz, 2H), 3.80 (s, 3H), 3.74 (s, 2H), 2.41 (s, 3H) ESI-MS *m/z* 469 $[C_{25}H_{22}ClN_3O_3+ Na]^+$, HPLC: retention time = 17.2 min, >99% pure.

Compound 15 was obtained as an off-white solid (53 mg, 13% isolated yield). Melting point = 181 ^{o}C, ^{1}H NMR ($CDCl_3$) δ 8.48 (dd, *J* = 1.6, 4.4 Hz, 2H), 7.65 (d, *J* = 13.1 Hz, 2H), 7.49 (d, *J* = 13.1 Hz, 2H), 7.04 (dd, *J* = 1.6, 4.4 Hz, 2H), 6.85 (m, 1H), 6.72 (dd, *J* = 2.5, 9.0 Hz, 1H), 5.83 (d, *J* = 7.8 Hz, 1H), 5.10 (quint, *J* = 7.4 Hz, 1H), 3.78 (s, 3H), 3.68 (s, 2H), 2.40 (s, 3H), 1.35 (d, *J* = 7.4 Hz, 3H) ESI-MS *m/z* 483 $[C_{26}H_{24}ClN_3O_3+ Na]^+$, HPLC: retention time = 16.2 min, >99% pure.

Compound 16 was obtained as a yellow solid (310 mg, 85% isolated yield). Melting

point = 163 °C, ^{1}H NMR ($CDCl_3$) δ 8.24 (d, *J* = 8.4 Hz, 1H), 8.10 (d, *J* = 5.9 Hz, 1H), 7.95 (s, 1H), 7.51 (d, *J* = 13.1 Hz, 2H), 7.08 (m, 1H), 6.94 (d, *J* = 2.4 Hz, 1H), 6.87(d, *J* = 9.0 Hz, 1H), 3.87 (s, 2H), 3.82 (s, 3H), 2.45 (s, 3H) ESI-MS *m/z* 455 $[C_{24}H_{20}ClN_3O_3+Na]^+$, HPLC: retention time= 17.1 min, >99% pure.

Compound 17 was obtained as a yellow solid (60 mg, 16% isolated yield). Melting point = 167 °C , ^{1}H NMR ($CDCl_3$) δ 8.61 (d, *J* = 4.9 Hz, 2H), 8.41 (br s, 1H), 7.69 (d, *J* = 13.1 Hz, 2H), 7.47 (d, *J* = 13.1 Hz, 2H), 7.02 (t, *J* = 3.2 Hz, 1H), 6.96 (d, *J* = 2.4 Hz, 1H), 6.87(d, *J* = 9.0 Hz, 1H), 6.69 (dd, *J* = 2.4, 9.0 Hz, 1H), 4.03 (s, 2H), 3.80 (s, 3H), 2.44 (s, 3H), ESI-MS *m/z* 456 $[C_{23}H_{19}ClN_4O_3 + Na]^+$, HPLC: retention time = 18.9 min, 98.0% pure.

Compound 18 was obtained as an off-white solid (250 mg, 59% isolated yield). Melting point = 177 °C, ^{1}H NMR (300 MHz,$CDCl_3$,ppm) δ 8.15 (d, 1H, J = 2.1 Hz), 7.50 (m, 5H), 7.422 (d, 1H, J = 8.4 Hz), 6.83 (m, 2H),6.69 (dd, J1 = 9 Hz, J2 =2.4 Hz 1H), 6.19 (br t, J = 6 Hz, 1H), 4.37 (d, J = 6Hz, 2H), 3.79 (s, 3H), 3.71(s, 2H), 2.36 (s, 3H), ESI-MS *m/z* (positive) 482 $[C_{25}H_{21}Cl_2N_3O_3]^+$, HPLC: retention time = 19.1 min, >99% pure.

Compound 19 was obtained as an off-white solid (264 mg, 69% isolated yield). Melting point = 183 °C, ^{1}H NMR (300 MHz,$CDCl_3$, ppm) δ 8.54 (s, 1H), 7.60 (m, 4H), 7.49 (m, 2H), 6.85 (m, 2H), 6.70 (d, J = 8.7 Hz, 1H), 6.12 (br s, 1H), 4.47 (s, 2H), 3.79 (s, 3H), 3.72 (s, 2H), 2.39 (s, 3H), ESI-MS *m/z* (positive) 516 $[C_{26}H_{21}ClF_3N_3O_3]^+$, HPLC: retention time =20.0 min, >99% pure.

Compound 20 was obtained as a yellow solid (280 mg, 59% isolated yield), Melting point = 188 ^{o}C, ^{1}H NMR (300 MHz,$CDCl_3$,ppm) δ 8.40 (d, J = 1.4 Hz, 1H), 8.32 (dd, J_1 = 4.7 Hz, J_2 = 1.4 Hz, 1H), 8.06 (m, 1H), 7.65 (d, J = 8.6, 2H), 7.48 (d, J = 8.6, 2H), 7.24 (m, 1H), 6.94 (d, J = 2.5 Hz, 1H), 6.86 (d, J = 9.0 Hz, 1H), 6.72 (dd, J_1 = 9.0, j_2 = 2.5, 1H), 5.61 (br s, 1H), 3.81 (s, 3H), 3.59 (s, 2H), 3.45 (m, 2H), 2.70 (t, J = 6.7 Hz, 2H), 2.04 (s, 3H) ESI-MS *m/z* (positive) 462 $[C_{26}H_{24}ClN_3O_3+H]^+$, HPLC: retention time = 15.1 min, >99% pure.

Compound 21 was obtained as an off-white solid (360 mg, 72% isolated yield). Melting point = 191 ^{o}C, ^{1}H NMR (300 MHz, $CDCl_3$, ppm) δ 7.65 (d, J = 8.6, 2H), 7.53 (br s, 1H), 7.48 (d, J = 8.6, 2H), 7.30 (m, 2H), 7.18 (dd, J_1 = 9.0, j_2 = 2.5, 1H), 6.94 (d, J = 2.5 Hz, 1H), 6.86 (d, J = 9.0 Hz, 1H), 6.72 (dd, J_1 = 9.0, j_2 = 2.5, 1H), 5.61 (br s, 1H), 3.81 (s, 3H), 3.59 (s, 2H), 3.45 (m, 2H), 2.70 (t, J = 6.7 Hz, 2H), 2.04 (s, 3H) ESI-MS *m/z* (positive) 495 $[C_{27}H_{24}Cl_2N_2O_3+H]^+$, HPLC: retention time =16.1 min, 98.1% pure.

Compound 22 was obtained as an off-white solid (301 mg, 62% isolated yield) Melting point = 180 ^{o}C, ^{1}H NMR (300 MHz, $CDCl_3$, ppm) δ 7.59 (d, J = 8.4 Hz, 2H), 7.47 (d, J = 8.4 Hz,, 2H), 7.13 (m, 3H), 6.90 (m, 4H), 6.71 (dd, J_1 = 8.9, j_2 = 2.4, 1H), 5.61 (br s, 1H), 3.81 (s, 3H), 3.59 (s, 2H), 3.45 (m, 2H), 2.70 (m, 1H), 2.04 (s, 3H), 1.28 (d, J = 6.8 Hz, 3H), ESI-MS *m/z* (positive) 475 $[C_{28}H_{27}ClN_2O_3+H]^+$, HPLC: retention time = 17.3 min, >99% pure.

Results and Discussion

TCCYP51 ligands found via HTS - Optical high throughput screening is based on the P450 property of changing the maximum of the Soret band absorbance upon ligand binding. The changes are connected with alterations in the surrounding environment of the heme iron [9]. Heterologously expressed CYP51s are usually purified in the oxidized low-spin ferric form (resting state of the iron- porphyrin complex with the Soret band maximum at 417 nm), the sixth coordinate position of the iron being occupied by a water molecule. Binding of a substrate-like ligand in the active center causes water displacement; the iron becomes penta-coordinated and pops out of the porphyrin plane. This triggers a low-to-high-spin transition in the iron-porphyrin complex, and the Soret band maximum shifts to 390 nm producing a so-called type 1 spectral response in the difference spectra. Alternatively, a type 2 spectral response (red shift in the Soret band maximum to 422-424 nm) reflects direct coordination of a ligand other than water to the low-spin heme iron.

All "substrate-like" ligands identified by HTS produced rather weak spectral responses in TCCYP51. The three best compounds (Figure 1A) revealed apparent dissociation constants in the concentration range of 50 -100 μM, which suggests binding affinities at least 50-fold lower than the affinity of the enzyme/substrate complex formation (K_d around 1 μM with the preferred substrate 24-methylenedihydrolanosterol) [9]. Correspondingly, the inhibitory potencies of these compounds in the reconstituted enzyme reaction were very low (I/E_2 >50 (not shown)). We believe this might be connected with the narrowness of the CYP51 substrate specificity [19]: to preserve their

catalytic function through hundreds of million of years of evolution the CYP51 family enzymes developed very strict requirements towards their substrates so that minor alterations in the spatial structure would differentiate a foreign compound and prevent it from being metabolized or interfere with the substrate in the CYP51 active center. The finding supports the notion that the most likely way to design potent substrate-analogous CYP51 inhibitors would be through the subtle modifications of the basic sterol structure in the regions adjusted to the reactive 14α-methyl group [8].

The HTS hits which induced type 2 spectral response in TCCYP51 demonstrated higher binding affinities; the most potent inhibitor (**5**) exhibiting a K_d of 0.44 μM and I/E_2 of about 10 (Table 1). Contrary to compounds **4** and **6**, which must interact with the TCCYP51 heme iron through their five-membered imidazole ring, **5** is most likely to coordinate through the pyridyl nitrogen. This has been supported by the results of the web-database search using compound **5** (*N*-(4-pyridyl)-formamide) as a template since similar structures tested (Figure 1B) produced the same spectral shift in the TCCYP51 absorbance (Soret band maximum 422 nm). On the other hand, differences in the calculated apparent binding affinities reflect influence of the configuration of the non-coordinated portion of the ligand molecule, which (similar to azole inhibitors) might enhance the inhibitory effect by forming additional interactions with the amino acid residues in the CYP51 substrate binding cavity. The strongest binding compounds **7 and 9 (**K_d = 0.75 and 0.24 μM, respectively) have bulky structures attached to the N-(4-pyridyl)-amide moiety. In **9** this portion of the molecule is larger and more flexible than it is in **7,** and this feature must be preferable since in the reconstituted enzyme reaction **9**

revealed more than one order of magnitude stronger potency as TCCYP51 inhibitor (I/E_2<1, Table 1).

Having an inhibitory effect on TCCYP51 comparable with the effects of antifungal azole drugs fluconazole and ketoconazole [9], compound **9** has potential to serve as a lead for the design of novel non-azole CYP51 inhibitors. Because high flexibility of the substrate binding cavity is known to be the basis of the P450 catalysis and ligand binding [20, 21], in the absence of TCCYP51 crystal structure, most preferably in a complex with **9,** molecular docking and computer modeling are very unlikely to produce reliable information on rational **9** structure modification, especially since sequence identity of TCCYP51 to the closest P450 template of known crystal structure is only 28%. Instead, we continued with investigation of structural similarity and tested as TCCYP51 inhibitors a number of INDO-amide derivatives which share structural features with **9.** All these compounds have the same INDO-amide moiety (Figure 1 C, shown in square) but differ in the length of the alkyl-linker and position of the nitrogen in the heterocycle (shown in blue); this part of the molecule is of special interest because it is expected to form the sixth coordinate bond with the P450 heme iron.

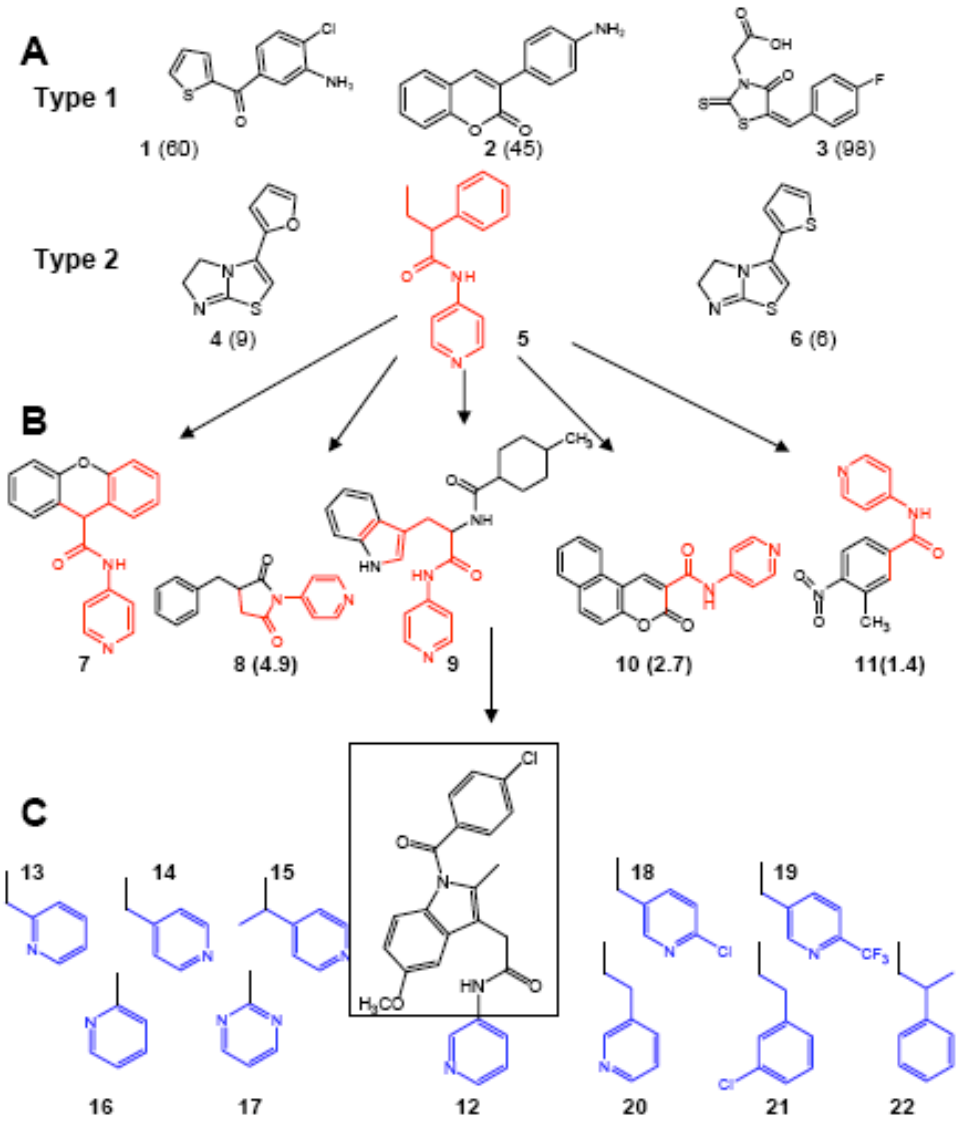

Figure 1. Search for TCCYP51 inhibitors.
(A) Ligands *found via* HTS; (B) inhibitors found using web-database search for structural similarity to **5**; (C) **9**-like INDO-amide derivatives. Calculated from spectral responses apparent dissociation constants (μM) for the compounds not included in Table 1 are shown in brackets.

INDO-amide derivatives as TCCYP51 ligands - While spectral responses of TCCYP51 to the compounds **7-11** were very similar to the responses caused by imidazole and triazole

derivatives, INDO-amides induced a variety of spectral changes in the hemoprotein (Figure 2, Table 1). It could be connected with the variations in the location of the nitrogen in the heterocyclic ring. Thus, when the nitrogen is in the para-position (as in compounds **7-11**) the Soret band maximum shows a normal shift to 422 nm (**14** and **15**). The same response is produced if the nitrogen is in the meta-position (**12**) and the ring does not contain any additional substituents. If it does (**18** and **19**), the maximum is observed at 420 nm. Taking into account that the same spectral changes are also caused by two compounds which do not carry any nitrogen atoms in the ring (**21** and **22**), it is not excluded that this modified type 2 response may result from accommodation of the inhibitor in the TCCYP51 active center, which would strengthen the water ligation to the heme iron. This can also be true for **13** (nitrogen in the ortho-position), though in this case the iron coordination is weaker and the absorbance maximum shifts only to 418 nm. Having a shorter arm between the ortho-nitrogen ring and the amide, **16** definitely does not participate in iron coordination as the compound causes very weak substrate-like type 1 spectral response in TCCYP51. Finally, **17** (pyrimidine ring with both nitrogens ortho to the arm) did not induce any spectral changes in TCCYP51,

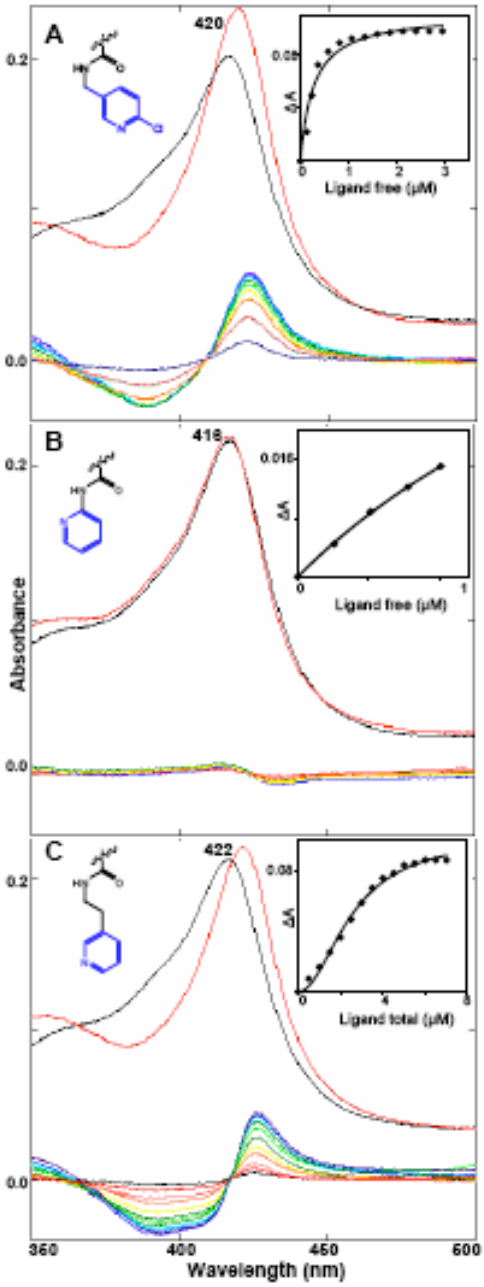

Figure 2. Spectral responses of TCCYP51 (2 μM) to three INDO-amide derivatives. (A) **18**; (B) **16**; (C) **20.** Upper spectra: Absolute absorbance in the Soret band region (black line – no ligand, red line – plus ligand. Lower: Difference spectra upon titration with the ligands (rainbow color sequence upon ligand addition in 0.5 μM steps. Insets: Titration curves.

Compound	Spectral response in TCCYP51			Effect on enzymatic activity (I/E_2)	
	Type	Soret band maximum, nm	Kd, μM	TCCYP51	Mouse COX2
5	2	422	0.44±0.02	10	
7	2	422	0.75±0.03	14	
9	2	422	0.24±0.01	<1	
12	2	422	0.29±0.01	9.1	2.1
13	2**	418	7.6±0.9	13	>10
14	2	422	0.54±0.02	10	10
15	2	422	0.37±0.05	8.5	1.7
16	1*	416	3.3±0.48	11	2.1
17	none	417	-	15	3.6
19	2**	420	0.56±0.08	7.7	<1
18	2**	420	0.26±0.04	4.2	<1
20	2***	422	2.31±0.09	6.3	2.4
21	2**	419	0.36±0.02	<1	<1
22	2**	419	0.15±0.01	<1	>40

Table 1. Binding parameters, inhibitory potencies and antiparasitic effects of selected TCCYP51 ligands

* weak type 1 response with only ~7% of P450 experiencing low to high spin transition;
**modified type 2 response with the smaller shift in the Soret band maximum,
***sigmoid curve, Hill coefficient 2.3±0.2 (see Figure 2)

Though they differ in the location of the Soret band maximum, the majority of the spectral responses upon titration of TCCYP51 with the increasing concentrations of the ligands produced typical hyperbolic curves. The only exception was observed in the case of **20** (Figure 2 C). The sigmoid shape of the titration curve was reproducible upon variations in the buffer composition, salt gradient, increase in the concentration of TCCYP51 or use for the titration of more soluble **20**-hydrochloride. The Hill coefficient

of 2.3 suggested a possibility of simultaneous binding of two inhibitor molecules to the enzyme. This has been tested and confirmed using ESI-mass spectrometry. Allosteric effects (non-Michaelis-Menten kinetics) have been reported for several microsomal drug-metabolizing CYPs (e.g 1A2, 2A6, 2C9, 3A4: [22]) but this is the first example in a CYP51 ortholog and binding of a second molecule may have no inhibitory effect.

Regardless of the quite pronounced differences in the apparent binding affinities calculated from the spectral responses, most of the INDO-amides demonstrated comparably strong inhibitory effects on TCCYP51 (I/E_2 around 5-10, reversible) except for **21** and **22** ($I/E_2<1$, functionally irreversible) (Table 1). Altogether this supports our previous observation that, being indicative of binding of a ligand near the heme iron, spectral responses do not necessarily reflect real inhibitory potency [9] and the interactions in the regions of the CYP51 substrate binding cavity, remote from the heme iron, might also provide strong inhibitory effect on the enzyme catalysis and should be considered in the design of new inhibitors.

Antiparasitic effect of CYP51 inhibitors in extracellular and intracellular trypanosomes - TC is an obligate parasite with a complex life cycle that includes four morphologically and metabolically different stages. Proliferative epimastigotes and infective metacyclic trypomastigotes are present in the insect vectors (kissing bugs). Upon infection of mammalian hosts, TC transforms into bloodstream trypomastigotes and proliferative intracellular amastigotes (amastigotes dominate in the chronic stage of Chagas). Pre-treatment of TC trypomastigotes with compounds **9, 13, 18,** and **20** produced a clear dose-dependent antiparasitic effect in both human forms of TC (Figure 3). At a 20 μM

compound concentration the parasite was practically eliminated from cardiomyocytes. The strongest growth inhibition (ED_{50}<1 μM in TC amastigotes) was observed with **20** which may be at least in part due to its better cellular permeability or the longest lifetime/highest metabolic stability[15].

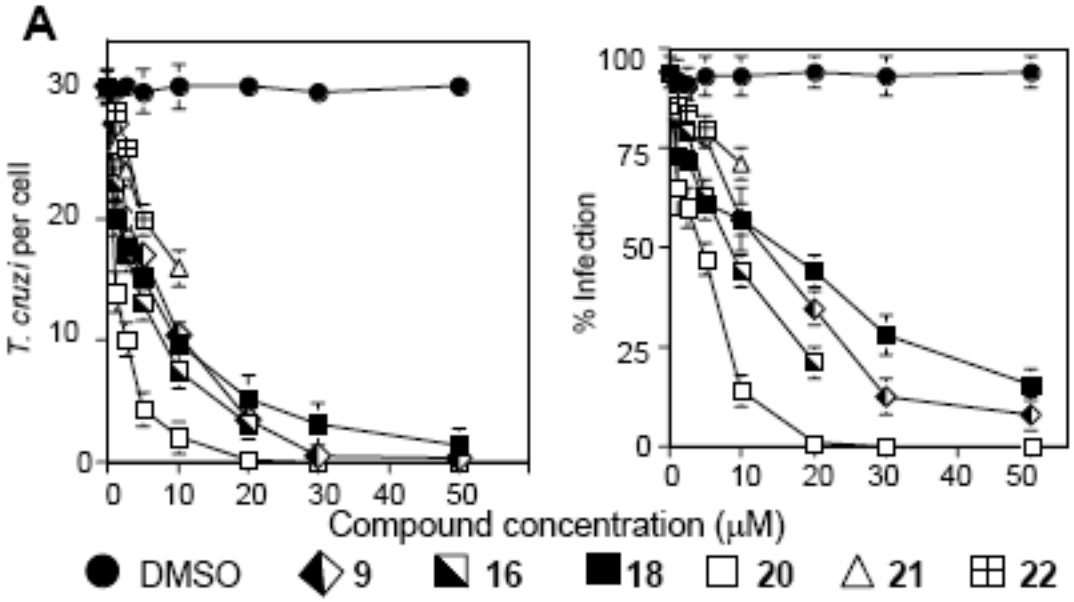

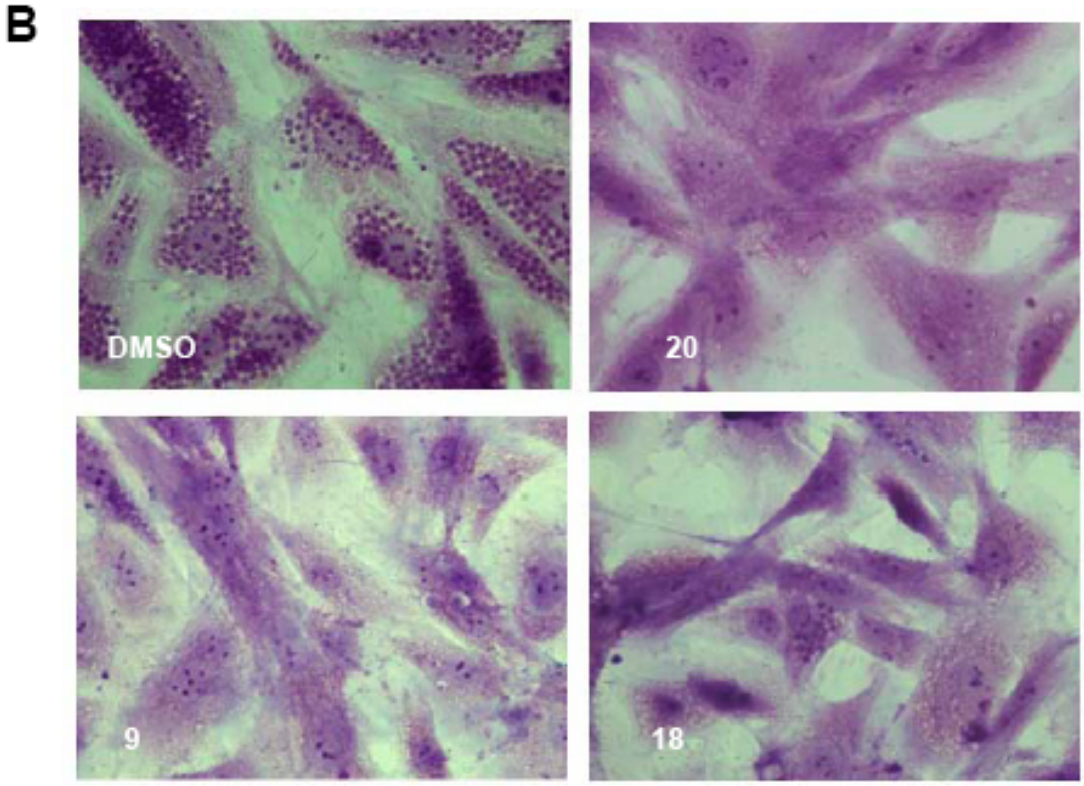

Figure 3. Cellular effects of TCCYP51 inhibitors in TC trypomastigotes and amastigotes.

(A) Dose-dependent inhibition of *T. cruzi* intracellular multiplication and infection in cardiomyoblasts by TCCYP51 inhibitors. Trypomastigotes were pre-treated with several concentrations of TCCYP51 inhibitors or mock-treated, exposed to cardiomyoblast monolayers and *T. cruzi* multiplication was evaluated at 72 h by determining the number of *T. cruzi*/cell (left panel) and the percent of infection (right panel). The data represent the mean $\pm$ standard deviation (SD) of results from triplicate samples. SD did not exceed 10% of the mean. The two most potent TCCYP51 inhibitors (**21** and **22**) show antiparasitic activities at $\leq$ 10 □M concentrations) but release cardiomyoblast monolayers at higher concentrations.

(B). Microscopic observation of the inhibition of *T. cruzi* multiplication by 20 □M TCCYP51 inhibitors within cardiomyoblasts at 72 hr. *T. cruzi* pre-treated with control DMSO showed high levels of parasite multiplication, whereas cells exposed to trypanosomes pre-incubated with the inhibitors showed a dramatic decrease in the number of intracellular parasites.

*Sterol composition of TC cells upon treatment with **20*** - We have shown recently that treatment of TC cells with a potent TCCYP51 inhibitor [9] profoundly alters their sterol composition. While untreated parasites, where sterol biosynthesis is highly efficient, essentially contain only the pathway products (ergosterol and its 24-ethylated analog) and exogenous cholesterol from the medium (Figure 4A), in the inhibitor-treated TC (SDZ-284629, 1μM) the pathway practically stops at the stage of the C14-methylated sterol precursors, predominantly lanosterol, the first cyclized compound of the pathway, and 24-methylenedihydrolanosterol, the preferred TCCYP51 substrate. Treatment of TC with 50 μM **20** produces a very similar effect on cellular sterol composition (Figure 4B) indicating that the mechanism of action of the compound is connected with blocking sterol biosynthesis in the parasite via inhibition of TCCYP51 activity.

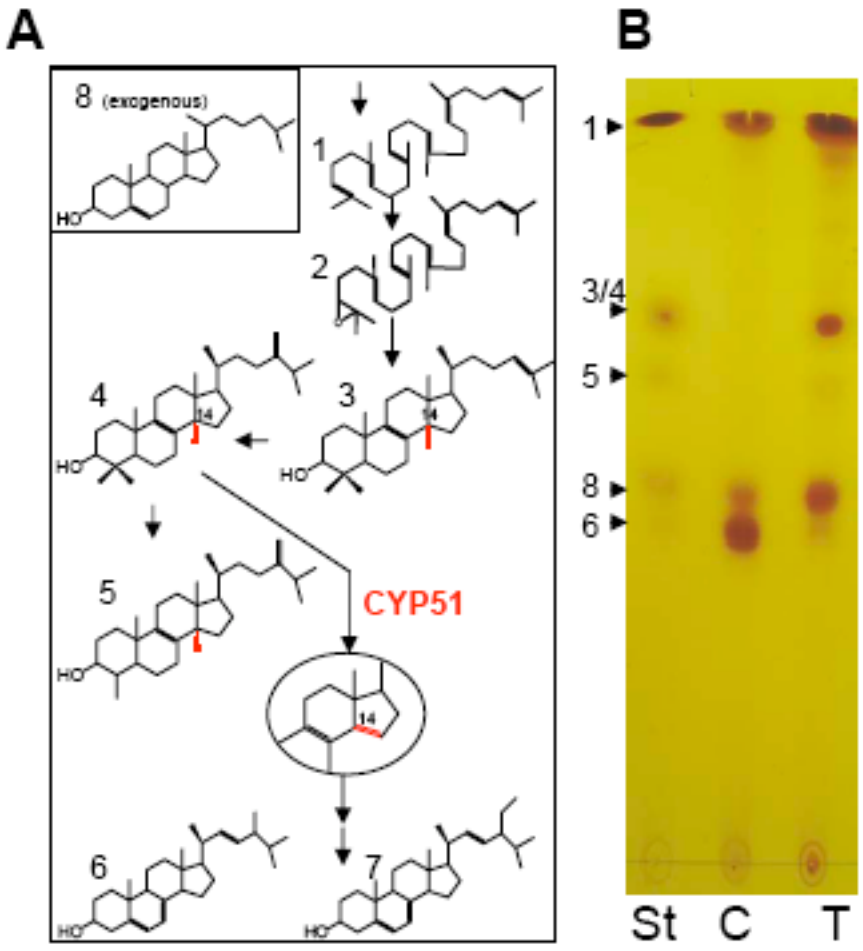

Figure 4. Sterols in TC.
(A) Structural formulas of neutral lipids formed upon sterol biosynthesis (1- squalene; 2-squalene epoxide; 3-lanosterol; 4 - 24-methylenedihydrolanosterol; 5 – obtusifoliol; 6-ergosterol; 7- 24-methylergosterol) or up taken from the media (8-cholesterol). 14α-methyl group and formed by CYP51 Δ14-15 double bond are shown in red.
(B) TLC analysis of sterols extracted from TC epimastigotes. St, sterol standards; C, sterols in untreated cells; T, sterols in TC incubated for 24 hours with 50 μM **20**.

Inhibition of sterol biosynthesis in TC is becoming one of the very promising directions in the development of anti-Chagasic drugs. Several antifungal azoles have recently entered clinical trials for anti-trypanosomal chemotherapy[4]. However, azole derivatives (at least those currently used as fungicides) have one serious disadvantage: upon long-term treatment they often cause resistance. Experimental development of resistance to fluconazole in the cultured TC cells also has been described[23]. Though strong inhibition of TCCYP51 with specific azoles might shorten the treatment time and decrease the probability of resistance, an alternative set of TCCYP51 inhibitors would be highly desirable. The strong antiparasitic effect of indomethacin amide derivatives in both extracellular and intracellular forms of human stages of TC indicates that this group of compounds might find a new application as potential anti-trypanosomal agents. While additional directed modifications, targeted to decrease COX-2 inhibitory potency might be desirable for use as a lead structure **20** in the chronic (especially cardiac) forms of Chagas, this class of compounds is particularly attractive for the acute stage since drugs traditionally aimed to ease non-specific symptoms of inflammation and fever can actually provide treatment to the disease. Finally, HTS of larger libraries of small bioactive molecules in combination with the database search for structural similarity may help to discover other novel CYP51 inhibitors.

References

1. Blood donor screening for chagas disease--United States, 2006-2007. *MMWR Morb Mortal Wkly Rep* **2007**, 56, (7), 141-3.
2. Ferreira, M. S.; Borges, A. S., Some aspects of protozoan infections in immunocompromised patients- a review. *Mem Inst Oswaldo Cruz* **2002**, 97, (4), 443-57.
3. Wilkinson, S. R.; Taylor, M. C.; Horn, D.; Kelly, J. M.; Cheeseman, I., A mechanism for cross-resistance to nifurtimox and benznidazole in trypanosomes. *Proc Natl Acad Sci U S A* **2008**, 105, (13), 5022-7.
4. Croft, S. L.; Barrett, M. P.; Urbina, J. A., Chemotherapy of trypanosomiases and leishmaniasis. *Trends Parasitol* **2005**, 21, (11), 508-12.
5. El-Sayed, N. M.; Myler, P. J.; Blandin, G.; Berriman, M.; Crabtree, J.; Aggarwal, G.; Caler, E.; Renauld, H.; Worthey, E. A.; Hertz-Fowler, C.; Ghedin, E.; Peacock, C.; Bartholomeu, D. C.; Haas, B. J.; Tran, A. N.; Wortman, J. R.; Alsmark, U. C.; Angiuoli, S.; Anupama, A.; Badger, J.; Bringaud, F.; Cadag, E.; Carlton, J. M.; Cerqueira, G. C.; Creasy, T.; Delcher, A. L.; Djikeng, A.; Embley, T. M.; Hauser, C.; Ivens, A. C.; Kummerfeld, S. K.; Pereira-Leal, J. B.; Nilsson, D.; Peterson, J.; Salzberg, S. L.; Shallom, J.; Silva, J. C.; Sundaram, J.; Westenberger, S.; White, O.; Melville, S. E.; Donelson, J. E.; Andersson, B.; Stuart, K. D.; Hall, N., Comparative genomics of trypanosomatid parasitic protozoa. *Science* **2005**, 309, (5733), 404-9.
6. Cammerer, S. B.; Jimenez, C.; Jones, S.; Gros, L.; Lorente, S. O.; Rodrigues, C.; Rodrigues, J. C.; Caldera, A.; Ruiz Perez, L. M.; da Souza, W.; Kaiser, M.; Brun, R.; Urbina, J. A.; Gonzalez Pacanowska, D.; Gilbert, I. H., Quinuclidine derivatives as potential antiparasitics. *Antimicrob Agents Chemother* **2007**, 51, (11), 4049-61.
7. Haughan, P. A., Goad, L.J., Lipid Biochemistry of Trypanomastids. *Biochemical Protozoology* **1991**, 312-328.
8. Lepesheva, G. I.; Zaitseva, N. G.; Nes, W. D.; Zhou, W.; Arase, M.; Liu, J.; Hill, G. C.; Waterman, M. R., CYP51 from Trypanosoma cruzi: a phyla-specific residue in the B' helix defines substrate preferences of sterol 14alpha-demethylase. *J Biol Chem* **2006**, 281, (6), 3577-85.
9. Lepesheva, G. I.; Ott, R. D.; Hargrove, T. Y.; Kleshchenko, Y. Y.; Schuster, I.; Nes, W. D.; Hill, G. C.; Villalta, F.; Waterman, M. R., Sterol 14alpha-demethylase as a potential target for antitrypanosomal therapy: enzyme inhibition and parasite cell growth. *Chem Biol* **2007**, 14, (11), 1283-93.
10. Espinel-Ingroff, Mechanisms of Resistance to Antifungal Agents: Yeasts and Filamentous Fungi. *Rev Iberoam Micol* **2008**, 2, 101-106.
11. Kalgutkar, A. S.; Crews, B. C.; Rowlinson, S. W.; Marnett, A. B.; Kozak, K. R.; Remmel, R. P.; Marnett, L. J., Biochemically based design of cyclooxygenase-2 (COX-2) inhibitors: facile conversion of nonsteroidal antiinflammatory drugs to potent and highly selective COX-2 inhibitors. *Proc Natl Acad Sci U S A* **2000**, 97, (2), 925-30.
12. Kalgutkar, A. S.; Marnett, A. B.; Crews, B. C.; Remmel, R. P.; Marnett, L. J., Ester and amide derivatives of the nonsteroidal antiinflammatory drug, indomethacin, as selective cyclooxygenase-2 inhibitors. *J Med Chem* **2000**, 43, (15), 2860-70.
13. Prusakiewicz, J. J.; Felts, A. S.; Mackenzie, B. S.; Marnett, L. J., Molecular basis of the time-dependent inhibition of cyclooxygenases by indomethacin. *Biochemistry* **2004**, 43, (49), 15439-45.

14. Omura, T.; Sato, R., The Carbon Monoxide-Binding Pigment of Liver Microsomes. Ii. Solubilization, Purification, and Properties. *J Biol Chem* **1964**, 239, 2379-85.
15. Remmel, R. P.; Crews, B. C.; Kozak, K. R.; Kalgutkar, A. S.; Marnett, L. J., Studies on the metabolism of the novel, selective cyclooxygenase-2 inhibitor indomethacin phenethylamide in rat, mouse, and human liver microsomes: identification of active metabolites. *Drug Metab Dispos* **2004**, 32, (1), 113-22.
16. Lepesheva, G. I.; Virus, C.; Waterman, M. R., Conservation in the CYP51 family. Role of the B' helix/BC loop and helices F and G in enzymatic function. *Biochemistry* **2003**, 42, (30), 9091-101.
17. Lepesheva, G. I.; Nes, W. D.; Zhou, W.; Hill, G. C.; Waterman, M. R., CYP51 from Trypanosoma brucei is obtusifoliol-specific. *Biochemistry* **2004**, 43, (33), 10789-99.
18. Nde, P. N.; Simmons, K. J.; Kleshchenko, Y. Y.; Pratap, S.; Lima, M. F.; Villalta, F., Silencing of the laminin gamma-1 gene blocks Trypanosoma cruzi infection. *Infect Immun* **2006**, 74, (3), 1643-8.
19. Lepesheva, G. I.; Waterman, M. R., Sterol 14alpha-demethylase cytochrome P450 (CYP51), a P450 in all biological kingdoms. *Biochim Biophys Acta* **2007**, 1770, (3), 467-77.
20. Lepesheva, G. I.; Seliskar, M.; Knutson, C. G.; Stourman, N. V.; Rozman, D.; Waterman, M. R., Conformational dynamics in the F/G segment of CYP51 from Mycobacterium tuberculosis monitored by FRET. *Arch Biochem Biophys* **2007**, 464, (2), 221-7.
21. Poulos, T. L., Cytochrome P450 flexibility. *Proc Natl Acad Sci U S A* **2003**, 100, (23), 13121-2.
22. Atkins, W. M., Non-Michaelis-Menten kinetics in cytochrome P450-catalyzed reactions. *Annu Rev Pharmacol Toxicol* **2005**, 45, 291-310.
23. Buckner, F. S., Sterol 14-demethylase inhibitors for Trypanosoma cruzi infections. *Adv Exp Med Biol* **2008**, 625, 61-80.

CHAPTER VI

SUMMARY

The tools available for the study of enzymes have proliferated over the past sixty years. The ability to study protein structure in fine detail took a giant leap forward in the 1950's with the solving of the first protein crystal structure (myoglobin) by Perutz and Kendrew. To date, there are now nearly 45,000 structures solved using X-ray crystallography in the Protein Data Bank free accessible to the world's scientists. Additionally, advances in the nuclear magnetic resonance spectroscopy have allowed for the analysis of larger proteins and have produced 7,500 structures in the Protein Data Bank. In concert with these advances, the advent of accessible molecular biology tools over the past twenty years have enabled mutagenesis studies to be accomplished much quicker. The tools available to study enzyme function have evolved in a synergistic fashion with these structural technologies. Instruments have been developed to measure on faster and faster time scales with greater and greater sensitivity (e.g. single molecule fluorescence studies). The computing power now available allows for more and more complex simulations of dynamic enzyme motions. All of this is to say it is an incredibly exciting, rich, and powerful time to be studying both structure and function and in turn, both biology and chemistry of enzymes and the small molecules (e.g. drugs) that interact with them.

The use of salicylic acid, secured from willow bark, by the ancient Egyptians to ease pain and swelling is the earliest know pharmacological blockade of cyclooxygenase

(COX) action. A derivatized salicylate brought commercial success for the Bayer Company when it released aspirin in 1899. However, it was not until over a half century later when the mechanism of action of aspirin was described by Smith and Vane to be the blockade of cyclooxygenase (COX) action. The identification in 1991 of a second COX isoform (COX-2), which had an extremely homologous sequence and seemingly identical enzymatic function to COX-1, was puzzling as the need for such redundancy was not apparent. The ability of drug companies and academic laboratories to develop inhibitors that could bind selectively to COX-2 was quite an accomplishment considering forthcoming crystal structures would show nearly identical three-dimensional structures of these two isoforms.

Neutralization of the acidic non-selective non-steroidal anti-inflammatory drug (NSAID) indomethacin (INDO) confers COX-2 selectivity, but the molecular basis for this selectivity was not revealed through prior crystallographic or mutagenesis studies. We have expressed and assayed a number of non-active site, divergent, COX-2 mutants to discover that mutation of position 472 (Leu in COX-2, Met in COX-1) reduces enzyme inhibition by INDO-amides. Crystal structures and molecular dynamics simulations reveal identical equilibrium enzyme structures around residue 472. However, the calculations indicate that the L472M mutation impacts local low-frequency dynamical COX constriction site motions, by stabilizing the active site entrance, slowing constriction site opening, and impeding inhibitor entry into the active site. Kinetic analysis reveals significantly reduced rates of inhibitor movement into the active site of L472M. The results of these studies may help inform future development of small moleculas that selectively bind to COX-2.

In addition to inhibitors binding selectively to COX-2, it has been reported that an endogenous fatty acid used for signaling in the nervous system binds selectively to COX-2. It has been reported from *in vitro* experiments that the endocannabinoid 2-arachidonoyl glycerol (2-AG) is a selective substrate for COX-2. However, recent studies with murine resident peritoneal macrophages indicated COX-1 contributes to 2-AG oxygenation because this activity was insensitive to COX-2-selective inhibitors and occurred in macrophages from cyclooxygenase-2 (-/-) animals. Mutagenesis studies identified that constriction site residues Arg-120 and Glu-524, conserved between both isoforms of cyclooxygenase, play a vital role in 2-AG turnover. However, the identity of a non-conserved second-shell residue, 472, can drastically alter the dynamics of the constriction site. We report mouse COX-1, unlike human or ovine COX-1, is able to metabolize 2-AG due, in part, to the species-divergent identity of residue 472. These results identify another important determinant of the substrate selectivity of cyclooxygenases. Additionally, these findings are a contribution to the field of animal model development as many studies of endocannabinoid pharmacology are routinely done in rodents.

The NSAIDs have been widely used for pain and swelling relief that is available over-the-counter. Unfortunately, long-term use of these drugs led to ulcerogenecity assumed to be caused by inhibition of the COX-1 isoform. Subsequently, the strategy was undertaken to design COX-2 selective inhibitors (COXIBs) and was proven to be successful with the commercial launch of both rofecoxib and celecoxib. It was also found that chemical neutralization of carboxylic acid-containing NSAIDs, such as INDO, to an ester or amide would afford a COXIB. Unexpectedly, unanticipated cardiovascular side

effects resulted in rofecoxib being pulled from the market and led to an FDA black-box warning on celecoxib.

The cause of the cardiovascular toxicity is still unclear, though it has been shown that administration of both rofecoxib and celecoxib decreases the level of vasodilating PGI_2 while having no effect on production of vasoconstricting TXA_2, both of which are downstream of COX action. Currently, one hypothesis is that restoration of the balance between these two vasoactive metabolites would eliminate cardiotoxicity of the, otherwise very effective, COXIBs. We report the design and synthesis of dual inhibitors of COX-2 and TXAS that we propose as proof-of-concept cardio-protective COXIBs.

One strategy for drug development for diseases in desperate need of chemotherapeutic intervention (e.g. Chagas disease) is to take a currently used drug (INDO) that combats with any measurable potency against said disease and use medicinal chemistry to tune out the original activity (e.g. COX inhibition) and tune in potency against the desired target (14α-demethylase of *Trypanasoma cruzi*). The strategy has been called Selective Optimization of Side Activities or SOSA. The advantage to this strategy is known pharmacokinetics and toxicity of the original molecule (INDO) with the hope that any derivitatization will not dramatically change these properties. We were able to tune out COX-1 inhibition through amidation and tune out COX-2 inhibition by changing the amine portion of the molecules synthesized. In addition, INDO-amides are particularly well-suited as treatment for a neglected tropical disease as they are chemically stable to both heat and light and can be made in minimal synthetic step from cheap and readily available materials. This research, in total, has highlighted the ability to

uncover new and interesting biology by modulating the chemical properties of a small molecule such as an INDO-amides.